

**DEVELOPMENT OF COORDINATED VOLTAGE
CONTROL MECHANISM FOR MV NETWORKS WITH
LARGE SCALE SOLAR PENETRATION**

Mutuantrige Kasun Darshana Peiris

(159314J)

Degree of Master of Science

Department of Electrical Engineering

University of Moratuwa

Sri Lanka

May 2019

**DEVELOPMENT OF COORDINATED VOLTAGE
CONTROL MECHANISM FOR MV NETWORKS WITH
LARGE SCALE SOLAR PENETRATION**

Mutuantrige Kasun Darshana Peiris

(159314J)

Thesis submitted in partial fulfillment of the requirements for the degree Master of
Science

Department of Electrical Engineering

University of Moratuwa

Sri Lanka

May 2019

DECLARATION

I declare that this is my own work and this thesis does not incorporate without acknowledgement any material previously submitted for a Degree or Diploma in any other University or institute of higher learning and to the best of my knowledge and belief it does not contain any material previously published or written by another person except where the acknowledgement is made in the text.

Also, I hereby grant to University of Moratuwa the non-exclusive right to reproduce and distribute my thesis, in whole or in part in print, electronic or other medium. I retain the right to use this content in whole or part in future works (such as articles or books).

Signature:

Date:

.....

M. K. D. Peiris

The above candidate has carried out research for the Masters thesis under my supervision.

Signature of the supervisor:

.....

Date:

Dr. J. V. U. P. Jayatunga

.....

Date:

Dr. D. P. Chandima

.....

Date:

Dr. H. M. Wijekoon

ABSTRACT

With the rapidly increasing solar PV penetration to the Utility Distribution Network (UDN) over the past decade, numerous operational challenges including Power Quality (PQ) problems have become substantial compared with the conventional UDN globally. Primarily, solar photovoltaic (PV) systems were connected to the UDN via Low Voltage (LV) side, however, global trend has been advanced to extract solar energy through Medium Voltage (MV) networks up to date via large scale solar farm integration.

Steady state voltage rise in the distribution feeders is reported as one of the main constraining factors for limiting solar PV deployment in LV and MV networks. In Sri Lankan context, recent studies proved that over voltages stay unavoidable in LV networks with high solar PV penetration. Further, preliminary system studies has shown that over voltages will give rise due to the connection of proposed 1 MW Solar Farms at MV level under the “Battle for Solar Energy” program.

This thesis is a comprehensive study to identify the PQ issues correlated to such MV networks, especially assesses the over voltage occurrences during the day time where solar penetration at its maximum. A coordinated decentralized control mechanism is adapted to control the over voltages and maintain the voltage levels within its stipulated limits. Coordination between two decentralized voltage controllers; reactive power control of solar PV inverter and distribution static compensator (DSTATCOM), is proposed to harness the maximum amount of clean energy into the UDN avoiding voltage violations, splitting the MV network into multiple controllable zones.

The coordinated voltage control mechanism was modeled using DIgSILENT PowerFactory simulation platform for IEEE 33-bus radial network, which was further extended to the Mauara feeder of the Embilipitiya Grid Substation of Sri Lanka in order to verify the mitigation of over voltages due to large scale solar penetrations. Finally, the influence of the DSTATCOM location and the dead band voltage of the PV inverter on the voltage profile of the Mauara feeder were analyzed.

Index Terms – Solar penetration, coordinated voltage control, IEEE 33 bus network, DSTATCOM

DEDICATION

To my parents, beloved wife and our daughter.

ACKNOWLEDGEMENT

First and foremost, I would like to express my sincere gratitude to my principal supervisor Dr. J. V. U. P. Jayatunga, Senior Lecturer from Electrical Engineering Department at University of Moratuwa, for the continuous support of my M.Sc. Study and research, for her motivation, enthusiasm, and enormous knowledge. Thanks also to my other supervisors Dr. D. P. Chandima, Senior Lecturer from Electrical Engineering Department at University of Moratuwa, and Dr. H. M. Wijekoon, Chief Engineer (Transmission Planning) from CEB for their guidance and continuous support throughout the study.

Second, I would like to thank the rest of the lecturers from Electrical Engineering Department at University of Moratuwa for their enthusiasm, encouragement and insightful comments, during the progress reviews.

Last but not the least, I would like to convey my sincere gratitude to my wife, parents and family members for their understanding, support in numerous ways to achieve my targets all the time.

M. K. D. Peiris

May 2019

TABLE OF CONTENTS

| | |
|------------------------------------------------------------|------|
| Declaration | i |
| Abstract | ii |
| Dedication | iii |
| Acknowledgement | iv |
| Table of Contents | v |
| List of Figures | viii |
| List of Tables | x |
| List of Abbreviations | xi |
| List of Appendices | xiii |
| 1. Introduction | 1 |
| 1.1 Background | 1 |
| 1.2 Problem Statement | 2 |
| 1.3 Objective | 3 |
| 1.4 Methodology | 4 |
| 1.5 Organization of the Thesis | 4 |
| 2. Problem Formulation with Large Scale Solar Penetration | 6 |
| 2.1 Overview | 6 |
| 2.2 Battle for Solar Energy Program | 7 |
| 2.3 Simulation Analysis | 8 |
| 2.3.1 Simulation 1: Embilipitiya GSS | 8 |
| 2.3.1.1 Study 1: Typical mid-day load condition | 10 |
| 2.3.1.2 Study 2: Minimum mid-day load condition | 11 |
| 2.3.2 Simulation 2: Anuradhapura GSS | 13 |
| 2.4 Conclusion | 15 |
| 3. Literature Review | 17 |
| 3.1 Overview | 17 |
| 3.2 Voltage Variations due to Distributed Energy Resources | 17 |
| 3.3 Conventional Over Voltage Control Techniques | 19 |
| 3.3.1 On-load tap changer transformer | 19 |

| | | |
|-------|--------------------------------------------------------------------|----|
| 3.3.2 | Capacitor bank | 19 |
| 3.3.3 | Voltage regulator | 20 |
| 3.3.4 | Static VAR compensator | 20 |
| 3.3.5 | Dynamic Voltage Restorer (DVR) | 21 |
| 3.3.6 | DSTATCOM | 21 |
| 3.4 | Control Structures | 23 |
| 3.4.1 | Local Control | 23 |
| 3.4.2 | Decentralized Coordinated Control | 24 |
| 3.4.3 | Centralized Control | 24 |
| 3.5 | Conclusion | 25 |
| 4. | Development of Dynamic Voltage Control Mechanism using DSTATCOM | 26 |
| 4.1 | Overview | 26 |
| 4.2 | Mathematical Modeling of DSTATCOM | 30 |
| 4.3 | DIgSILENT PowerFactory Modeling | 34 |
| 4.3.1 | IEEE 33 Bus Distribution Network Model | 34 |
| 4.3.2 | DSTATCOM Model | 37 |
| 4.3.3 | Discussion | 41 |
| 4.4 | Development of Modified DSTATCOM Model | 43 |
| 4.4.1 | Introduction | 43 |
| 4.4.2 | Local Controllable Zones | 43 |
| 4.4.3 | Discussion | 47 |
| 5. | Voltage Control Co-ordination between Solar PV Inverter & DSTATCOM | 49 |
| 5.1 | Overview | 49 |
| 5.2 | Voltage-Reactive Power (Volt-Var) | 51 |
| 5.3 | Co-ordination between DSTATCOM and DER | 52 |
| 5.4 | Simulation | 54 |
| 5.5 | Discussion | 56 |
| 6. | Voltage Management in Embilipitiya GSS with Proposed Solar Farms | 57 |

| | | |
|-------|---------------------------------------------------------------|----|
| 6.1 | Overview | 57 |
| 6.2 | Adoption of Coordinated Voltage Control Mechanism | 57 |
| 6.2.1 | Typical mid-day load condition | 58 |
| 6.2.2 | Minimum mid-day load condition | 61 |
| 6.3 | Influence of DSTATCOM Location on Voltage Profile | 63 |
| 6.4 | Influence of Dead Band Voltage of Solar PV on Voltage Profile | 64 |
| 6.5 | Conclusion | 66 |
| 7. | Conclusions and Recommendations | 67 |
| 7.1 | General Conclusions | 67 |
| 7.2 | Research Findings | 68 |
| 7.3 | Suggestions for Future Work | 69 |
| | References | 70 |
| | Appendices | 74 |

LIST OF FIGURES

| | Page | |
|------------|-------------------------------------------------------------------------------------------------------|----|
| Figure 1.1 | Solar PV global capacity and annual additions, 2007-2017 | 1 |
| Figure 1.2 | Sri Lanka 2050 electricity generation mix: 100 percent RE | 2 |
| Figure 2.1 | Mauara Feeder model with 6 nos. of solar farms | 9 |
| Figure 2.2 | Voltage variation along Mauara Feeder (Typical mid-day load condition) | 10 |
| Figure 2.3 | Simulation results of voltage variation along the Mauara feeder in SynerGi simulation platform | 11 |
| Figure 2.4 | Voltage variation along the Mauara Feeder (Minimum mid-day load condition) | 12 |
| Figure 2.5 | Simulation results of voltage variation along the Mauara feeder in SynerGi simulation platform | 12 |
| Figure 2.6 | AOld-Vavuniya feeder model with 4 nos. of solar farms | 14 |
| Figure 2.7 | Voltage variation along the AOld-Vavuniya Feeder | 14 |
| Figure 2.8 | Simulation results of voltage variation along the AOld-Vavuniya feeder in SynerGi simulation platform | 15 |
| Figure 2.9 | Voltage comparison of typical & minimum mid-day load conditions of Mauara feeder | 16 |
| Figure 3.1 | A simple radial distribution network with DG | 18 |
| Figure 3.2 | Typical SVC configuration | 20 |
| Figure 3.3 | Typical DVR configuration | 21 |
| Figure 3.4 | Typical DSTATCOM configuration | 22 |
| Figure 3.5 | Differentiation between centralized, decentralized & local control structures | 23 |
| Figure 4.1 | Configuration of DSTATCOM | 27 |
| Figure 4.2 | Terminal characteristics of DSTATCOM | 28 |
| Figure 4.3 | Basic vector diagrams of DSTATCOM | 28 |
| Figure 4.4 | Block diagram of the DSTATCOM | 30 |
| Figure 4.5 | DSTATCOM control block diagram | 32 |
| Figure 4.6 | Single Line Diagram of IEEE 33Bus Network | 35 |
| Figure 4.7 | IEEE 33 Bus Voltage Profile | 37 |
| Figure 4.8 | Single line diagram of test system with DSTATCOM | 38 |

| | | |
|-------------|---------------------------------------------------------------------------|----|
| Figure 4.9 | DSTATCOM control frame | 39 |
| Figure 4.10 | DSTATCOM control block diagram | 39 |
| Figure 4.11 | Single Line Diagram of DSTATCOM connected to 33 rd bus | 40 |
| Figure 4.12 | IEEE 33 Bus Voltage Profile with DSTATCOM | 41 |
| Figure 4.13 | Comparison of voltage variation due to DSTATCOM | 42 |
| Figure 4.14 | Change of voltage due to DSTATCOM at 33rd bus | 42 |
| Figure 4.15 | LCZ concept adaption for a distribution network | 43 |
| Figure 4.16 | LCZ representation of the test system with DSTATCOM | 45 |
| Figure 4.17 | Control frame diagram of modified DSTATCOM model | 46 |
| Figure 4.18 | Control block diagram of modified DSTATCOM model | 46 |
| Figure 4.19 | Comparison of voltage variation due to typical & modified DSTATCOM | 47 |
| Figure 4.20 | Voltage change due to typical & modified DSTATCOM | 48 |
| Figure 5.1 | Voltage-Reactive power characteristic | 51 |
| Figure 5.2 | Representation of voltage magnitudes | 52 |
| Figure 5.3 | Flow Diagram of the co-ordination between DSTATCOM and DER | 53 |
| Figure 5.4 | Network configuration of coordinated voltage control | 55 |
| Figure 5.5 | Comparison of bus voltages of the test system | 55 |
| Figure 6.1 | Comparison of Mauara feeder voltages under different simulation platforms | 58 |
| Figure 6.2 | Identification of LCZ consists of solar PV and DSTATCOM | 59 |
| Figure 6.3 | Voltage profile of 06 locations under TLC | 59 |
| Figure 6.4 | Complete voltage profile variation of Mauara feeder | 60 |
| Figure 6.5 | Comparison of Mauara feeder voltages under different simulation platforms | 61 |
| Figure 6.6 | Voltage profile of 06 locations under MLC | 62 |
| Figure 6.7 | Identification of LCZs of DSTATCOMs | 63 |
| Figure 6.8 | Mauara feeder voltage against DSTATCOM location | 64 |
| Figure 6.9 | Reactive power absorption vs dead band voltage of DER | 65 |

LIST OF TABLES

| | | Page |
|-----------|-------------------------------------------------------------------------------------|------|
| Table 2.1 | Identified large scale solar PV locations under the battle for solar energy program | 7 |
| Table 2.2 | Summary of the simulation scenarios Mauara feeder | 8 |
| Table 2.3 | Summary of the simulation scenarios Vavuniya feeder | 13 |
| Table 4.1 | Functionality of modules of DSTATCOM control block | 32 |
| Table 4.2 | IEEE 33 Bus Network Data | 36 |
| Table 4.3 | Parameters of the DSTATCOM model | 40 |
| Table 4.4 | Summary of the IEEE 33 bus network under three cases | 48 |
| Table 5.1 | Differentiation of control modes | 49 |
| Table 5.2 | Summary of the IEEE 33 bus network under coordinated control mode | 56 |
| Table 5.3 | Summary of the LCZ under coordinated control mode | 56 |
| Table 6.1 | Voltage summary of the 06 locations under TLC | 60 |
| Table 6.2 | Voltage summary of the 06 locations under MLC | 62 |
| Table 6.3 | Reactive power absorption vs dead band voltage | 65 |
| Table 7.1 | Summary of the Mauara Feeder simulations | 68 |

LIST OF ABBREVIATIONS

| Abbreviation | Description |
|--------------|---------------------------------------------------|
| AC | Alternating current |
| CEB | Ceylon electricity board |
| CSD | Current synchronous detection |
| CSP | Concentrating solar thermal power |
| DC | Direct current |
| DER | Distributed energy resource |
| DG | Distributed generation |
| DMS | Distribution management system |
| DSL | DIgSILENT-PowerFactory simulation language |
| DSTATCOM | Distribution static compensator |
| DVR | Dynamic voltage restorer |
| EMD | Empirical decomposition |
| EPLL | Enhanced phase locked loop |
| FACTS | Flexible alternative current transmission system |
| GSS | Grid substation |
| GW | Giga watt |
| HV | High voltage |
| IEEE | Institute of Electrical and Electronics Engineers |
| IGBT | Insulated-gate bipolar transistor |
| IO | Input output |
| ISCT | Instantaneous symmetrical component theory |
| LCZ | Local controllable zone |
| LECO | Lanka Electricity Company (Pvt) Ltd |
| LV | Low voltage |
| MLC | Minimum mid-day load condition |
| MOSFET | Metal oxide semiconductor field effect transistor |
| MV | Medium voltage |

| | |
|--------|-------------------------------------------------------|
| MW | Mega watt |
| OLTC | On-load tap changer |
| PBT | Power balance theory |
| PCC | Point of common coupling |
| PI | Proportional integral |
| PLL | Phase locked loop |
| PV | Photovoltaic |
| PQ | Power quality |
| RE | Renewable energy |
| SLSEA | Sri Lanka sustainable energy authority |
| SRF | Synchronous reference frame |
| SVC | Static var compensator |
| TCR | Thyristor-controlled reactor |
| TLC | Typical mid-day load condition |
| TSC | Thyristor-switched capacitor |
| UDN | Utility distribution network |
| UNFCCC | United Nations Framework Convention on Climate Change |

LIST OF APPENDICES

| Appendix | Description | Page |
|----------|-----------------------------------------------------------------------------------------------------------------------------------------|------|
| A1 | Power Quality in Distribution Network | 74 |
| A2 | Overview of major FACTS devices | 75 |
| A3 | Summary of Power System Analysis Modelling Capability | 76 |
| A4 | Phase Locked Loop | 77 |
| A5 | Voltage-Reactive Power (Volt-Var) | 78 |
| A6 | Active Power-Reactive Power (Watt-Var) | 80 |
| A7 | Voltage-Active Power (Volt-Watt) | 81 |
| A8 | Records Generated for IEEE 33 Bus Network in DIgSILENT PowerFactory | 83 |
| A9 | Records Generated for IEEE 33 Bus Network with DSTATCOM in DIgSILENT PowerFactory | 86 |
| A10 | Records Generated for IEEE 33 Bus Network with Modified DSTATCOM in DIgSILENT PowerFactory | 89 |
| A11 | Records Generated for Coordinated Voltage Control between DSTATCOM & Solar PV of IEEE 33 Bus Network in DIgSILENT PowerFactory | 92 |
| A12 | Records Generated for Coordinated Voltage Control between DSTATCOM (@39 bus) & DER of Mauara Feeder in DIgSILENT PowerFactory under TLC | 95 |
| A13 | Records Generated for Coordinated Voltage Control between DSTATCOM (@52 bus) & DER of Mauara Feeder in DIgSILENT PowerFactory under MLC | 98 |
| A14 | Records Generated for Coordinated Voltage Control between DSTATCOM (@52 bus) & DER of Mauara Feeder in DIgSILENT PowerFactory under TLC | 101 |

CHAPTER 1

INTRODUCTION

1.1 Background

While considering the electricity generation, Renewable Energy (RE) sources have become highly prioritised due to the nature of free carbon dioxide emissions. Out of RE sources, solar PV is considered as the fast-growing RE source in the world, compared with the other RE sources; hydropower, wind power, bio-power, ocean, concentrating solar thermal power (CSP) & geothermal power [1].

The key factor for this attractiveness is the possibility of installing solar PV systems into distribution network via either LV side or MV side. Subsequently, electricity generation is being shifted from centralized to decentralized generation over the past decade.

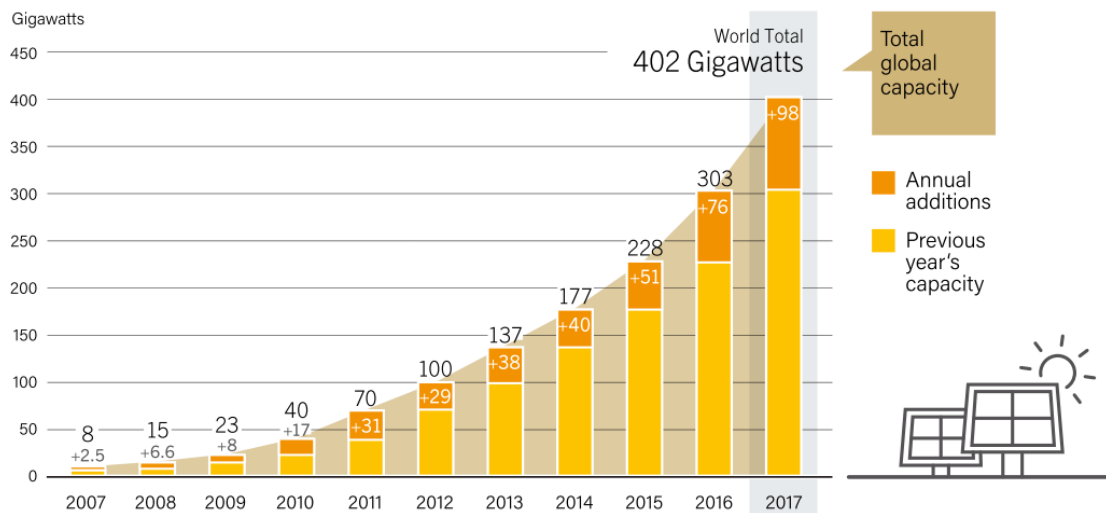


Figure 1.1: Solar PV global capacity and annual additions, 2007-2017

Source: Renewables 2018, Global Status Report (www.ren21.net)

The worldwide solar PV installed capacity has been climbed up from 8 GW in 2007 to 402 GW in 2017 within 10 years of duration. In addition, year 2017 was a remarkable year for solar PV industry as more solar PV capacity was added in 2017 than the net additions of coal, gas and nuclear combined.

At the 22nd United Nations Framework Convention on Climate Change (UNFCCC) Conference of Parties in Marrakech, Morocco, Sri Lanka pledged to use 100% Renewable Energy (RE) for electricity generation by 2050 [2].

According to the [2], the electricity generation mix of Sri Lanka by 2050 has been developed as in figure 3.1. Solar and wind play the key roles of RE generation where energy market for wind and solar tend to be amplified accordingly.

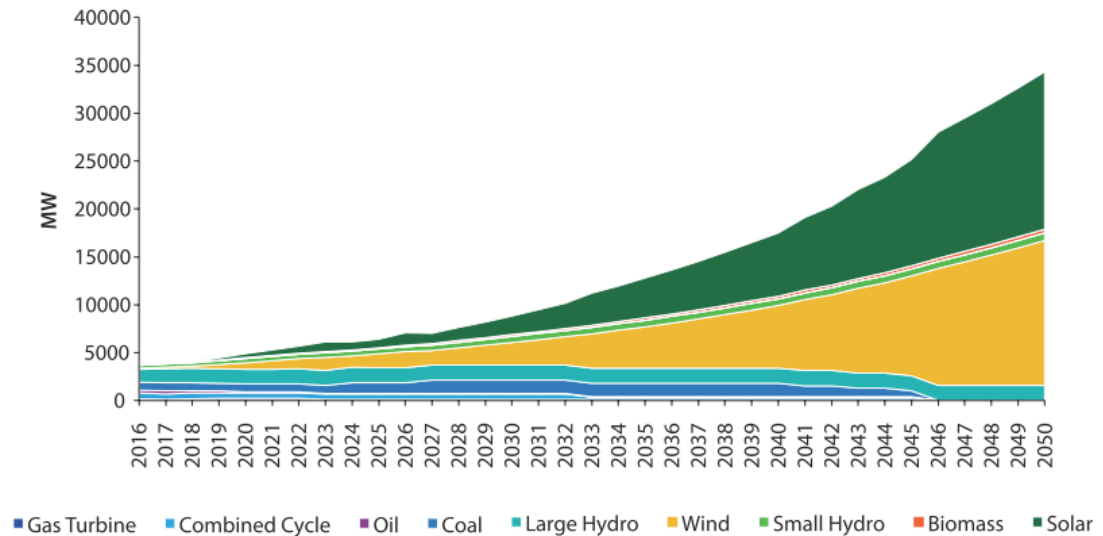


Figure 1.2. Sri Lanka 2050 electricity generation mix: 100 percent RE

Source: “100% ELECTRICITY GENERATION THROUGH RENEWABLE ENERGY BY 2050”, Assessment of Sri Lanka’s Power Sector, Co-publication of the Asian Development Bank and the United Nations Development Programme.

1.2 Problem Statement

Although solar PV systems can provide numerous paybacks to the network operation and environmental sustainability, it also carries significant challenges in terms of voltage quality disturbances with regards to PQ. The unreliable characteristics of intermittent solar PV can deteriorate the power system stability by introducing voltage regulatory problems and reverse power flow into transmission network from distribution network. At the network operator’s point of view, revenue patterns can be changed abruptly.

In fact, the voltage quality disturbances refer to the extensive subject contains voltage dips, over voltages, harmonics, unbalances and voltage fluctuations. Out of those

issues over voltages is the commonly experiencing PQ issue up to date. The degree of over voltages with regards to PQ, directly proportional to the amount of installed solar PV capacities in a particular feeder and the distance to the each solar PV capacity from feeder starting point. In general, for a radial distribution feeder without distribution generation (DG), maximum voltage persists at the feeder starting point which is considered as 1.0 pu, in which the voltage decreases towards the feeder end. More and more solar PV penetrates to the system and which exceeds the amount of feeder loading, the surplus power will be transferred towards the feeder starting point which is called back feeding. As a result of back feeding, maximum voltage point no longer exists at the feeder starting point, but a location where a solar PV is connected. Consequently, over voltages can be occurred at feeder ends against the addition of large scale solar PVs in to the distribution network.

With reference to the Sri Lankan context, over voltages are unavoidable due to the promotion of connecting 1 MW solar farms to Sri Lankan distribution network at MV level by CEB under the initiative of “Battle for Solar Energy” program.

Currently, PV Solar systems have been mostly connected at LV level and quiet large no. of studies have been performed to assess voltage quality impact at LV side. However, the necessity of performing studies to assess the voltage quality impact (i.e. feeder voltage profile change) in connection to the “Battle for Solar Energy” program, was emphasized. This thesis mainly investigates the changing of feeder voltage profile in MV networks due to increased solar PV penetration. Decentralized voltage control solutions and coordination among two decentralized controllers have been discussed to mitigate over voltage occurrences at MV level.

1.3 Objective

The main objective of this thesis is to develop a coordinated decentralized voltage control mechanism for MV networks with the large scale solar penetration. The coordination between two decentralized voltage controllers; reactive power control of solar PV inverter and DSTATCOM, to be implemented to enhance the PQ (i.e. voltage) of the MV distribution network.

1.4 Methodology

The research methodology used to mitigate the over voltages mainly performed based on Sri Lankan context. The complete Sri Lankan MV network has been modeled in SynerGi simulation platform by CEB Engineers and same existing models were used to simulate the large scale solar PV penetrations under the “Battle for Solar” program to justify the over voltage concerns. The key developments for voltage control mechanism are as follows.

1. Development of IEEE 33-bus radial distribution network in DIgSILENT PowerFactory simulation platform which includes DSTATCOM model to operate under voltage droop characteristics as the primary voltage control.
2. Development of solar PV inverter to operate under decentralized voltage control method; the reactive power control depend on the voltage, as the secondary voltage control.
3. Coordination between solar PV inverter and DSTATCOM to provide voltage support by splitting MV network into multiple controllable zones.
4. Adapt the developed control mechanism to Mauara feeder of the Embilipitiya GSS, Sri Lanka in order to mitigate over voltages and analyze the influences of DSTATCOM location and dead band voltage of primary voltage controller.

1.5 Organization of the Thesis

The thesis contains 7 chapters.

Chapter 2 refers the problem formulation related to the large-scale solar addition in to Sri Lankan distribution network. Though there are several PQ issues associated with the DG, over-voltage issues are only concerned in this thesis. Theoretical background behind the over-voltage occurrences are discussed and adopted in to Sri Lankan network. Mauara & Vavunia feeders were selected and simulated in Synergi

simulation platform in order to assess the impact of large-scale solar addition under the “Battle for Solar” program.

Chapter 3 refers the literature review of the existing over-voltage mitigating techniques. The differentiation between several control structures; local, decentralized & centralized, were identified and decentralized control structure was selected for the implementation in this thesis. Coordination between two voltage support devices; DSTATCOM and volt-var control of DG, was implemented in this study.

Chapter 4 refers the development of modified DSTATCOM model in DIgSILENT PowerFactory simulation platform in which, DSTATCOM is capable of actively monitor multiple bus bars of the distribution network. DSTATCOM modeling was incorporated with IEEE 33 bus distribution network where the test system is split in to multiple Local Controllable Zones (LCZ). Typical DSTATCOM model was implemented and then modified to monitor the voltage of each bus in the LCZ.

Chapter 5 refers the development of volt-var control of DG as the secondary voltage support and the coordination principle behind decentralized control structure. Coordination between modified DSTATCOM and the volt-var control of DG in test system were simulated and analyzed deeply.

Chapter 6 refers the adaption of developed control structure in to the Sri Lankan distribution network. Initially, Mauara feeder of the Embilipitiya Grid Substation (GSS) was modeled in DIgSILENT PowerFactory simulation platform and compared the results in chapter 2. Once the model is verified, the developed control structure in chapter 5 is introduced to the Mauara Feeder and results are analyzed.

Chapter 7 refers to the conclusions and recommendations.

CHAPTER 2

PROBLEM FORMULATION WITH LARGE SCALE SOLAR PENETRATION

2.1 Overview

The problems associated with solar penetration has been furthered with the introduction of distributed energy resources (DER) in terms of PQ. In simply, PQ refers to a vital measure of the power system which adheres to an ideal sinusoidal voltage and current waveform [3]. Power quality disturbances in distribution networks based on IEEE Std. 1159-2009 are mentioned in the appendix 1 (A1). The power produced by the DER is considered as absolutely sinusoidal in nature and the distortion of voltage and current waveforms from its original sinusoidal waveform occurs mainly due to the addition of active devices or loads to the transmission or distribution network [4].

Although, the phrase “large scale” is quite frequent in latest discussions related to RE industry, there is no precise definition as to what size constitutes. Generally, large scale solar PV systems differ from roof-mounted solar PV systems as they supply power at utility level, with a scale of at least 1 MW to multi-megawatt systems [5]. The capacity of roof-mounted systems determined by the extent of the roof concentrated to the load centers, however, large scale solar PV systems may be installed far away from load centers.

Several initiatives were taken by Ministry of Power & Renewable Energy to extract solar energy into Sri Lankan system. “Battle for Solar Energy” program launched in 2016 is the most successful project at present, which targeted to connect large scale (1 MW each) solar power plants into Sri Lankan distribution network via MV level. In addition, tenders have been initiated to construct 10MW solar farms at Vavunathivu & Polonnaruwa by CEB.

2.2 Battle for Solar Energy Program

Ministry of Power & Renewable Energy in collaboration with CEB, Sri Lanka Sustainable Energy Authority (SLSEA) and Lanka Electricity Company Pvt Ltd (LECO), launched a project called “Battle for Solar Energy” (Soorya Bala Sangramaya) expecting to achieve solar electricity generation of 200MW by 2020 and 1000MW by 2025 including large scale solar farms as well as rooftop solar [6].

As per the program, development of large scale solar farms was initiated in two phases. Under the Phase I, 36 nos of 1MW solar PV systems were awarded. Similarly, under the phase II, 90 nos. of 1MW solar PV systems to be awarded. The identified locations for the 1MW solar farms by CEB can be found in table 2.1.

Table 2.1. Identified large scale solar PV locations under the battle for solar energy program

| No | Grid Substation | Phase I | Phase II | Total |
|--------------|--------------------|-----------|-----------|------------|
| 1 | Anuradhapura | 3 | 4 | 7 |
| 2 | Habarana | - | 7 | 7 |
| 3 | Kilinochchi | 3 | - | 3 |
| 4 | Maho | 3 | 7 | 10 |
| 5 | Pannala | 1 | 5 | 6 |
| 6 | Polonnaruwa | 2 | - | 2 |
| 7 | Valachchenai (New) | 3 | 5 | 8 |
| 8 | Vavuniya | 3 | 5 | 8 |
| 9 | Horana | 3 | - | 3 |
| 10 | Panadura | 1 | - | 1 |
| 11 | Embilipitiya | 3 | 7 | 10 |
| 12 | Beliatta | 1 | 3 | 4 |
| 13 | Galle | - | 3 | 3 |
| 14 | Matara | - | 3 | 3 |
| 15 | Matugama | 1 | 3 | 4 |
| 16 | Ampara | 2 | 7 | 9 |
| 17 | Mahiyanganaya | 3 | 7 | 10 |
| 18 | Monaragala | 3 | 5 | 8 |
| 19 | Pallekele | 1 | 5 | 6 |
| 20 | Vavunathivu | - | 7 | 7 |
| 21 | Trincomalee | - | 7 | 7 |
| Total | | 36 | 90 | 126 |

2.3 Simulation Analysis

Higher the amount solar PV penetration, higher the impact of voltage variation occurs in the distribution line. As mentioned in 1.2, bi-directional power flow occurs from distribution network to transmission network when the solar PV penetration exceeds the feeder loading itself. Simply, this scenario occurs mostly in rural areas where day time loading at its minimum and the solar PV generates becomes maximum.

Two GSSs were selected for the analysis of large scale solar PV addition into Sri Lankan distribution network; Embilipitiya GSS & Anuradhapura GSS. The complete MV distribution network of Sri Lanka has been modeled in SynerGi simulation platform by CEB Engineers. Since, the validated models are available in CEB, Embilipitiya & Anuradhapura GSSs SynerGi models were obtained from CEB.

2.3.1 Simulation 1: Embilipitiya GSS

For the Embilipitiya GSS, there is a total of 10 nos. of 1MW solar PV systems to be connected. It was assumed that 6 nos. of solar farms to be connected to the Mauara feeder under phase I & II of battle for solar energy program (3 nos. each under phase I & II).

Details of the simulation feeder are as follows.

- Selected Feeder: Mauara Feeder
- Length: 85 km
- Simulation Year: 2020

Table 2.2. Summary of the simulation scenarios Mauara feeder

| | Solar Generation (MW) |
|------------|-----------------------|
| Base Case | 0 |
| Scenario 1 | 3 |
| Scenario 2 | 6 |

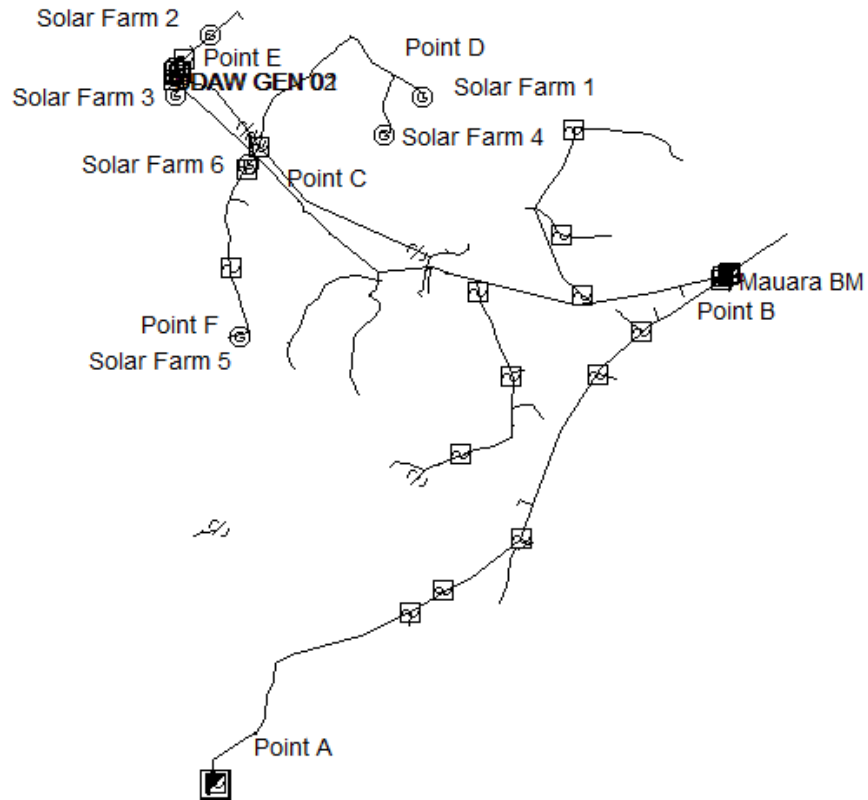


Figure 2.1. Mauara Feeder model with 6 nos. of solar farms

In distribution sector of CEB, there is no real time demand monitoring facility throughout the day. Therefore, maximum demand is considered during the night time of a particular day in March, which is considered as the hottest day of the year. Based on this maximum load, typical and worst case scenarios are developed by planning branches of distribution divisions.

The same concept was adopted to assess the impact of DER in this thesis. Two scenarios were considered related to Mauara feeder called typical mid-day load condition and minimum mid-day load condition (worst case).

Study 1: Typical mid-day load condition where demand is assumed as 35% of the maximum demand

Study 2: Minimum mid-day load condition (worst case) where demand is assumed as 20% of the maximum demand

2.3.1.1 Study 1: Typical mid-day load condition

As per the locations marked in figure 2.1, 6 nos. of solar farms were installed to Mauara feeder and voltages at 6 locations along the feeder were monitored. Feeder load prior connecting any DER is 1539kW and 820 kVar.

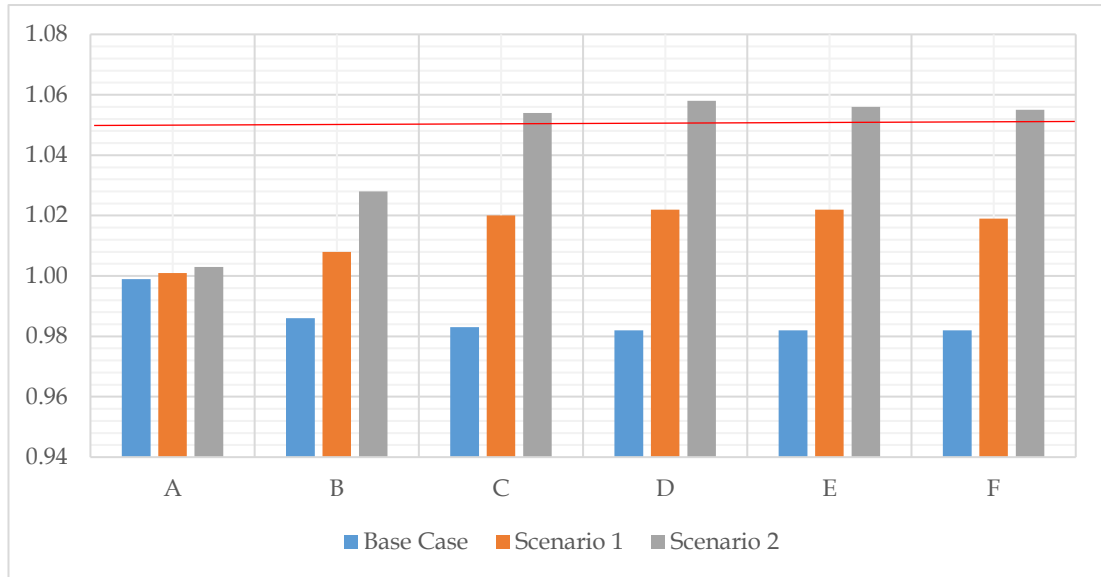


Figure 2.2. Voltage variation along the Mauara Feeder (Typical mid-day load condition)

According to the simulation results in figure 2.2, it was noted that the over voltages will be occurred with the connection of DER to the Mauara feeder.

The maximum voltages of 1.02 pu and 1.06 pu will be occurred at location point D under the scenario 1 & 2 respectively.

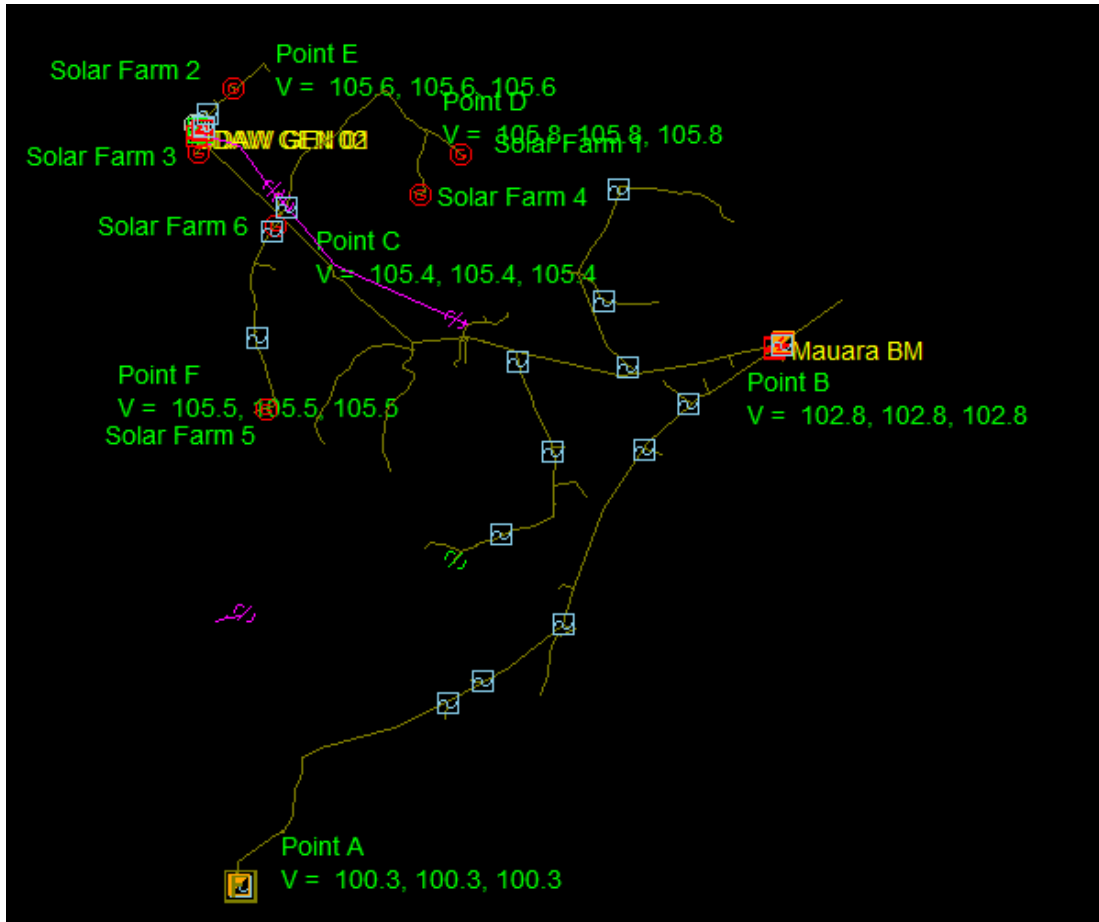


Figure 2.3. Simulation results of voltage variation along the Mauara feeder in SynerGi simulation platform

2.3.1.2 Study 2: Minimum mid-day load condition

As per the same locations used for the study 1, voltages along the feeder were monitored. Feeder load prior connecting any DER is 792 kW and 420 kVar.

According to the simulation results in figure 2.4, it was noted that the magnitudes of the over voltage at measuring locations have been increased compared to the study 1.

The maximum voltages of 1.03 pu and 1.07 pu will be occurred at location point D under the scenario 1 & 2 respectively.

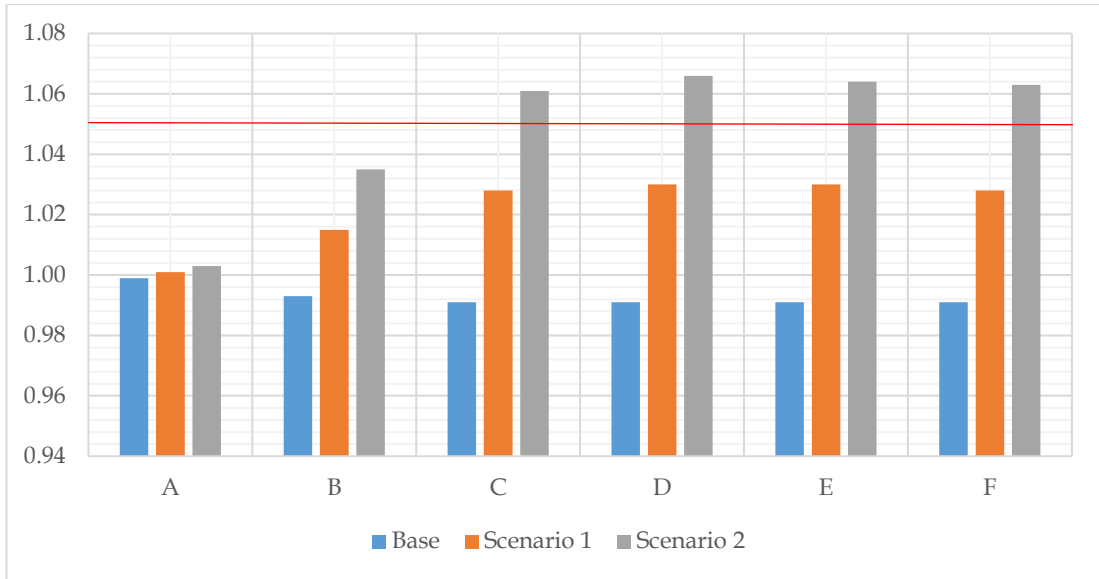


Figure 2.4. Voltage variation along the Mauara Feeder (Minimum mid-day load condition)

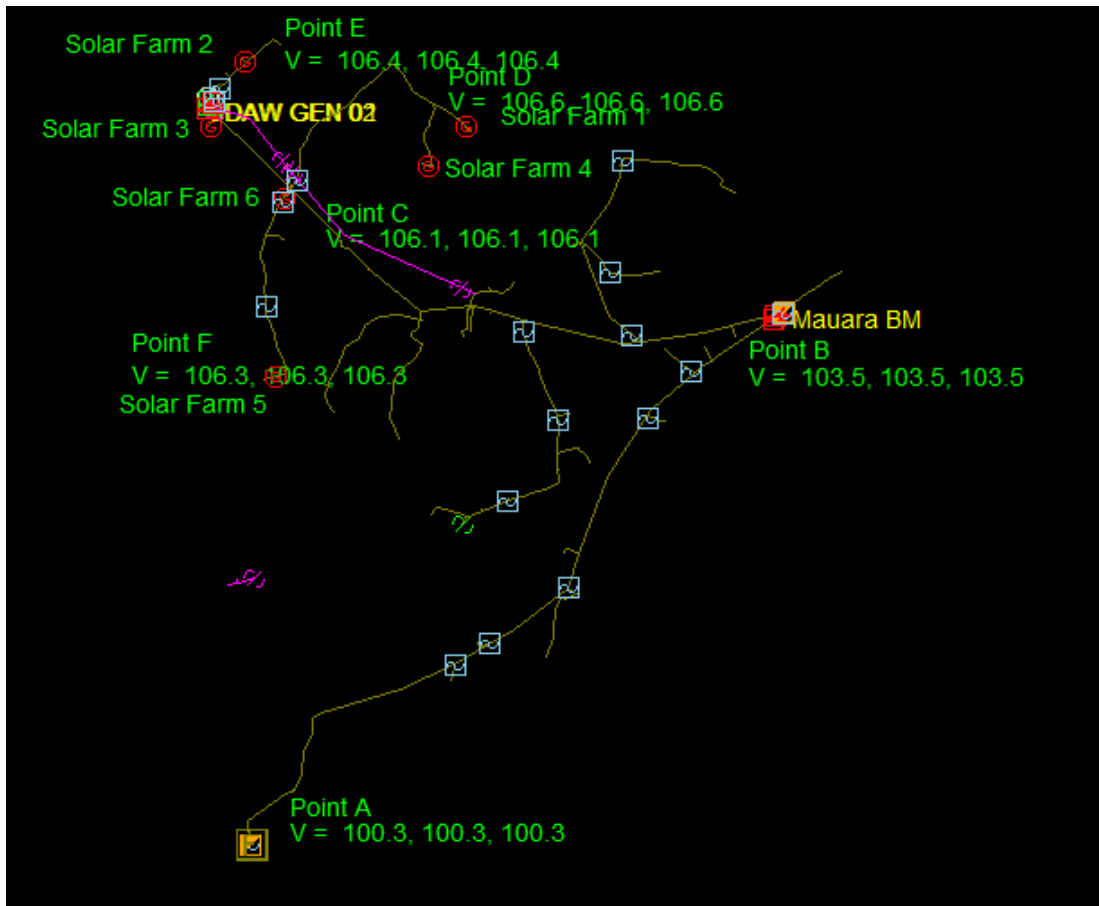


Figure 2.5. Simulation results of voltage variation along the Mauara feeder in SynerGi simulation platform

2.3.2 Simulation 2: Anuradhapura GSS

For the Anuradhapura GSS, there is a total of 7 nos. of 1MW solar PV systems to be connected. It was assumed that 4 nos. of solar farms to be connected to a particular feeder under phase I & II of battle for solar energy program (2 nos. each under phase I & II).

Details of the simulation are as follows.

- Selected Feeder: AOld-Vavuniya Feeder
- Length: 160 km
- Simulation Year: 2020

Table 2.3. Summary of the simulation scenarios Vavuniya feeder

| | Solar Generation (MW) |
|------------|-----------------------|
| Base Case | 0 |
| Scenario 1 | 2 |
| Scenario 2 | 4 |

Irrespective of the simulation performed to the Embilipitiya GSS, typical mid-day load condition was considered for the Anuradhapura GSS. It can be assumed that the problems associated with DER are persists on typical mid-day load condition, minimum mid-day load condition experiences the same problems with greater magnitudes.

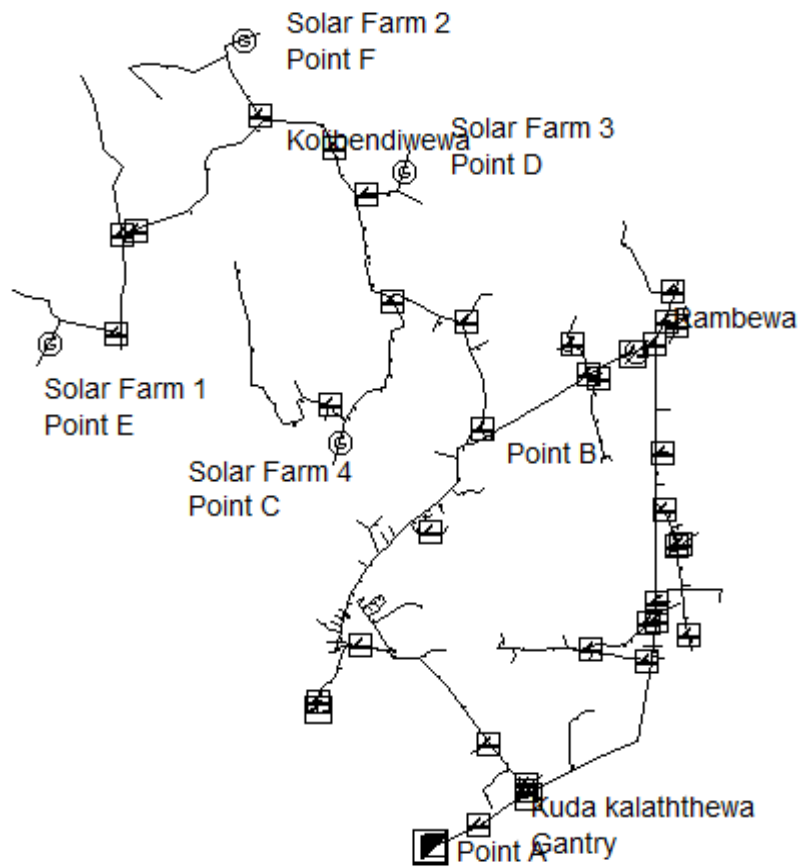


Figure 2.6. AOld-Vavuniya feeder model with 4 nos. of solar farms

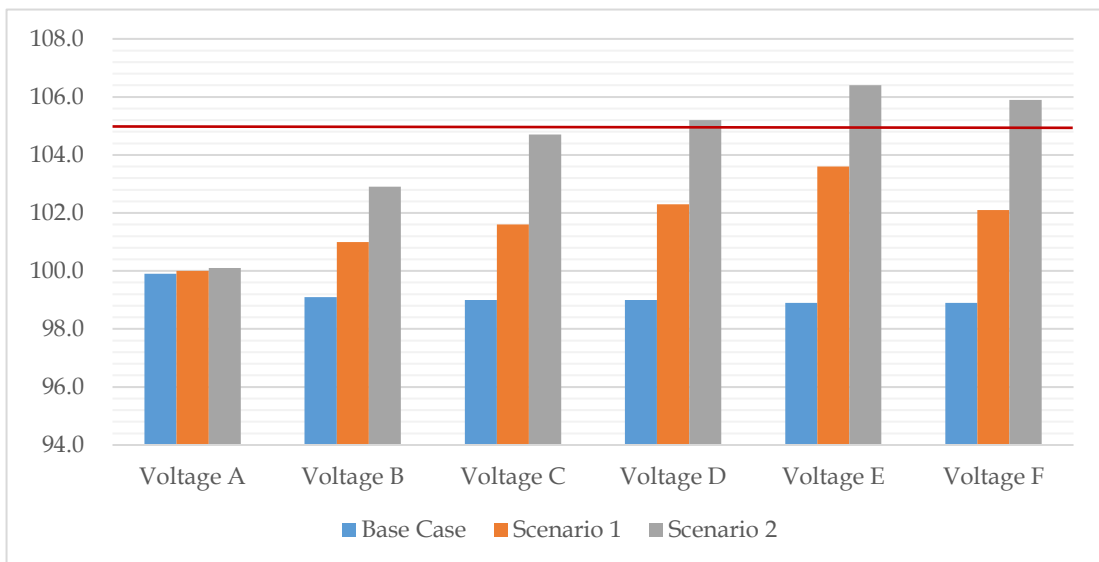


Figure 2.7. Voltage variation along the AOld-Vavuniya Feeder

According to the simulation results in figure 3.6, it was noted that the maximum voltages of 1.036 pu and 1.064 pu will be occurred at location point D under the scenario 1 & 2 respectively.

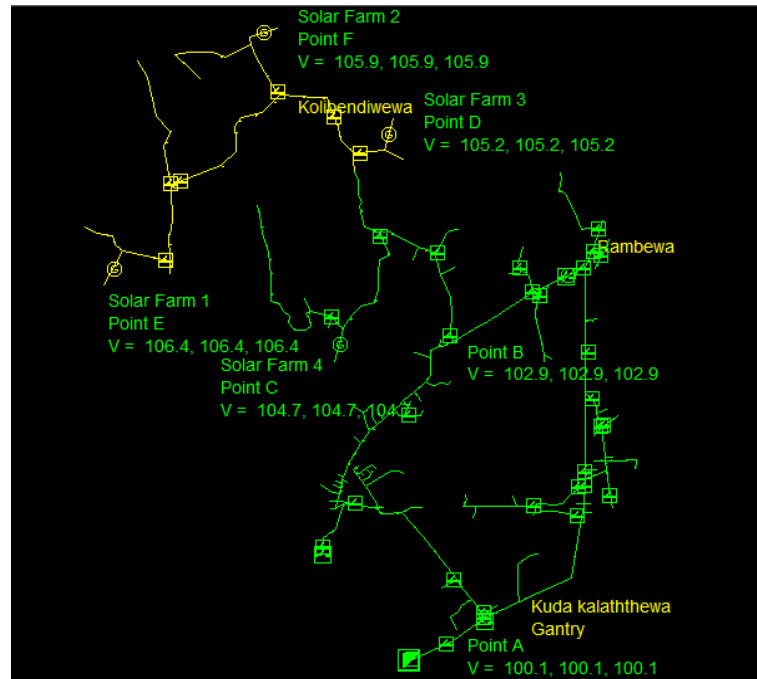


Figure 2.8. Simulation results of voltage variation along the AOld-Vavuniya feeder in SynerGi simulation platform

The voltages above 1.0500 pu after the simulation are marked in Yellow color as in figure 2.6 and 2.7. It was observed that the solar farms concentrated areas have been experienced heavy voltage violations.

2.4 Conclusion

In Sri Lankan context, solar farms connected to the distribution network shall operate within voltage range from 0.95pu to 1.05pu. If the distribution network voltage differs from the said voltage range, solar PV inverter automatically disconnects the solar PV penetration from the distribution network.

While performing studies with different load conditions it was observed that the feeder loading becomes minimum, the situation gets worse since the magnitude of the over voltage becomes substantial.

While connecting 6 nos. of DER to the Mauara feeder irrespective of the loading condition, over voltages sustain. As per the figure 2.9, maximum voltage at point D of the Mauara feeder during typical and minimum mid-day load conditions are 1.06 pu and 1.07 pu respectively.

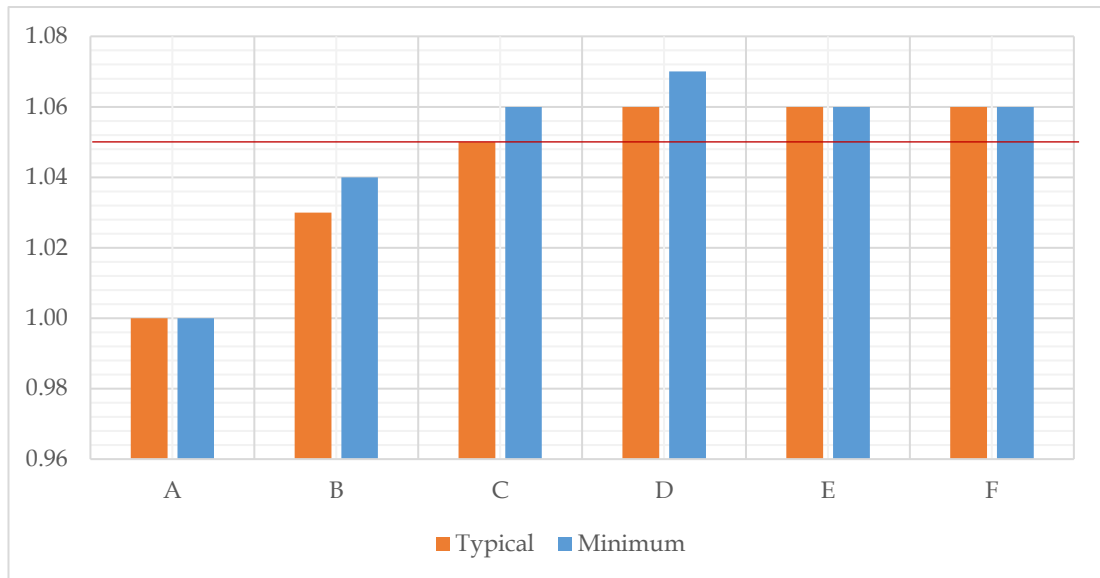


Figure 2.9. Voltage comparison of typical & minimum mid-day load conditions of Mauara feeder

The same over voltage issue persists on the AOld-Vavuniya feeder of the Anuradhapura GSS, as connecting 4 nos. of DER to the Mauara feeder irrespective of the loading condition, over voltages sustain.

Primary goal of the network operator is to harness the maximum amount of RE to the network which should not disrupt the system stability. In this thesis, coordinated voltage control mechanism has developed to mitigate over voltages (above 1.05) and the analysis of the control mechanism is intensely discussed in forthcoming chapters.

CHAPTER 3

LITERATURE REVIEW

3.1 Overview

Apart from the conventional power plants fueled by coal, hydro or gas, latest technology has diversified the grid to accommodate DER into distribution network and allowing bi-directional power flows. PQ issues in relation to DERs either in micro scale or large scale are uncommon. The requirements related to the performance, operation, testing, safety considerations, and maintenance of the interconnection are explained in the standard IEEE 1547-2018 [7].

In addition to the environmental sustainability of the large scale solar PV systems, it also introduces significant challenges in terms of PQ such as voltage variations, voltage fluctuations & flicker, voltage imbalance, harmonic distortions, direct current injection [8]. Summary of power quality disturbances of a power system is mentioned in appendix A.

This report only focuses on voltage variations due to large scale solar PV systems and propose coordinated voltage control mechanism to enhance the power quality.

3.2 Voltage Variations due to Distributed Energy Resources

The traditional distribution networks allowed one directional power flow, from the substation to the consumer loads, without DER. However, the injection of real power to the distribution networks by DER affected the bi-directional power flow as well as the change of voltage levels within the network.

The change of voltage level of the network due to DER with the injection of real and reactive power can be explained using Figure 3.1 as follows.

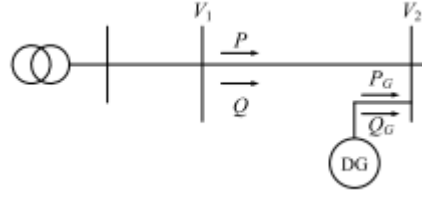


Figure 3.1. A simple radial distribution network with DG

Without DER, the voltage drop between buses 1 & 2 can be written as in (3.1)

$$\Delta V = V_1 - V_2 = \frac{PR + QX}{V_2} \quad (3.1)$$

Where P & Q are the real and reactive power injected from the bus 1 respectively. R & X are the resistance and the reactance between buses 1 & 2 respectively. In per unit, voltage of the bus 2 (V_2) can be assumed as 1.0 p.u., thus, 3.1 can be rewritten as:

$$\Delta V = V_1 - V_2 = PR + QX \quad (3.2)$$

If the case that a DER is connected at bus 2, which injects real and reactive power into the system, P_G and Q_G respectively, then 2.2 can be written as:

$$\Delta V = V_1 - V_2 = (P - P_G)R + (Q - Q_G)X \quad (3.3)$$

It is found that the injection of both real and reactive power from the DER may reduce the terms $(P - P_G)$ and $(Q - Q_G)$, thus the term ΔV decreases. In other words, voltage at the DER bus (bus 2) will increase when DER is supplying power into the distribution network. While considering solar PV systems as DER, they mostly operates at unity power factor providing only the real power. The voltage change in such situations will occur only due to the real power injection which is very significant in MV level, due to the fact that having higher R/X ratios in overhead distribution networks [9].

The voltage rise at the DER bus can be reduced, if the reduction of term $(P - P_G)$ can be compensated by the term $(Q - Q_G)$. In other words, if the DER is injecting real power

into the system and it is capable of absorbing reactive power from the system, the voltage rise can be reduced [10].

The method of absorbing reactive power by solar PV inverter is further discussed in this report to mitigate voltage rises.

3.3 Conventional Over Voltage Control Techniques

There are several conventional voltage regulatory techniques used across the world at MV level. With the advancement of power electronics, modern custom power devices capable of supporting static and dynamic voltage control.

3.3.1 On-load Tap Changer Transformer

The on-load tap changer (OLTC) is a device committed to a transformer for the purpose of regulating of the secondary side of the transformer which is considered as one of the very old techniques used to regulate the voltage level. The same concept can be applied for either power transformers or substation transformers depending on the voltage to be regulated [11]. The main disadvantage of this system is, all the feeders connected to the transformer will be effected by the OLTC operation irrespective of the feeders with DER.

The challenge is to set the optimal tap position of the OLTC safeguarding that the voltage level of each and every feeder connected to the transformer within the allowed voltage level.

3.3.2 Capacitor Bank

The capacitor bank is another common technique used to regulate the voltage of the distribution network. Generally, capacitor bank is a set of shunt capacitors connected to a particular distribution location in order to supply reactive power to the network, hence, voltage control or power factor correction is achieved [12].

3.3.3 Voltage Regulator

The voltage regulator is a kind of OLTC transformer which is typically installed in very long radial distribution networks for the purpose of mitigating under voltages at the feeder end by adjusting its tap position. The radial network is divided into two sections under the voltage regulator, in which provides voltage support for the latter section omitting excessive voltage drops [13].

3.3.4 Static VAR Compensator

The Static VAR Compensator (SVC) is a member of Flexible Alternating Current Transmission System (FACTS) family, which comprises of electrical devices aimed to provide fast acting reactive power compensation into the network [14]. The SVC is generally designed using fixed capacitors in parallel with a thyristor-controlled reactor (TCR), or a TCR in parallel with a thyristor-switched capacitor (TSC).

When the power system is operating under leading power factor (capacitive load), the SVC uses TCR to consume VARs from the system, hence, the system voltage is lowered. Similarly, under lagging power factor (inductive load), the capacitor banks are automatically switched in, thus the system voltage is increased.

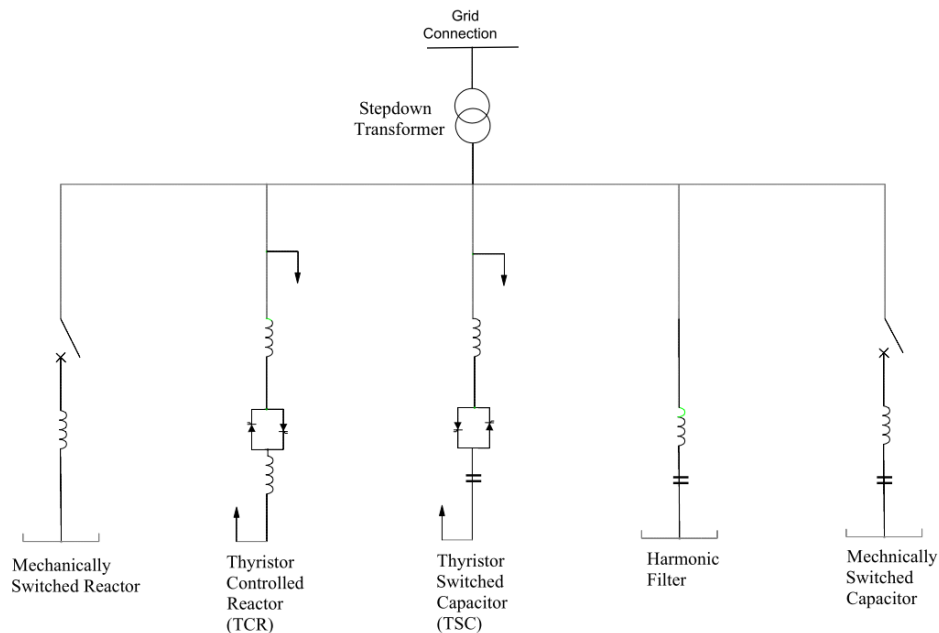


Figure 3.2. Typical SVC configuration

The very fast acting response to changes in the system voltage is the core advantage of SVCs compared with typical mechanically switched compensation schemes. In addition to the instantaneous response, SVCs are quite famous as it's cheaper, higher capacity, faster and more reliable device than dynamic compensation schemes.

When SVCs are utilized in industrial applications, they are placed near sudden varying loads, i.e. arc furnaces, as they are capable of smoothing flicker voltage [15].

3.3.5 Dynamic Voltage Restorer (DVR)

The dynamic voltage restorer (DVR), is a member of a FACTS devices family connected in series to the network which behaves as a voltage source [16]. This mode of connection capable of direct injection of voltage into the distribution network and regulate voltage as required. The configuration of a typical DVR is shown in figure 2.2.

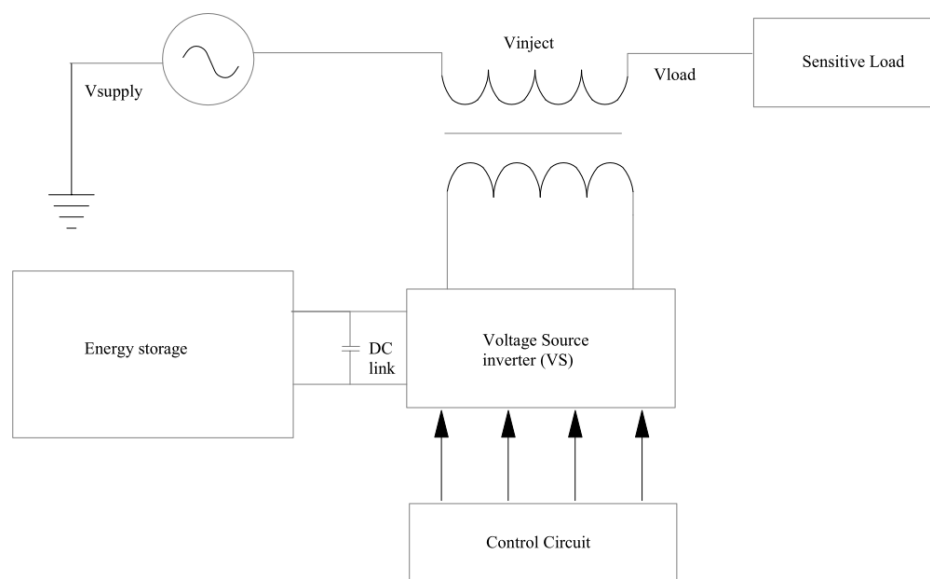


Figure 3.3. Typical DVR configuration

3.3.6 DSTATCOM

A Distribution static compensator (DSTATCOM), is the adaptation of STATCOM used in the distribution network, connected in parallel to the network which provides

a complete solution for reactive power compensation and voltage regulation. DSTATCOM comprises of three main components: coupling transformer/inductor, voltage source converter (VSC), DC energy storage, as shown in Figure 2.3.

The VSC of the DSTATCOM is based on power electronics and can be act as either a sink or a source to the reactive power of a distribution network. DSTATCOM is smaller in size, have better dynamic performance over the other FACTS devices [17].

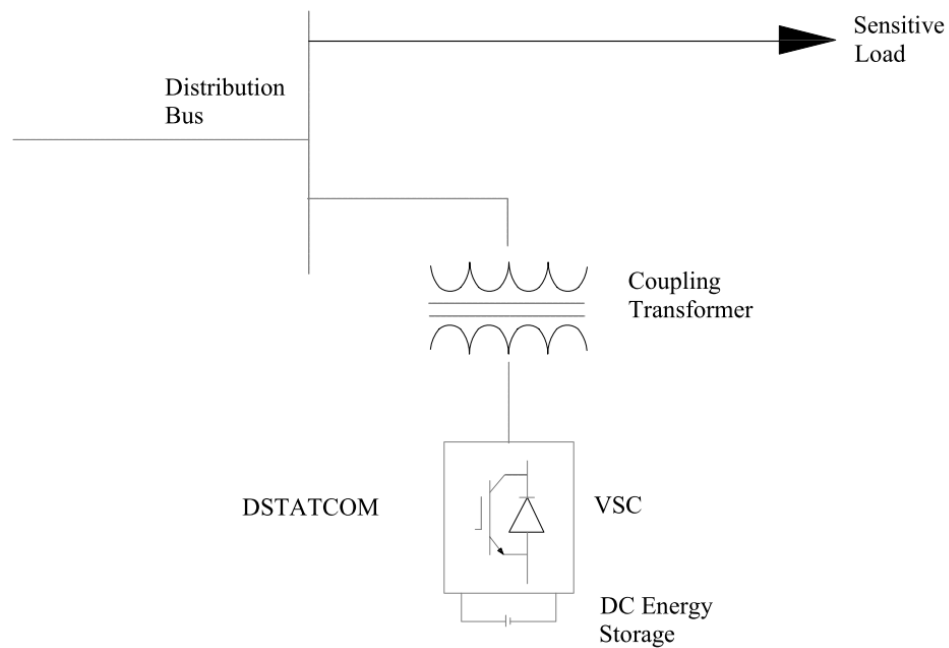


Figure 3.4. Typical DSTATCOM configuration

The Overview of major FACTS devices and their characteristic comparison can be found in appendix A2.

Typical DSATCOM monitors only the voltage at point of common coupling (PCC) and compensate reactive power accordingly as per the droop control characteristics defined in controller. However, in this thesis an advanced DSTATCOM model is developed in DIgSILENT PowerFactory simulation platform to monitor several buses of the distribution network and provide reactive power accordingly.

The performance of the developed DSTATCOM model as the primary voltage support, is deeply analyzed in chapter 4.

3.4 Control Structures

In addition to the control devices explained in 3.3, the control architectures have been developed from individual control device to few different control devices operate with a coordinated manner.

There are three control structures are defined as local control, decentralized control and centralized control in which basic dissimilarities are summarized in Figure 2.4 [18].

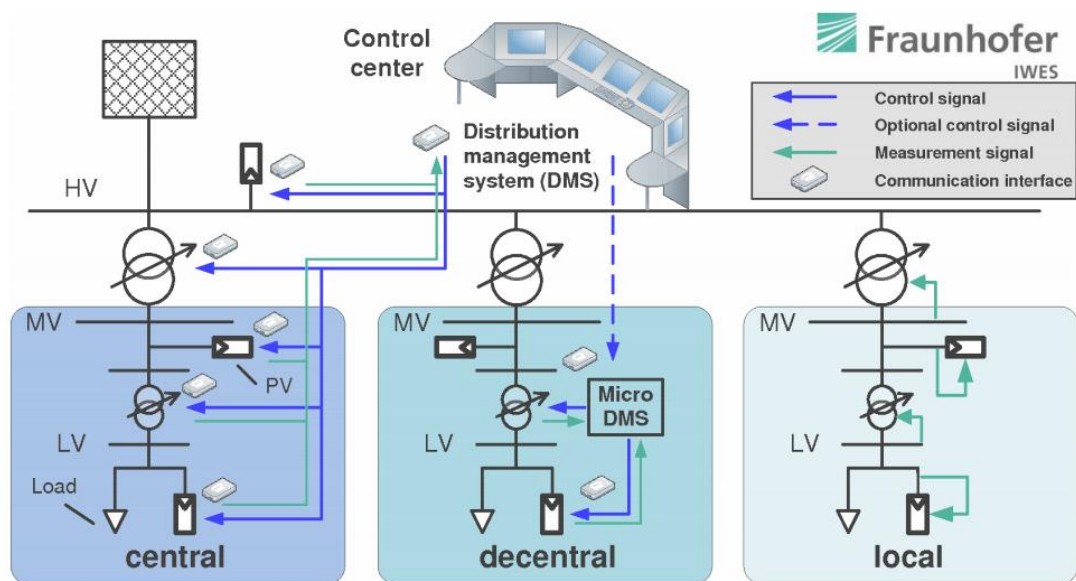


Figure 3.5. Differentiation between centralized, decentralized & local control structures
Source: Time in the sun, IEEE Power & Energy Magazine, vol. March/ April, 2013.

3.4.1 Local Control

Local control mechanism is considered as the elementary control structure, as it does not involve any kind of communication between voltage control devices of the distribution network. Stand-alone operation is performed within its control device, once the measurement values are recorded, processed and interpreted by the respective controlling entity itself.

Less complexity of the control action due to its own decision making facility and cheaper in cost due to its simple architecture are the key advantages of this mechanism compared with other control mechanisms.

3.4.2 Decentralized Coordinated Control

Decentralized coordinated control is generally achieved by linking two different control devices together and they are ranked according to their fast response and the amount of reactive power support. The device with highest amount of reactive power compensation availability shall operate first as the primary voltage support with complying the ranking order [19].

However, if the primary voltage control support is adequate enough to maintain the voltage limits within stipulated limits, rest of the control devices should remain idle. Similarly, when the primary voltage support is insufficient to maintain the voltage levels, secondary voltage support shall be delivered.

This is the famous among the three control mechanisms due to its effectiveness compared with the costs involved.

3.4.3 Centralized Control

The centralized control mechanism is the most advanced and complex control mechanism which collects the complete information from the whole network. Control decision is generated based on the data collected from the whole network and the control action is originated by the coordinator /centralized controller at the distribution management system (DMS).

The infrastructure development of this mechanism is challenging due to its complexity and fast communication links to be used to utilize its maximum benefit out of it. In Sri Lankan context, no developments have been initiated to incorporate DMS for distribution network.

3.5 Conclusion

Moreover to the voltage control devices explained in 3.3, concerns have been raised to compensate reactive power from DER as a local voltage control support. For instance, solar PV inverter, one of the DER type, shall have the facility to either absorb or inject reactive power into the distribution network monitoring the system voltage. At present, coordination between several control devices can be found across the globe to enhance the PQ of the distribution network: DER with SVC, DER with OLTC and OLTC with DSTATCOM [20].

Under this thesis, mainly targets to develop a coordinated decentralized control mechanism between the DSTATCOM and the solar PV inverter to mitigate voltage variations of the distribution network due to large scale solar farms. DSTATCOM is modeled to monitor several buses of the network and facilitate the reactive power accordingly. Solar PV inverter is modeled to operate under “reactive power control depend on the voltage” mode.

DSTATCOM operates as the primary voltage support device due to its fast acting and the higher amount of reactive power compensation feasibility. However, solar PV inverter acts as the secondary voltage support device due to its lesser amount of reactive power compensation feasibility compared to the DSTATCOM.

CHAPTER 4

DEVELOPMENT OF DYNAMIC VOLTAGE CONTROL MECHANISM USING DSTATCOM

4.1 Overview

The theory of the Flexible AC Transmission Systems (FACTS) was initially developed for transmission line network. However, over the last 15 years, it has been extended to improve the power quality not only in transmission line network but also distribution line network. DSTATCOM is a mature technology for the mitigation of the power quality problem such as poor power factor, poor voltage regulation, current harmonic and unbalanced current [21]. As explained in chapter 3.3.6, DSTATCOM is operated based on VSC which involves power electronic devices with turn-off capability i.e. IGBT and a capacitive energy storage facility.

DSTATCOMs are basically categorized in to three types based on its configuration.

1. Single-Phase Two-Wire
2. Three-Phase Three-Wire
3. Three-Phase Four-Wire

Single-phase two-wire configuration is used for low voltage applications which is not a famous configuration as nowadays most of the distribution systems are either three-phase three-wire or three-phase four-wire. In addition, the availability of neutral conductor defines the configuration between three-phase three-wire and three-phase four-wire distribution systems.

Single line diagram of DSTATCOM configuration is illustrated in figure 4.1. For voltage regulation, DSTATCOM regulates PCC voltage by either injecting (over-excited operation) or absorbing reactive power (under-excited operation) to the system through VSC.

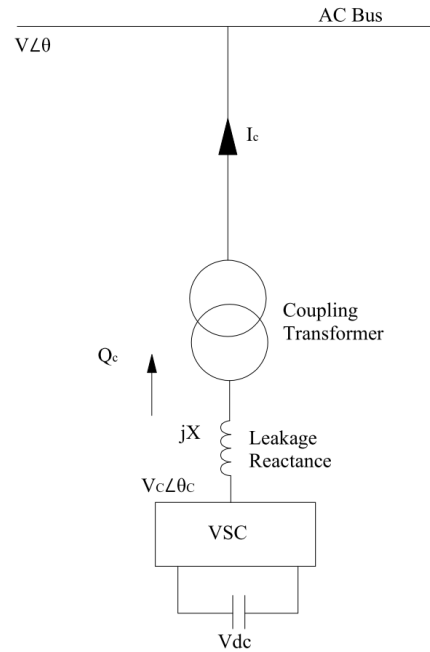


Figure 4.1 Configuration of DSTATCOM

During the steady state operation, the AC voltage generated by the VSC, V_c , is in phase with the system voltage V . Thereby, only the reactive power (Q_c) will flow within the DSTATCOM and the system where real power flow (P_c) becomes zero. The amount of reactive power flow (Q_c) is given in (4.1).

$$Q_c = \frac{V(V - V_c)}{X} \quad 4.1$$

When the system voltage is high, DSTATCOM absorbs reactive power and operates in induction mode. Similarly, DSTATCOM generates reactive power and injected in to the system in capacitive mode, when the system voltage becomes low. This is clearly understood by examining the terminal characteristics of the DSTATCOM and basic vector diagrams of DSTATCOM as shown in figure 4.2 and figure 4.3 respectively.

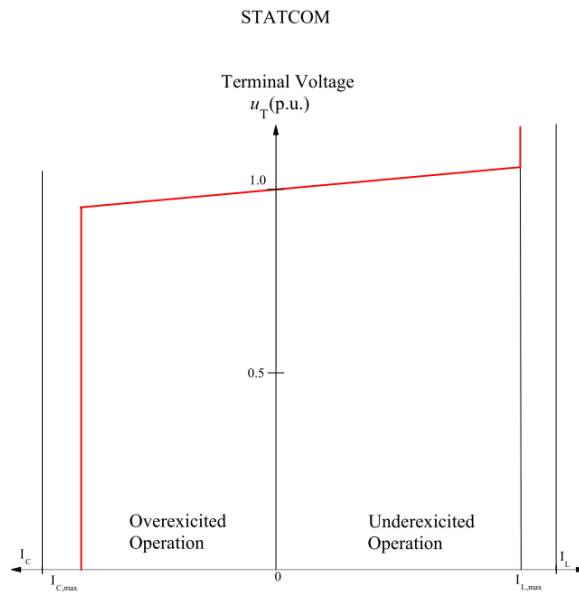


Figure 4.2 Terminal characteristics of DSTATCOM

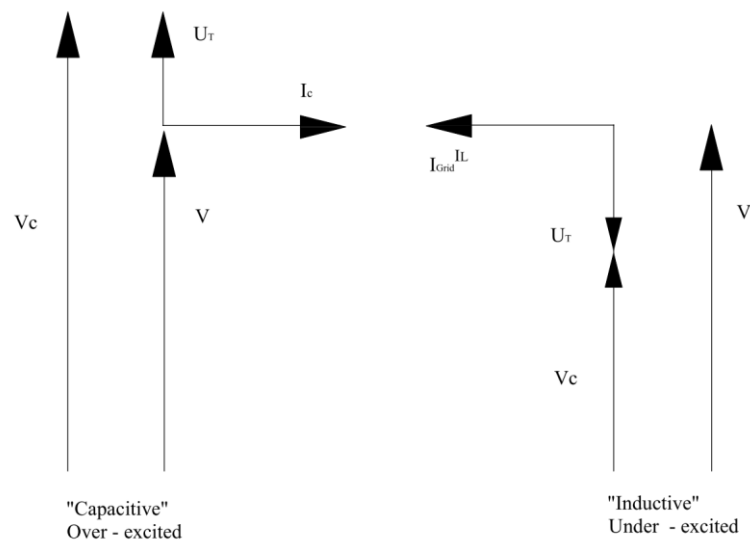


Figure 4.3 Basic vector diagrams of DSTATCOM

The primal objective of the control algorithm of the DSTATCOM is to estimate reference signals against the sensed signals. Accordingly, DSTATCOM sense the voltage of point of common coupling and derive switching signals of IGBT of the VSC based on the feedback signals.

The reference signals are estimated by means of following of control algorithms which are mainly divided in to time domain and the frequency domain control algorithms [22].

Time-domain control algorithms

1. Decoupled control of real and reactive power theory
2. Unit template technique or PI controller-based theory
3. Power balance theory (PBT)
4. $I \cos(\phi)$ control algorithm
5. Current synchronous detection (CSD) method
6. Instantaneous reactive power theory, also known as PQ theory or α - β theory
7. Synchronous reference frame (SRF) theory, also known as d-q theory
8. Instantaneous symmetrical component theory (ISCT)
9. Single-phase PQ theory
10. Single-phase DQ theory
11. Neural network theory (Widrow's LMS-based Adaline algorithm)
12. Enhanced phase locked loop (EPLL)-based control algorithm
13. Conductance-based control algorithm
14. Adaptive detecting control algorithm, also known as adaptive interference canceling theory

Frequency-domain control algorithms

1. Fourier series theory
2. Discrete Fourier transform theory
3. Fast Fourier transform theory
4. Recursive discrete Fourier transform theory
5. Kalman filter-based control algorithm
6. Wavelet transformation theory
7. Stockwell transformation (S-transform) theory
8. Empirical decomposition (EMD) transformation theory
9. Hilbert-Huang transformation theory

Out of aforementioned control algorithms, two control algorithms are commonly used for DSTATCOM modeling; Instantaneous reactive power theory (PQ theory or α - β theory) and SRF theory (d-q theory).

4.2 Mathematical Modeling of DSTATCOM

DSTATCOM is modeled by using DIgSILENT PowerFactory Simulation Language (DSL) related to this project. The size of the DSTATCOM is primarily decided by the parameters governed for the amount of reactive power compensated with the system. The decoupled active and reactive power control algorithm was used to model the DSTATCOM.

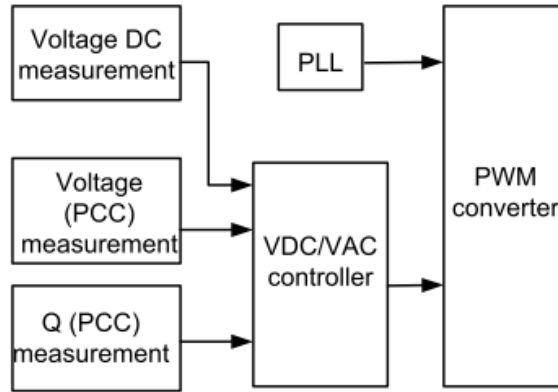


Figure 4.4 Block diagram of the DSTATCOM

The outputs of the DSTATCOM controller are i_{d_ref} and i_{q_ref} which are the reference currents in the d-q coordinate system. Those two parameters are to be calculated in order to assess the power injection by the DSTATCOM as in (4.2) and (4.3) [23].

$$P = V_i(i_d \cos \theta_i + i_q \sin \theta_i) = v_d i_d + v_q i_q \quad 4.2$$

$$Q = V_i(i_d \sin \theta_i + i_q \cos \theta_i) = -v_d i_q + v_q i_d \quad 4.3$$

Where;

V_i = Controller output voltage

i_d = Controller d-axis output current

i_q = Controller q-axis output current

θ = the phase angle

v_d = d-axis voltage

v_q = q-axis voltage

Considering a balanced three phase operation and taking the d-axis voltage vector v_d to match with the positive sequence voltage vector v , v_d and v_q can be simplified to (4.4) and (4.5).

$$v_d = |v_d| = |v| = v \quad 4.4$$

$$v_q = |v_q| = 0 \quad 4.5$$

Substituting (4.4) and (4.5) in to (4.2) and (4.3), active and reactive power injected to the distribution network can be rationalized to (4.6) and (4.7).

$$P = v_d i_d \quad 4.6$$

$$Q = -v_d i_q \quad 4.7$$

By controlling the i_d and i_q which are being the d and q components of the current injected to the distribution network, active and reactive power injected to the distribution network can be controlled independently. The controllable reactive power of DSTATCOM allows for a rapid control of bus voltage and power factor at point of common coupling as a fast-acting voltage supporting device.

The DSTATCOM control block diagram incorporating above equations is illustrated in figure 4.5.

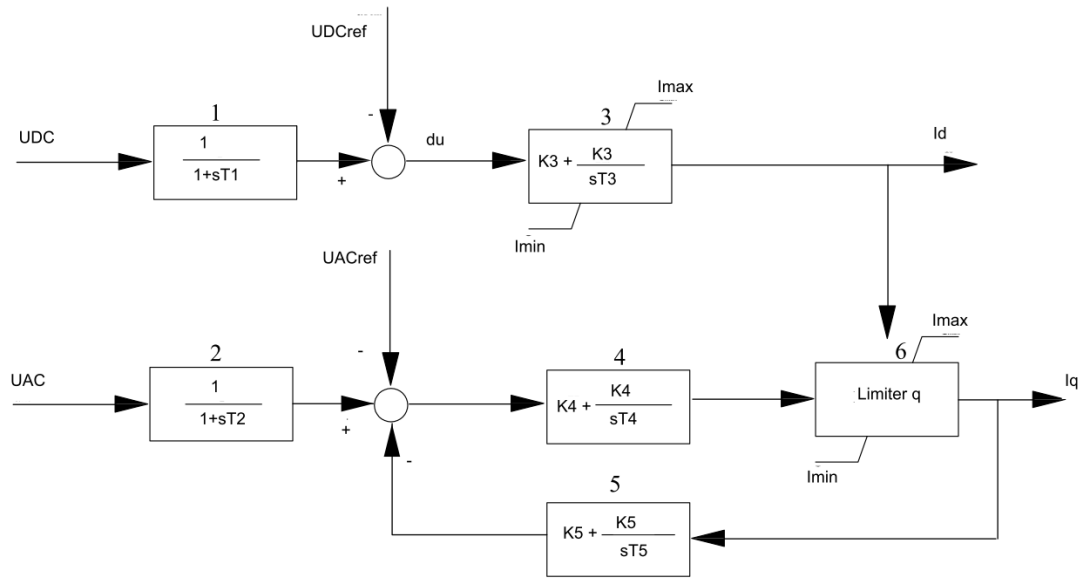


Figure 4.5 DSTATCOM control block diagram

Voltage measurement signals are introduced to the DSTATCOM control system at the point of connection of alternating voltage to the network (u_{AC}) and the voltage value in the DC circuit (u_{DC}), expressed in pu. The voltage values which are to be achieved in the system; AC (u_{ACref}) and DC (u_{DCref}), are set in the controller. Output signals in the controller are the current values in axes d (i_d) and q (i_q), expressed in pu.

Table 4.1 Functionality of modules of DSTATCOM control block

| Module No. | Function |
|------------|----------------------------------------------------------------------------------------------------------------------------------|
| 1 | Reflects the delay of voltage measuring signal of DC circuit (u_{DC}). |
| 2 | Reflects the delay of voltage measuring signal of AC circuit (u_{AC}). |
| 3 | Limits the inverter current component in d-axis (i_d), thereby the current does not exceed the limit value for the inverter. |

| | |
|---|-----------------------------------------------------------------------------------------------------------------------------------------------------|
| 4 | The same role as module 3, but in the AC circuit, and its output signal is not restricted inside it |
| 5 | Located in the feedback loop of the AC voltage control path and allows, among others, to introduce droop to the model. |
| 6 | Limits of the inverter current component in q-axis, depending on the current component value in d-axis and the limit current value in the inverter. |

While developing the typical DSTATCOM model, the ability to control the inverter in both d and q axis were concerned since, in DSTATCOM there is a need of controlling two voltages: the voltage on the capacitor in the DC circuit and the voltage at the PCC to compensate the reactive power in the MV network.

As per the figure 4.5, there are two voltage control paths in the control system. One path is in relation with the voltage control in the DC circuit, whereas the other one in relation with the AC circuit. Voltage control of the DC circuit is associated with the active power consumption from the power system, thus, the inverter shall be able to control the active current component in the inverter.

Voltage control at the point of connection to the power system is associated with the reactive power compensation between the power system and DSTATCOM. Therefore, the inverter shall be able to control the reactive current component in the inverter.

The value of the inverter current comprises of the both active current component in d axis and the reactive current component in q axis. Thus a method of controlling both d and q axis currents has been used for development of the model called ‘decoupled control of real & reactive power’.

For the proper operation of DSTATCOM, capacitors should not be discharged in the DC circuit of the inverter. Therefore, the voltage control path in the DC circuit has been assumed as the primary path. Restrictions of component values of the inverter current in axis d and q have been introduced in the model since the value of the inverter

current is an important limitation in the compensator operation. Fundamentally, the restriction of the reactive current component reflects the active current component in such a way as to ensure that the limit value of the inverter current is not exceeded [24].

For effective control DSTATCOM shall be placed closed to the load bus since farther to the load bus impact of DSTATCOM control capability decreases which can be clearly understood by the sensitivity analysis shown in figure 4.14 in forthcoming chapter 4.3.3.

4.3 DIgSILENT PowerFactory Modeling

DIgSILENT PowerFactory simulation platform (2018 SP5 thesis license) which is considered as one of the most advanced simulation tools up to now is used to model the DSTATCOM. A comparison of several simulation platforms can be found in Appendix 3.

Accordingly, IEEE 33 bus distribution network is modeled in DIgSILENT Power Factory software and then DSTATCOM model is introduced thereto. The voltage improvement of IEEE 33 bus network due to the DSTATCOM model is discussed to end with the chapter 4.

4.3.1 IEEE 33 Bus Distribution Network Model

IEEE 33 bus distribution network represents a single line diagram of the 12.66kV, 33-bus test radial distribution system which is shown in figure 4.6. It has one feeder with four different laterals, 32 branches and a total peak load of 3715kW and 2300kVar. The initial statuses of all the sectionalizing switches (switches No. 1-32) are closed while all the tie switches (switch No.33-37) are open [25].

The dashed lines represent the tie lines (normally open). The system data including line parameters and load connections can be found in Table 4.2.

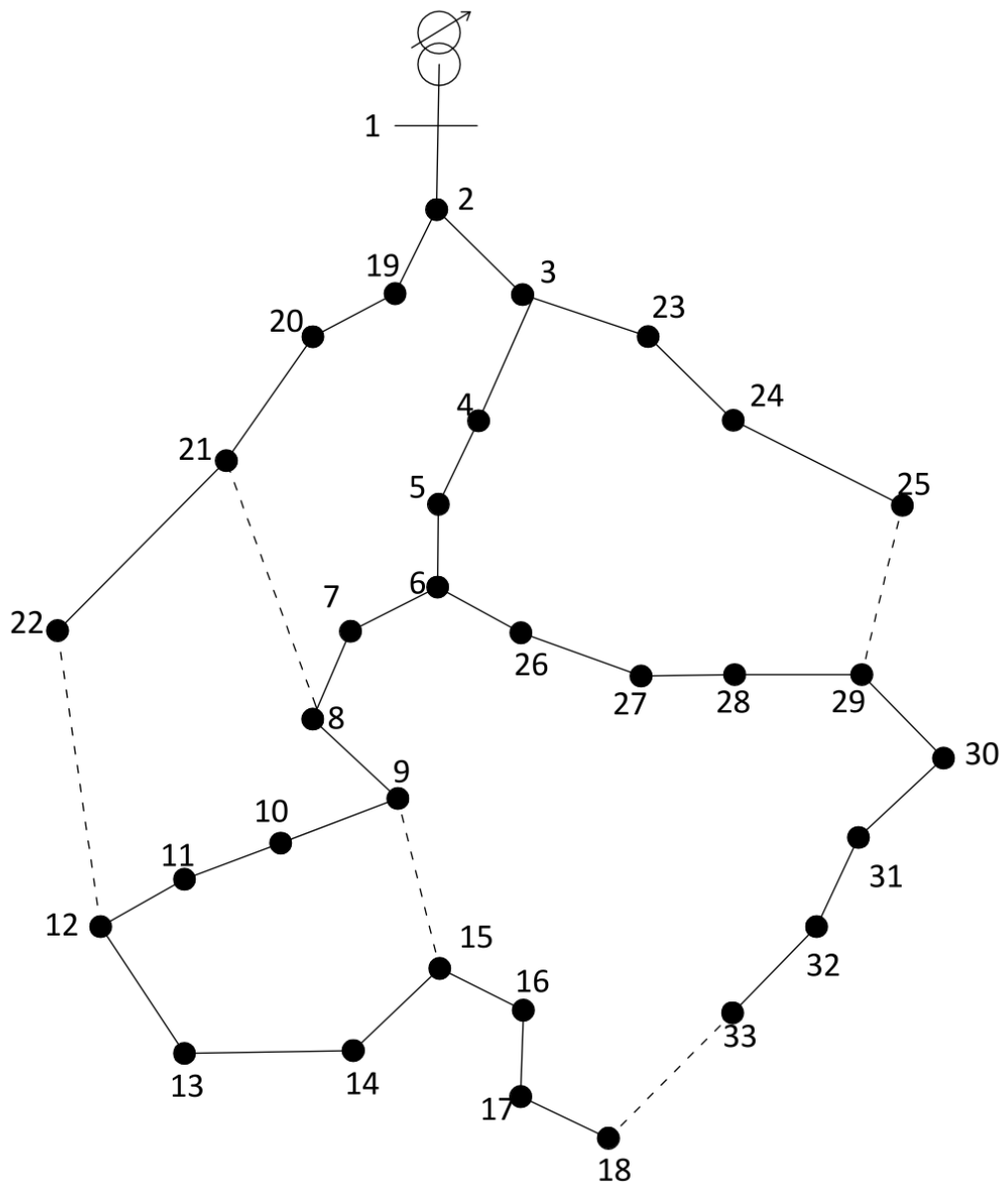


Figure 4.6 Single Line Diagram of IEEE 33Bus Network

Table 4.2: IEEE 33 Bus Network Data

| Line No. | From Bus | To Bus | Section Resistance (Ohm) | Section Reactance (Ohm) | End bus Real Load (kW) | End bus Reactive Load (kVar) |
|----------|----------|--------|--------------------------|-------------------------|------------------------|------------------------------|
| 1 | 1 | 2 | 0.0922 | 0.0470 | 100.00 | 60.00 |
| 2 | 2 | 3 | 0.4930 | 0.2511 | 90.00 | 40.00 |
| 3 | 3 | 4 | 0.3660 | 0.1864 | 120.00 | 80.00 |
| 4 | 4 | 5 | 0.3811 | 0.1941 | 60.00 | 30.00 |
| 5 | 5 | 6 | 0.8190 | 0.7070 | 60.00 | 20.00 |
| 6 | 6 | 7 | 0.1872 | 0.6188 | 200.00 | 100.00 |
| 7 | 7 | 8 | 0.7114 | 0.2351 | 200.00 | 100.00 |
| 8 | 8 | 9 | 1.0300 | 0.7400 | 60.00 | 20.00 |
| 9 | 9 | 10 | 1.0440 | 0.7400 | 60.00 | 20.00 |
| 10 | 10 | 11 | 0.1966 | 0.0650 | 45.00 | 30.00 |
| 11 | 11 | 12 | 0.3744 | 0.1238 | 60.00 | 35.00 |
| 12 | 12 | 13 | 1.4680 | 1.1550 | 60.00 | 35.00 |
| 13 | 13 | 14 | 0.5416 | 0.7129 | 120.00 | 80.00 |
| 14 | 14 | 15 | 0.5910 | 0.5260 | 60.00 | 10.00 |
| 15 | 15 | 16 | 0.7463 | 0.5450 | 60.00 | 20.00 |
| 16 | 16 | 17 | 1.2890 | 1.7210 | 60.00 | 20.00 |
| 17 | 17 | 18 | 0.7320 | 0.5740 | 90.00 | 40.00 |
| 18 | 2 | 19 | 0.1640 | 0.1565 | 90.00 | 40.00 |
| 19 | 19 | 20 | 1.5042 | 1.3554 | 90.00 | 40.00 |
| 20 | 20 | 21 | 0.4095 | 0.4784 | 90.00 | 40.00 |
| 21 | 21 | 22 | 0.7089 | 0.9373 | 90.00 | 40.00 |
| 22 | 3 | 23 | 0.4512 | 0.3083 | 90.00 | 50.00 |
| 23 | 23 | 24 | 0.8980 | 0.7091 | 420.00 | 200.00 |
| 24 | 24 | 25 | 0.8960 | 0.7011 | 420.00 | 200.00 |
| 25 | 6 | 26 | 0.2030 | 0.1034 | 60.00 | 25.00 |
| 26 | 26 | 27 | 0.2842 | 0.1447 | 60.00 | 25.00 |
| 27 | 27 | 28 | 1.0590 | 0.9337 | 60.00 | 20.00 |
| 28 | 28 | 29 | 0.8042 | 0.7006 | 120.00 | 70.00 |
| 29 | 29 | 30 | 0.5075 | 0.2585 | 200.00 | 600.00 |
| 30 | 30 | 31 | 0.9744 | 0.9630 | 150.00 | 70.00 |
| 31 | 31 | 32 | 0.3105 | 0.3619 | 210.00 | 100.00 |
| 32 | 32 | 33 | 0.3410 | 0.5320 | 60.00 | 40.00 |
| 33 | 8 | 21 | 2.0000 | 2.0000 | - | - |
| 34 | 9 | 15 | 2.0000 | 2.0000 | - | - |
| 35 | 12 | 22 | 2.0000 | 2.0000 | - | - |
| 36 | 18 | 33 | 0.5000 | 0.5000 | - | - |
| 37 | 25 | 29 | 0.5000 | 0.5000 | - | - |
| Total | | | | | 3,715.00 | 2,300.00 |

The voltage profile of the IEEE 33 bus network can be found in figure 4.7. The detailed simulation report produced by DIgSILENT software related to test system is attached in appendix 8 (A8).

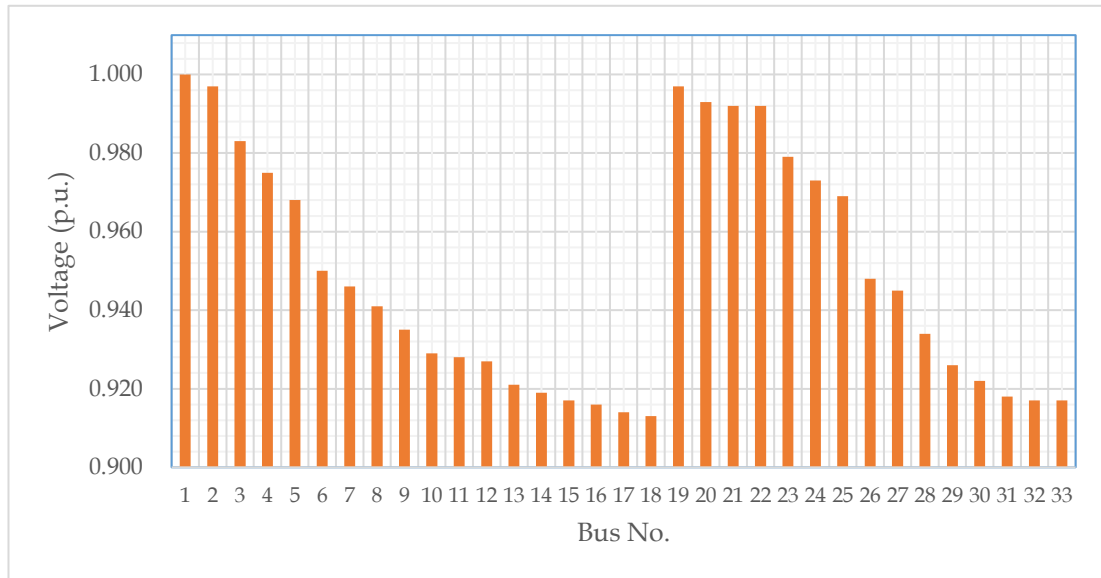


Figure 4.7 IEEE 33 Bus Voltage Profile

The minimum voltage of the test system equals to 0.913 pu at bus no. 18 and the maximum voltage equals to 1.000 pu at bus no. 1.

4.3.2 DSTATCOM Model

A typical DSTATCOM model which has one voltage input was developed in DIgSILENT Power Factory software for the IEEE 33 bus network. The DSTATCOM model was connected to the bus no. 33 (feeder end) to identify the voltage regulation. As per the table 4.2 total load of the test system is 3.7 MW & 2.3 MVar. Accordingly, the model is selected to achieve a compensation of 5 MVar with the distribution network.

There are two types of diagrams to be used for the DIgSILENT modeling; frame diagram and block diagram. The frame does consist of slots and signals connecting them. The frame is the basis of a composite model, where elements can be inserted into the slots.

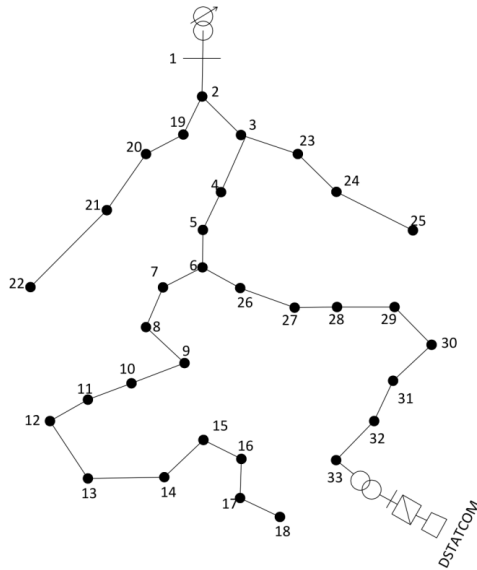


Figure 4.8 Single line diagram of test system with DSTATCOM

The block diagram doesn't have any slots but can be made up using different blocks or equations, where each block will define a function. The input/output parameters of the block diagram have to match those defined in the associated slot. Also the parameter names of the function have to match the I/O names used in the function block. The block diagram is the basis of a DSL element, which can be inserted into the slots of a composite model.

Simply, the input output relationship of the DSTATCOM model is defined in control frame which is illustrated in figure 4.9. The converter gets the current reference from the VDC/VAC-Controller and the phase reference from a phase measurement device PLL (phase-locked-loop). In order to keep the DC voltage, the AC voltage and the reactive power output constant, the controller gets its input from the DC, AC and reactive power measurement, respectively.

The basic structure of a PLL is explained in annexure 4 (A4)

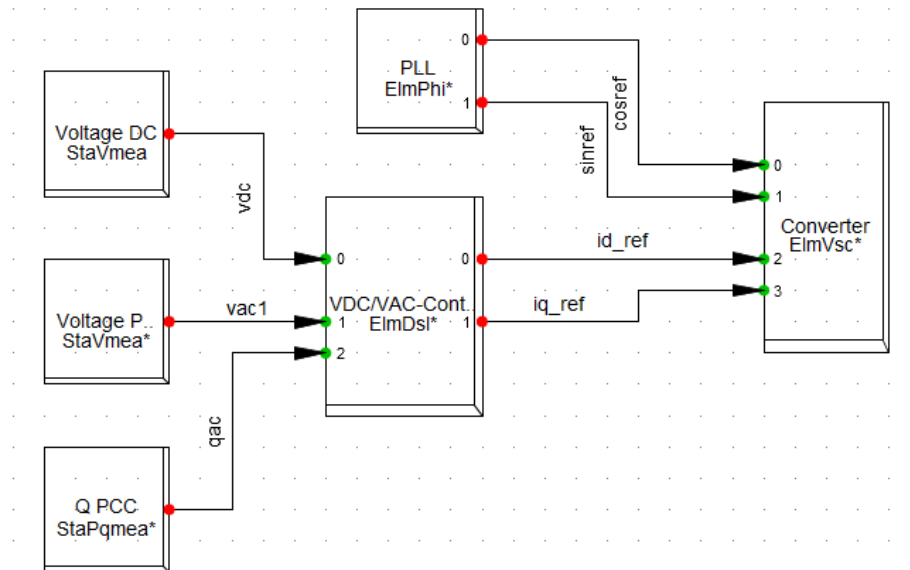


Figure 4.9 DSTATCOM control frame

The block diagram of the DSTATCOM is illustrated in figure 4.10 in which all the equations are defined within each block.

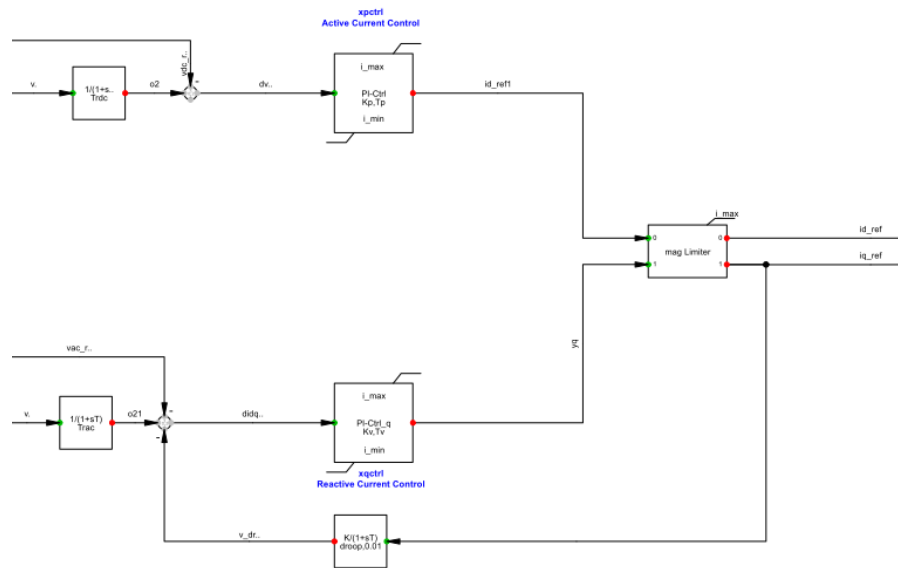


Figure 4.10 DSTATCOM control block diagram

With respect to the aforementioned frame diagram and the block diagram, DSTATCOM was capable of injecting or absorb reactive power to regulate the voltage level at point of common coupling. The modeled DSTATCOM in the IEEE 33 bus network is illustrated in figure 4.11 and the parameter values are shown in table 4.3.

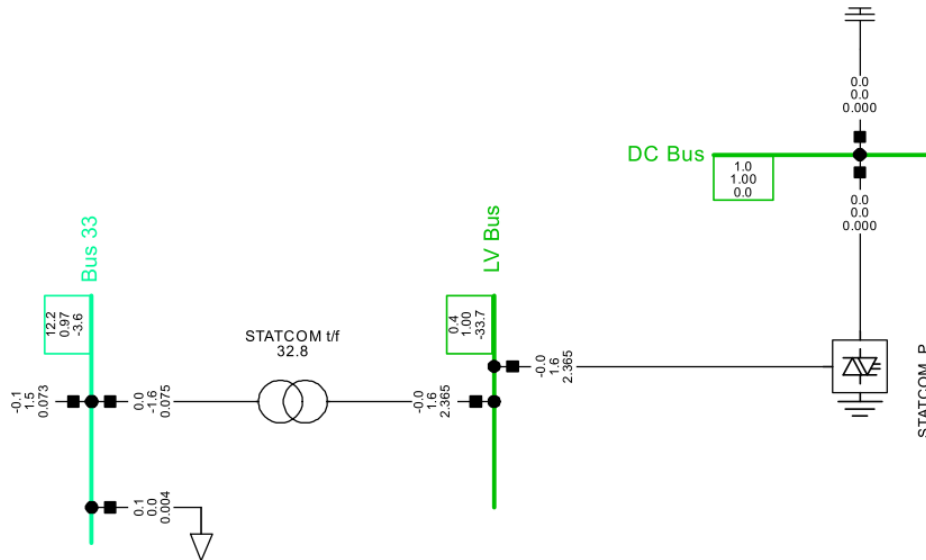


Figure 4.11 Single Line Diagram of DSTATCOM connected to 33rd bus

Table 4.3 Parameters of the DSTATCOM model

| No. | Parameter Description | Parameter Value |
|-----|---------------------------------------------------|-----------------|
| 1 | Active Power Control Gain (Kp) [pu] | 25.00 |
| 2 | Active Power Control Time Constant (Tp) [s] | 1.00 |
| 3 | Voltage Control Gain (Kv) [pu] | 2.00 |
| 4 | Voltage Power Control Time Constant (Tv) [s] | 0.10 |
| 5 | Droop | 0.06 |
| 6 | DC Voltage Measurement Delay Time Constant (Trdc) | 0.10 |
| 7 | AC Voltage Measurement Delay Time Constant (Trac) | 0.10 |
| 8 | Minimum Current Setting of the Inverter (i_min) | -2.00 |
| 9 | Maximum Current Setting of the Inverter (i_max) | 2.00 |

The voltage profile of IEEE 33 bus network after introducing DSTATCOM at the 33rd bus is shown in figure 4.12. Primarily, DSTATCOM monitors the voltage at the PCC,

in here 33rd bus, and try to maintain its voltage at 1.00 pu either operating under inductive or capacitive mode.

During the steady state operation of DSTATCOM, it has injected 1.6 MVar in to the distribution network. The voltage of 33rd bus has been increased up to 0.967 pu and the DSTATCOM has been loaded 32.8 % of its rated value. The minimum voltage of the test system equals to 0.925 pu at bus no. 18 and the maximum voltage equals to 1.000 pu at bus no. 1.

The detailed simulation report produced by DIgSILENT software related to test system with DSTATCOM is attached in annexure 9 (A9).

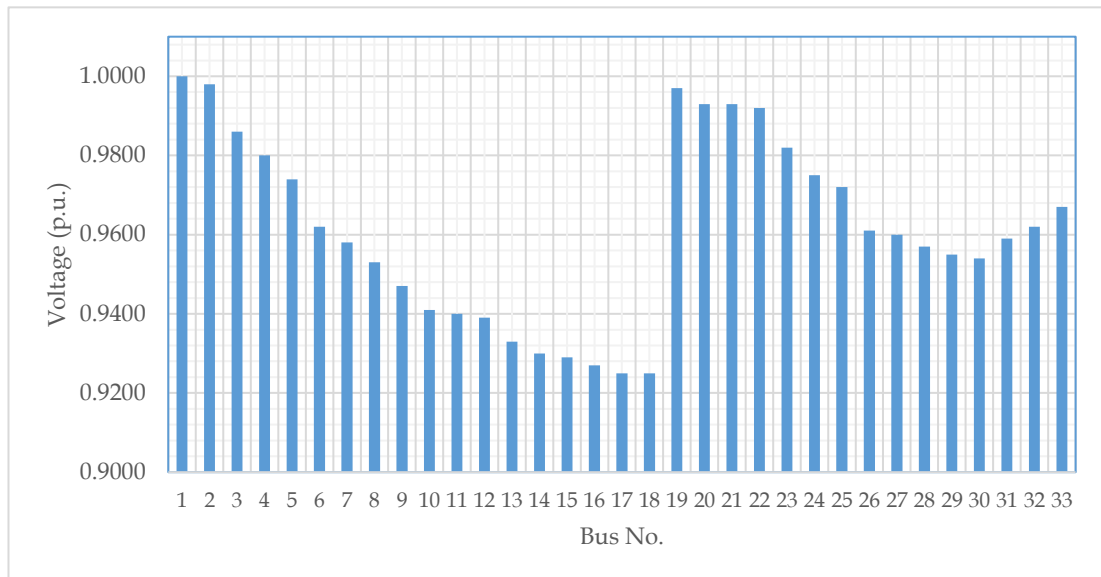


Figure 4.12 IEEE 33 Bus Voltage Profile with DSTATCOM

4.3.3 Discussion

The role of the modeled DSTATCOM as the voltage regulator is studied in this section comparing voltage of each bus before and after connecting DSTATCOM. The voltage variation is shown in figure 4.13.

Base case refers the IEEE 33 bus network without connecting DSTATCOM. Similarly, figure 4.8 and figure 4.12 are plotted in the same graph to understand the impact of DSTATCOM which is shown in figure 4.13. In addition, change of voltage due to the 1.6 MVar reactive power injection was plotted in figure 4.14 as a sensitivity analysis to the test network.

The voltage of 33rd bus has been hiked to 0.967 pu which is an increase of 0.05 pu due to the addition of DSTATCOM. Bus no. 33 shows the maximum voltage improvement of 5.45% compared to the base case where buses 1, 19, 20 and 22 shows no voltage change.

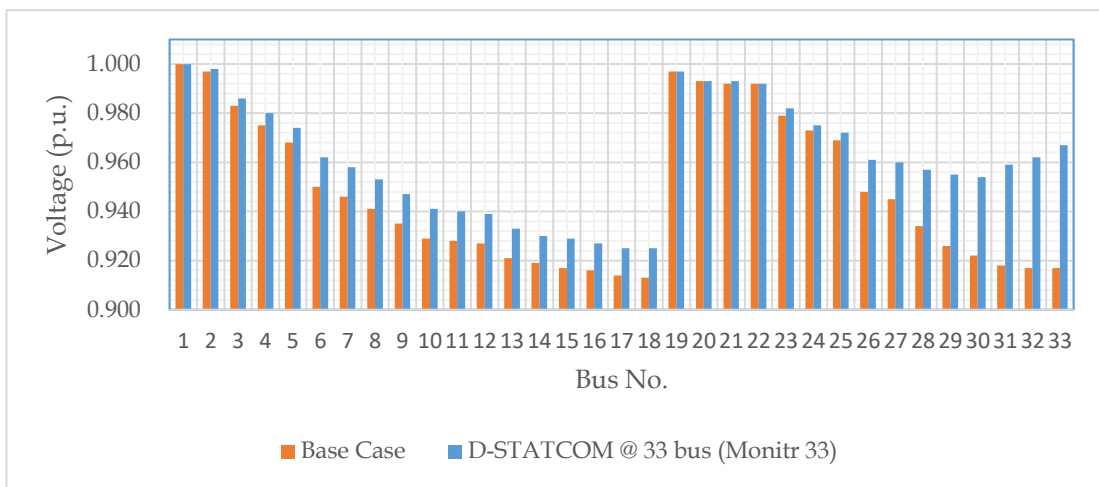


Figure 4.13 Comparison of voltage variation due to DSTATCOM

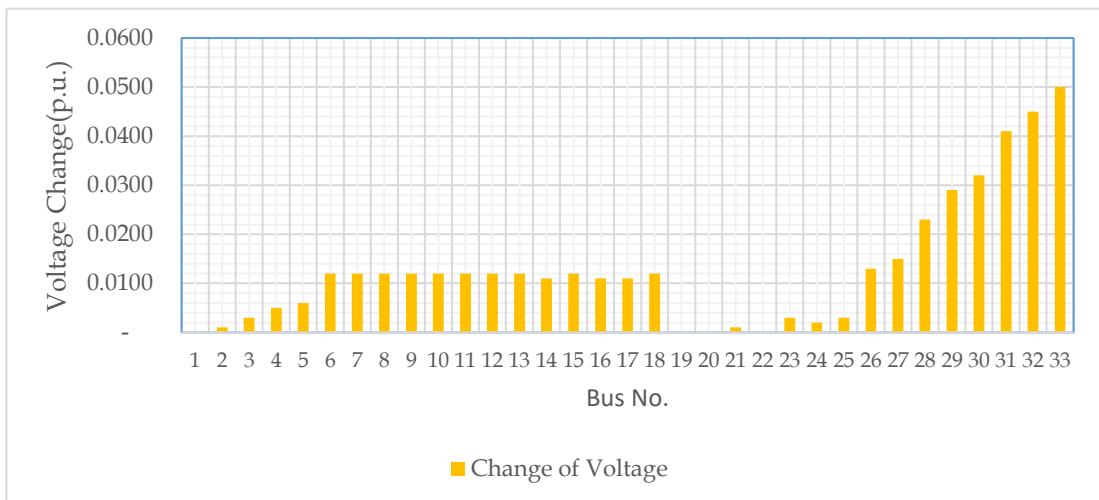


Figure 4.14 Change of voltage due to DSTATCOM at 33rd bus

4.4 Development of Modified DSTATCOM Model

4.4.1 Introduction

As explained in chapter 3, there are three control structures to control different types of control devices. i.e. local control, decentralized control & centralized control. Since decentralized control mechanism guiding few control devices in a coordinated manner, the response shall be more effective than local control mechanism.

Chapter 4.3 refers the typical DSTATCOM model which acts as a local control device for voltage regulation. In addition, a modified DSTATCOM to be implemented to act as a primary control device of decentralized control structure.

4.4.2 Local Controllable Zones

Local Controllable Zones (LCZ) are introduced for the purpose of simplification of an electrical network which consist of few bus bars of a particular feeder. The complete electrical network may consist of multiple LCZs. The concept of LCZ for a distribution network is illustrated in figure 4.15.

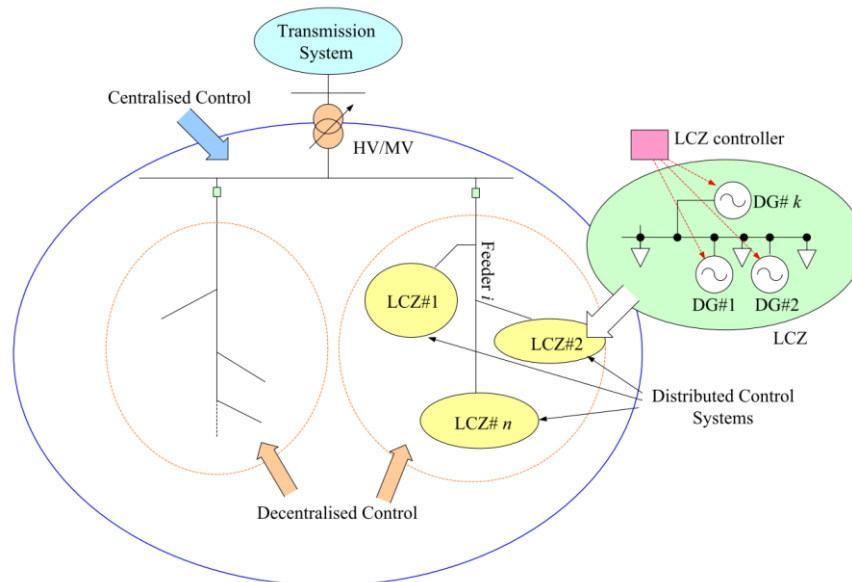


Figure 4.15 LCZ concept adaption for a distribution network

The LCZs provide proper voltage controllability over the local control but centralized control.

When considering the research there are two voltage support devices i.e. DSTATCOM and solar PV inverter, as explained earlier. Both two devices have the local control capability where each device monitors only the voltage of its PCC. However, LCZ are defined in such a way that both devices include in a particular LCZ.

Since the solar PV inverter acts as the secondary voltage support, injection or absorption of reactive power in to the distribution network is limited, mainly depends on the active power generation at a particular time. In addition, implementation of coordinated voltage control requires an advanced modification of voltage controlling method of DSTATCOM.

DSTATCOM shall not be limited to monitoring the voltage at PCC only, since it will not be available to react for voltage violation of different bus bar within the LCZ. Therefore, it is necessary to monitor two or more buses including secondary voltage support device in order to provide better performance of the DSTATCOM device.

In this study, DSTATCOM model is modified to monitor four (04) adjacent buses of the distribution network irrespective of a single bus bar. The DSTATCOM model developed in chapter 4.3.2 is further modified to monitor several bus bars of the IEEE 33 bus network, in which control frame diagram and the control block diagram are illustrated in figure 4.17 and 4.18 respectively.

The control signal of reactive power control is determined by monitoring four (04) bus voltages ie. bus nos 30, 31, 32 and 33. If one of the monitoring buses violates the stipulated voltage limits, DSTATCOM compensate the reactive power and try to maintain all the monitoring buses at healthy state (within stipulated limits).

The detailed simulation report produced by DIgSILENT software related to test system with modified DSTATCOM is attached in annexure 10 (A10).

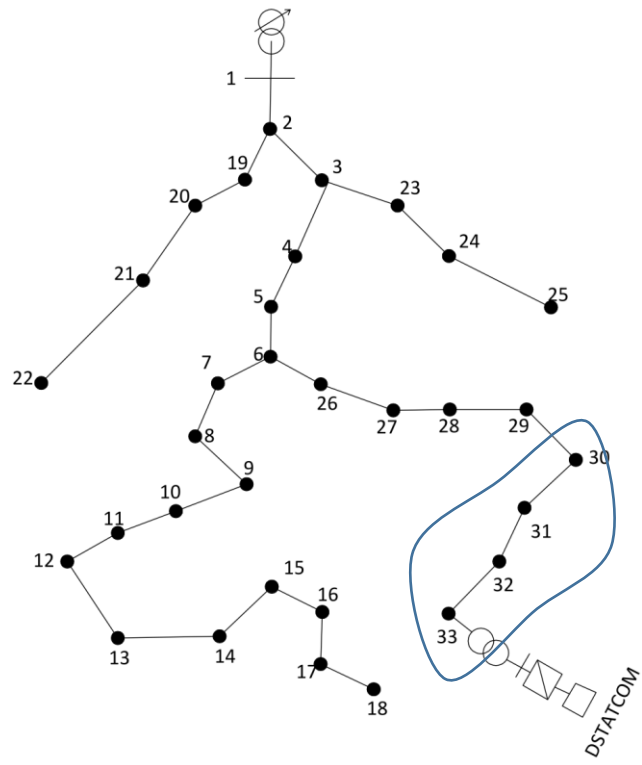


Figure 4.16 LCZ representation of the test system with DSTATCOM

Under the chapter 4.4, performance of the developed DSTATCOM has been discussed without coordinating the secondary voltage support device. However, coordinated voltage control is further discussed in forthcoming chapters 5 & 6.

The same parameters mentioned in table 4.3 were used for the modified DSTATCOM model.

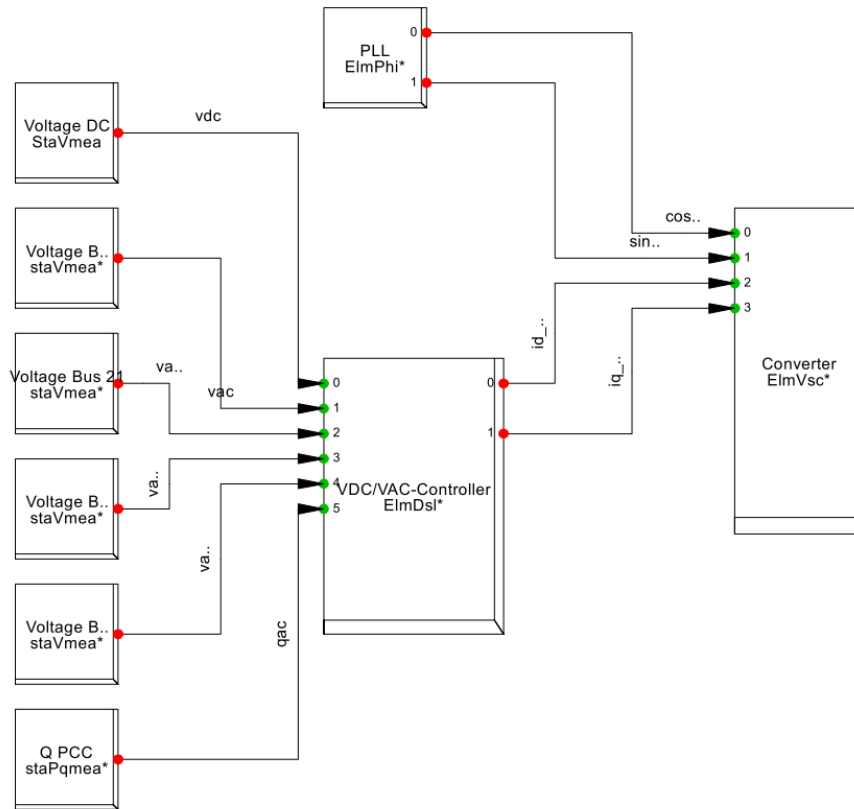


Figure 4.17 Control frame diagram of modified DSTATCOM model

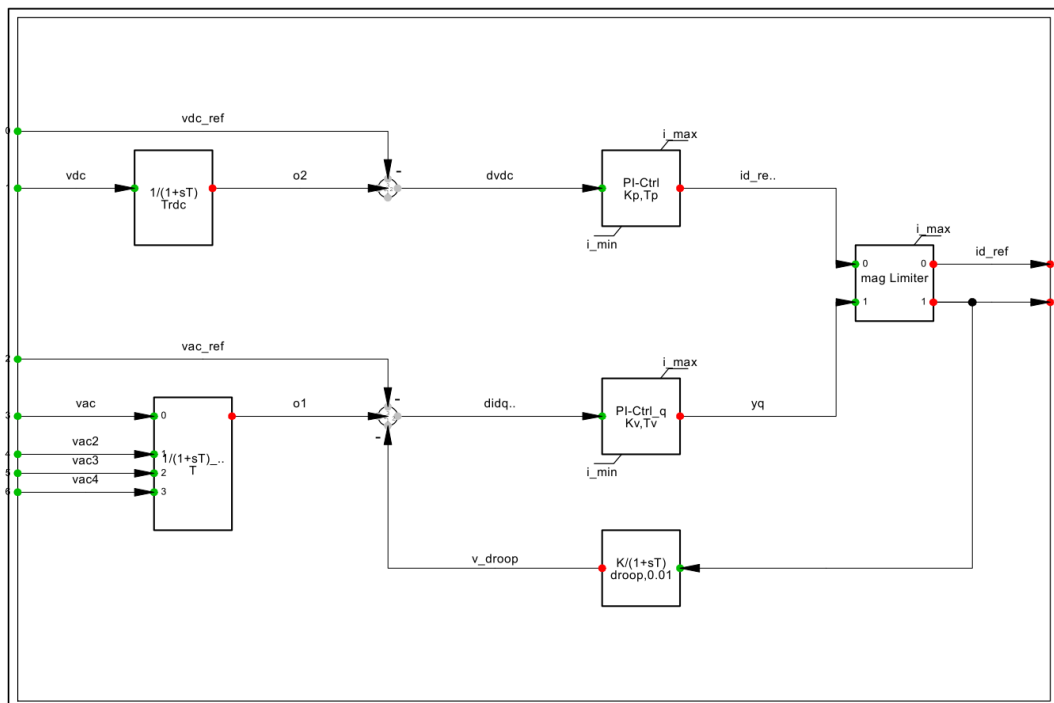


Figure 4.18 Control block diagram of modified DSTATCOM model

4.4.1 Discussion

Voltage improvement due to typical DSTATCOM and the modified DSTATCOM has been illustrated in figure 4.19. Base case refers the IEEE 33 bus distribution network without introducing any voltage support devices. Then DSTATCOM is introduced to the network at the bus no. 33 to monitor the voltage at its PCC only. Finally the DSTATCOM at bus no. 33 is modified to monitor four (04) bus voltages i.e. bus nos. 30, 31, 32 and 33.

All these three cases are plotted in figure 4.19 where three cases related to IEEE 33 bus distribution network are as follows.

1. Base Case : No voltage support devices
2. Case 1 : DSTATCOM at 33rd bus which monitors 33 bus voltage only
3. Case 2 : DSTATCOM at 33rd bus which monitors 30, 31, 32 and 33 bus voltages

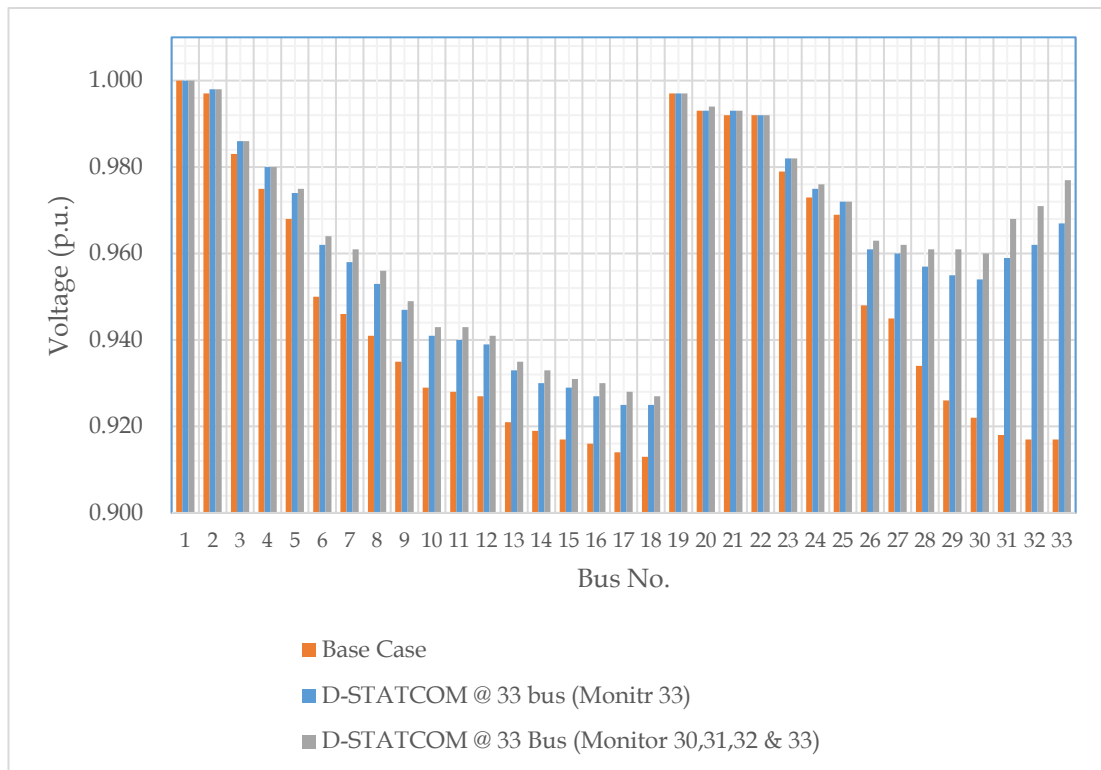


Figure 4.19 Comparison of voltage variation due to typical & modified DSTATCOM

Table 4.4 Summary of the IEEE 33 bus network under three cases.

| No. | Description | Base Case | Case 1 | Case 2 |
|-----|---------------------------------------------|-----------|--------|--------|
| 1 | Min. Voltage (pu) | 0.913 | 0.925 | 0.927 |
| 2 | Min Voltage bus | 18 | 18 | 18 |
| 3 | Max. Voltage (pu) | 1.000 | 1.000 | 1.000 |
| 4 | Max. Voltage bus | 1 | 1 | 1 |
| 5 | Voltage of 33 rd bus | 0.917 | 0.967 | 0.977 |
| 6 | Voltage improvement of 33 rd bus | - | 5.45% | 6.54% |

In addition, change of voltage due to the reactive power injection was plotted in figure 4.20 as a sensitivity analysis to the test network.

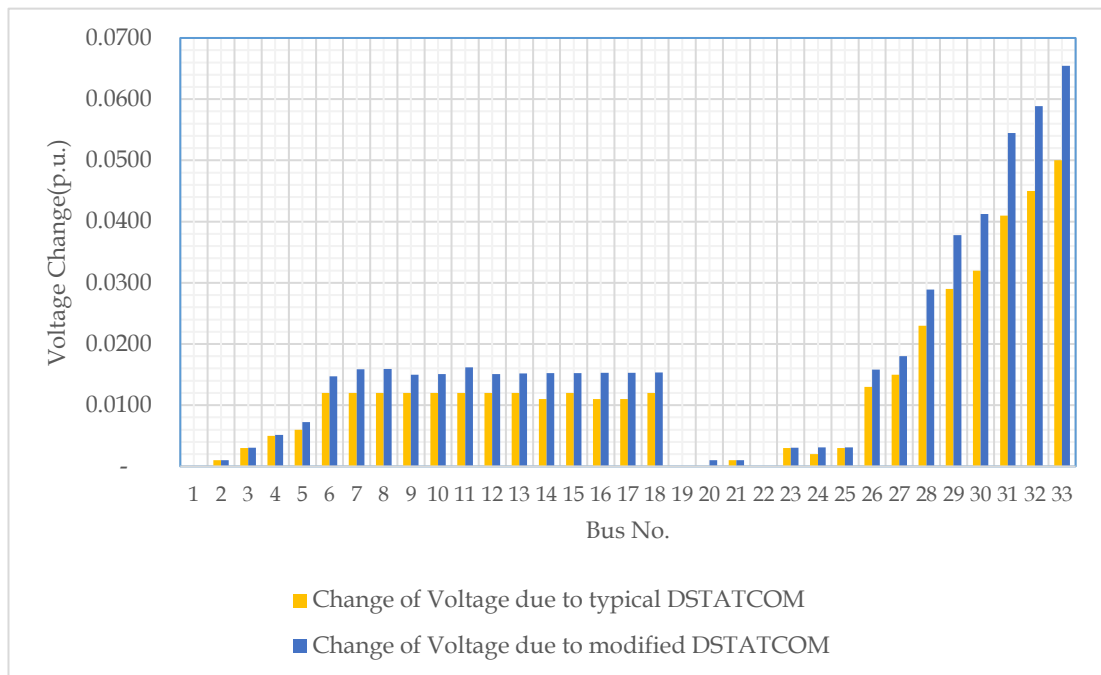


Figure 4.20 Voltage change due to typical & modified DSTATCOM

The voltage of 33rd bus has been hiked to 0.977 pu which is an increase of 0.06 pu due to the modified DSTATCOM. Bus no. 33 shows the maximum voltage improvement of 6.54% compared to the base case where buses 1, 19 and 22 shows no voltage change.

CHAPTER 5

VOLTAGE CONTROL CO-ORDINATION BETWEEN SOLAR PV INVERTER & DSTATCOM

5.1 Overview

Out of several types of DER in the distribution network, this study refers to the solar PV as the DER which means that the DER mentioned in this report talks only about solar PV. There are several control mechanisms currently available for solar PV inverter, each plays a significant role for the operation of solar PV inverter. According to the latest IEEE 1547-2015 standard, following five (05) control modes have been discussed deeply.

1. Constant power factor mode
2. Voltage-reactive power (volt-var) mode
3. Active power-reactive power (watt-var) mode
4. Constant reactive power mode
5. Voltage-active power (volt-watt) mode

Constant power factor mode at unity power factor is the default control mode setting of the solar PV inverter. Differentiation of each control mode can be understood by table 5.1 [7].

Table 5.1 Differentiation of control modes

| No. | Control Mode | Description |
|----------------------------------------------|-----------------------|--------------------------------------------------------------------------------------------------------------------------------------------------------------------------------------|
| Voltage regulation by reactive power control | | |
| 1 | Constant power factor | DER operates at a constant power factor which setting can be adjusted locally and/or remotely. The maximum DER response time to maintain constant power factor shall be 10s or less. |

| | | |
|----------------------------------|-------------------------------------------|--------------------------------------------------------------------------------------------------------------------------------------------------------------------------------------------------------------------------------------------------------------------------------------------|
| 2 | Voltage-reactive power (volt-var) | DER actively controls its reactive power output as a function of voltage following a voltage-reactive power piecewise linear characteristic. Refer appendix 5 (A5). |
| 3 | Active power-reactive power (watt-var) | DER actively controls the reactive power output as a function of the active power output following a target piecewise linear active power-reactive power characteristic, without intentional time delay. Refer appendix 6 (A6). |
| 4 | Constant reactive power | DER maintains a constant reactive power. The target reactive power level and mode (injection or absorption) shall be specified. |
| Voltage and active power control | | |
| 5 | Voltage-active power (volt-watt) | DER actively limits the DER maximum active power as a function of the voltage following a voltage-active power piecewise linear characteristic. If enabled, the voltage-active power mode remains active while any of the voltage-reactive power modes are enabled. Refer appendix 7 (A7). |

5.2 Voltage-Reactive Power (Volt-Var)

Out of control modes mentioned in chapter 5.1, Voltage-reactive power is considered in this study as the secondary voltage support. Solar PV inverter actively controls its reactive power output according to a voltage-reactive power piecewise linear characteristic as illustrated in figure 5.1.

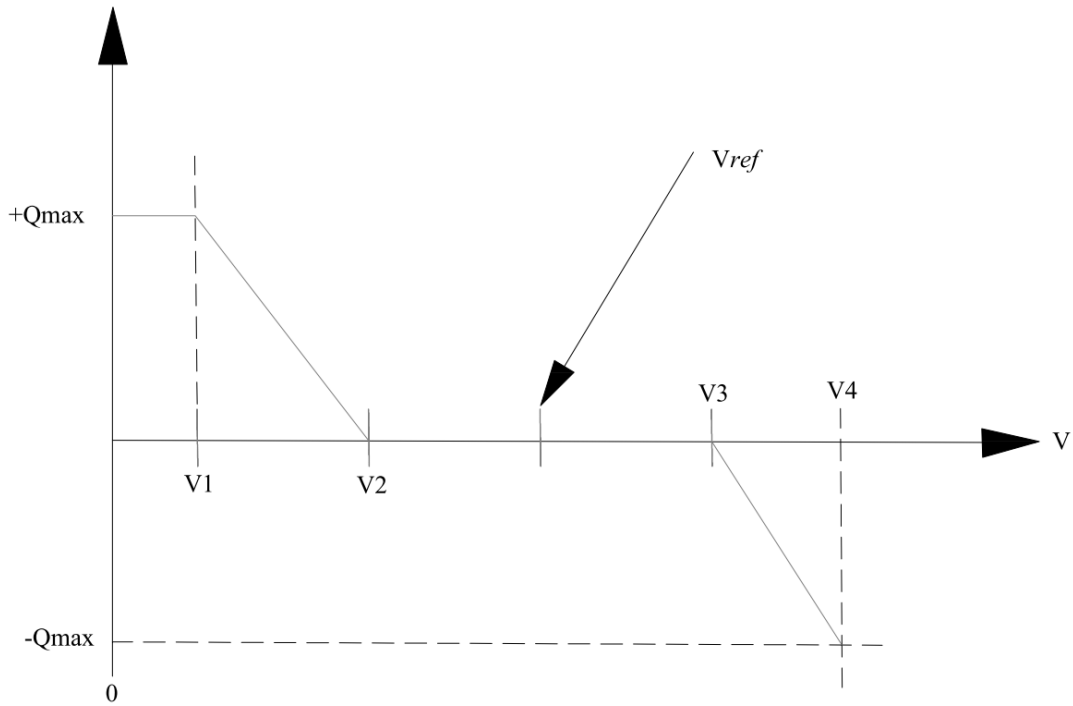


Figure 5.1 Voltage-Reactive power characteristic

In this mode, the DER continuously monitors the voltage at PCC and if this voltage lies outside the dead band voltage (U_2 - U_3), it will absorb/ inject reactive power in order to maintain the voltage at stipulated levels. Principally, if the voltage drops down beyond the dead band voltage, reactive power will be injected to the system vice versa.

Ultimately, the DER act as a voltage control device based on compensation of reactive power depending on the voltage at PCC. Further, the response is very fast as power electronic devices i.e. MOSFET are used for the inverter. This is the main reason for the adoption of this particular control mode for this research.

In addition, maximum power injection/ absorption has been defined by IEEE 1547-2018 standard which is 44% of the nameplate apparent power rating.

5.3 Co-ordination between STATCOM and DER

The coordination between two voltage support devices is developed as per the flow diagram mentioned in figure 5.3. Typically reactive power compensation capability of a DSTATCOM is in the range of few MVar and a 1MVA DER is within 0.5 Mvar. Therefore, DSTATCOM has the higher reactive power control capability compared to the DER, thus, DSTATCOM acts as the primary voltage support device and DER acts as the secondary voltage support device. Reactive power compensation responses of each device are very fast since both devices consist of power electronics components.

The main principle of the co-ordination is primary voltage support device acts initially and attempts to maintain the voltages under stipulated levels. If the primary device is unable to do so, the secondary voltage support device is operated in order to bring the voltages under stipulated levels.

Voltage relationship of the primary and secondary voltages are mentioned in (5.1) and (5.2).

$$V_{\min, \text{secondary}} < V_{\min, \text{primary}} \quad 5.1$$

$$V_{\max, \text{secondary}} > V_{\max, \text{primary}} \quad 5.2$$

The operational voltage band of the primary device is less than the same of the secondary device. The (5.1) and (5.2) can be re-written incorporating DSTATCOM and Solar PV and simple representation is illustrated in figure 5.2.

$$V_{\min, \text{PV}} < V_{\min, \text{DSTATCOM}} \quad 5.1$$

$$V_{\max, \text{PV}} > V_{\max, \text{DSTATCOM}} \quad 5.2$$

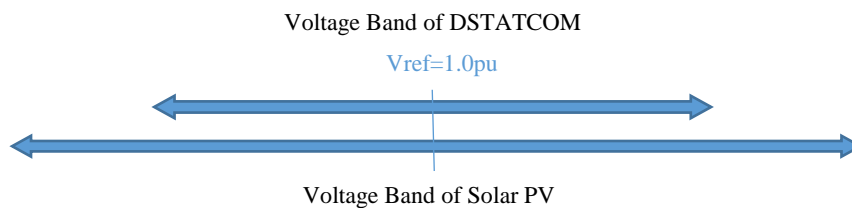


Figure 5.2. Representation of voltage magnitudes

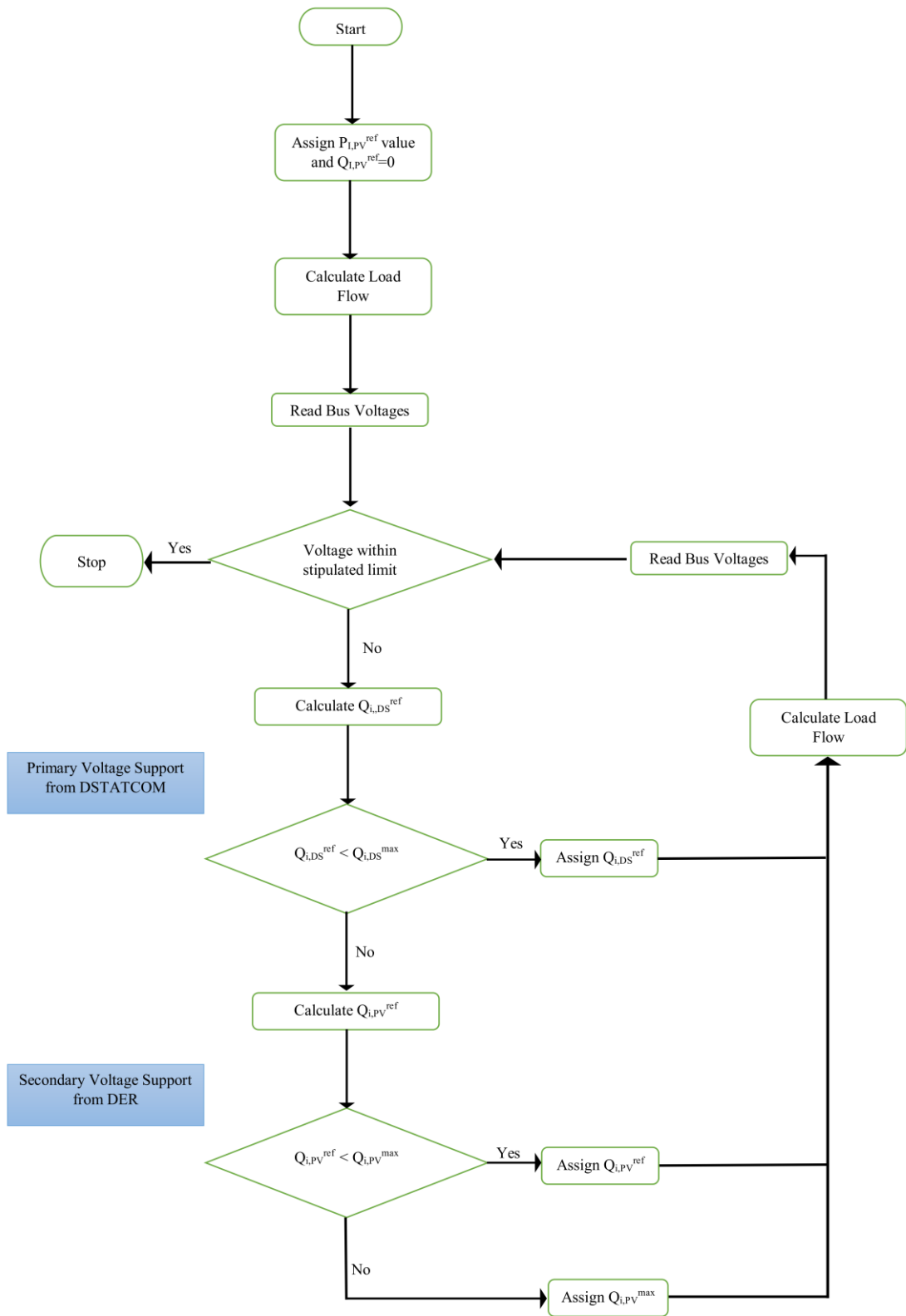


Figure 5.3 Flow Diagram of the co-ordination between DSTATCOM and DER

5.4 Simulation

The simulation was performed for the IEEE 33 bus distribution network. As per the chapter 2 (Problem formulation), this thesis addresses the over voltage issues pertaining to the large-scale solar PV installations connected at MV level. Therefore, making an over-voltage situation in the test system and adopt the coordinated voltage control mechanism was simulated.

The base case refers the IEEE 33 bus test system with 1MW and 2 MW solar PV systems are connected at bus nos. 12 and 22 respectively. The solar PV systems operated at unity power factor. No reactive power support from any device is considered.

The case 1 refers to the introduction of secondary voltage control support from solar PV inverter to the base case. The solar PV inverter operation mode is switched to unity power factor to voltage-reactive power mode in order to identify the voltage improvement. Each solar PV system's control mode in the test system changed to voltage-reactive power mode.

The case 2 refers to the introduction of primary voltage control support from DSTATCOM to the base case. A modified DSTATCOM is used for the simulation as explained in chapter 4.4, which monitors 4 buses of the distribution network i.e. 19, 20, 21 & 22. The LCZ for this case is consists of buses 19, 20, 21 and 22 which includes DSTATCOM and a solar PV system in the same LCZ.

The detailed simulation report produced by DIgSILENT software related to coordination control between DSTATCOM and DER is attached in appendix 11 (A11).

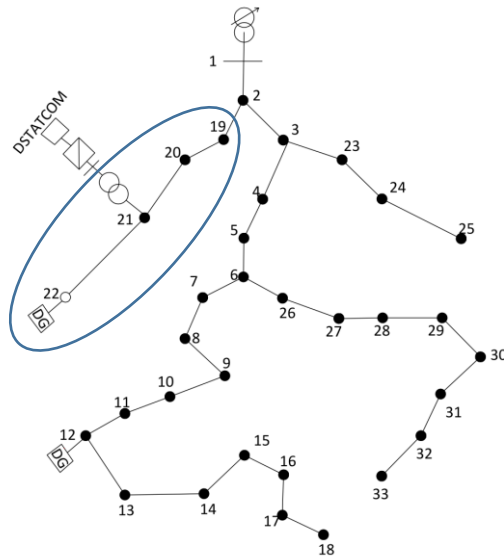


Figure 5.4 Network configuration of coordinated voltage control

In this case 2, solar PV inverter at bus no. 22 acts as the secondary voltage support device. However, solar PV inverter at bus no. 12 acts as the primary voltage support device which is being the only voltage control support device within its LCZ.

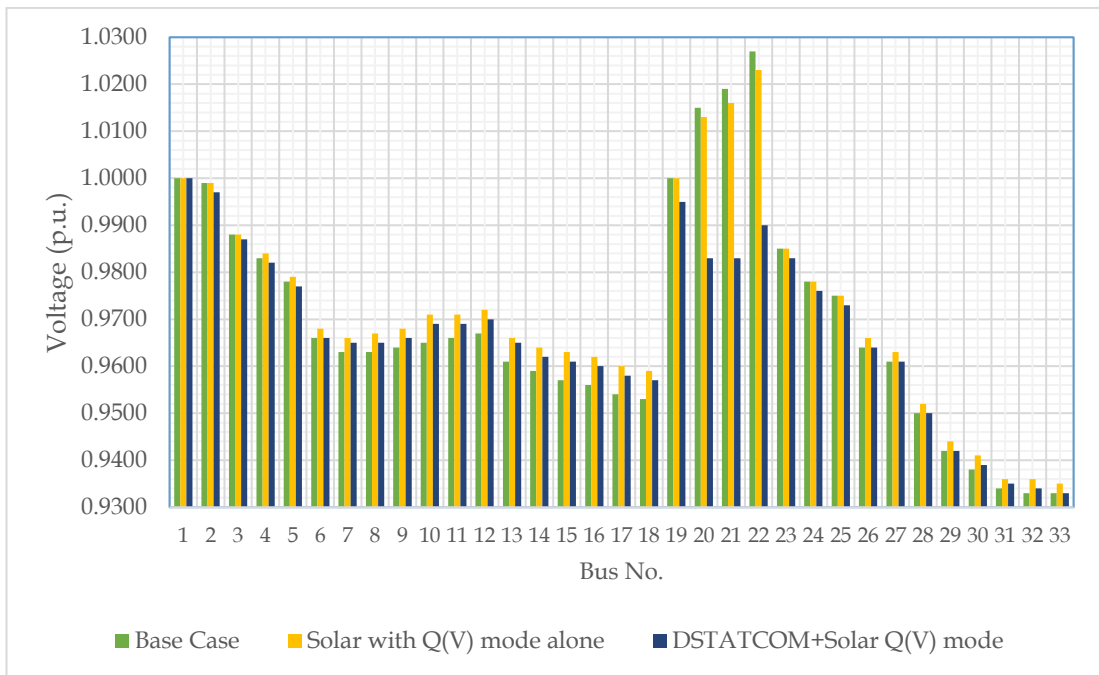


Figure 5.5 Comparison of bus voltages of the test system

5.5 Discussion

The LCZ and its voltage control devices' locations can be understood by figure 5.5. It is clearly seen that the voltage improvement of due to the coordinated voltage control mechanism can be applied between solar PV systems and DSTATCOMs. The voltage details of the complete 33 bus network is tabulated in table 5.2.

Table 5.2 Summary of the IEEE 33 bus network under coordinated control mode

| No. | Description | Base Case | Case 1 | Case 2 |
|-----|-------------------|-----------|--------|--------|
| 1 | Min. Voltage (pu) | 0.933 | 0.935 | 0.933 |
| 2 | Min Voltage bus | 33 | 33 | 33 |
| 3 | Max. Voltage (pu) | 1.027 | 1.023 | 1.000 |
| 4 | Max. Voltage bus | 22 | 22 | 1 |

The LCZ of the study consists of four (04) bus bars, i.e. bus nos. 19, 20, 21 and 22, each bus bar voltage is being monitored by DSTATCOM. In addition to the voltage details of the complete 33 bus network, voltage details of LCZ can be found in table 5.3.

Table 5.3 Summary of the LCZ under coordinated control mode

| No. | Description | Base Case | Case 1 | Case 2 |
|-----|-----------------------|-----------|--------|--------|
| 1 | Voltage of Bus no. 19 | 1.0000 | 1.0000 | 0.9950 |
| 2 | Voltage of Bus no. 20 | 1.0150 | 1.0130 | 0.9830 |
| 3 | Voltage of Bus no. 21 | 1.0190 | 1.0160 | 0.9830 |
| 4 | Voltage of Bus no. 22 | 1.0270 | 1.0230 | 0.9900 |

In the base case study, maximum voltage recorded at bus no. 22 which is equivalent 1.027 pu. Due to the coordinated voltage control mechanism it has reduced to 0.99 pu which shows a 3.60% reduction.

CHAPTER 6

VOLTAGE MANAGEMENT IN EMBILIPITIYA GSS WITH PROPOSED SOLAR FARMS

6.1 Overview

This chapter basically focuses on applying the developed coordinated voltage control mechanism in to Sri Lankan distribution network. As mentioned in the chapter 02 (Problem formulation), Embilipitiya GSS and Anuradhapura GSS were identified as possible victims of the “Battle for Solar” program. This chapter tries to consider only the Mauara feeder of Embilipitiya GSS for the simulations of coordinated voltage control mechanism.

In addition to the voltage control mechanism adoption, this chapter focuses on identifying the following influences related to the voltage profile of Sri Lankan network.

1. Influence of DSTATCOM location
2. Influence of dead band voltage of solar PV

6.2 Adoption of Coordinated Voltage Control Mechanism

During the problem formulation, simulations were performed under SynerGi simulation platform which is the distribution-network-planning software used by CEB. However, the research study was performed under DIgSILENT PowerFactory simulation platform. Created the existing SynerGi network model in DIgSILENT software and compared the results to verify the DIgSILENT model as the initial step.

The Mauara feeder in the Embilipitiya GSS was selected for the implementation of coordinated voltage control mechanism, which is having a length of 85km and a demand during day time in the year 2020. As mentioned in chapter 2.3.1 Mauara feeder was simulated in two scenarios. Scenario 1 refers to addition of 3 nos. of 1 MW solar PV systems whereas scenario 2 refers 6 nos. of 1 MW solar PV systems.

6.2.1 Typical mid-day load condition

As explained in earlier chapter 2.3.1.1, typical mid-day load condition (TLC) was simulated in DIgSILENT PowerFactory software. The comparison of voltages under the scenario 2 (having connected 6 nos. of solar PV systems) with two different simulation packages are illustrated in figure 6.1.

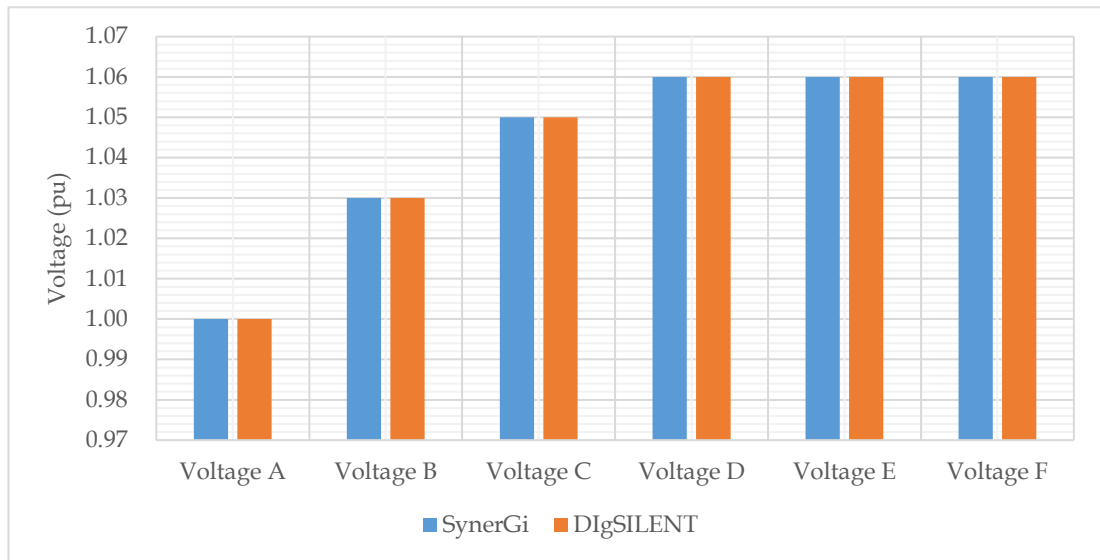


Figure 6.1 Comparison of Mauara feeder voltages under different simulation platforms

The voltages of Mauara feeder under SynerGi & DIgSILENT PowerFactory simulation software are approximately equal as per the figure 6.1. Therefore, it is understood that the DIgSILENT Powerfactory model under TLC is verified and ready to adopt the voltage control mechanism thereto.

Four (04) simulations were performed for Mauara Feeder under TLC as stated below.

Study 1 : Solar PV systems are operating under unity power factor.

Study 2 : Solar PVs operated under volt-var control mode alone. No any other voltage support devices.

Characteristics- Droop: 6% , Dead band voltage: 0.98 pu - 1.02 pu

Study 3 : Solar PVs operated under unity power factor alone. DSTATCOM is the only voltage support device which monitors 6 bus bars as mentioned in figure 6.2. *Characteristics - Droop : 6%*

Study 4 : Coordinated voltage control mechanism between solar PV and DSTATCOM. Refer appendix 12 (A12)

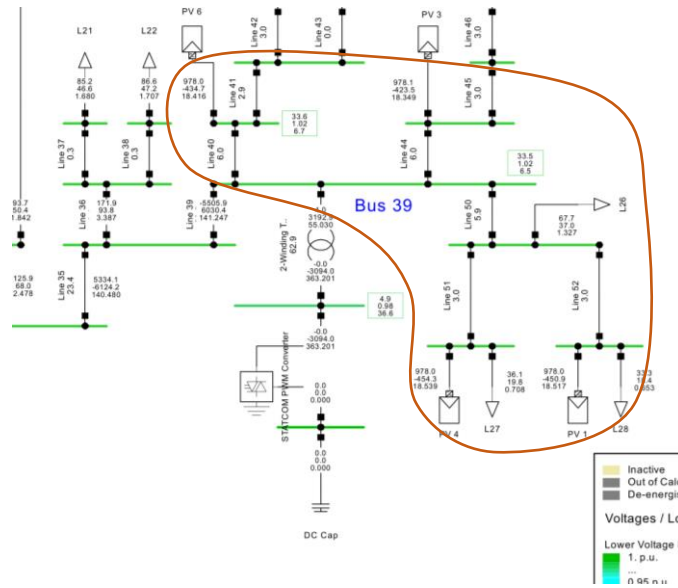


Figure 6.2 Identification of LCZ consists of solar PV and DSTATCOM

The voltages of six (06) locations as marked in appendix 12 (A12) pertaining to the aforementioned studies are illustrated in figure 6.3 and the voltage summary of the each locations and overall voltage improvement of study 4 compared to the study 1 are tabulated in table 6.1.

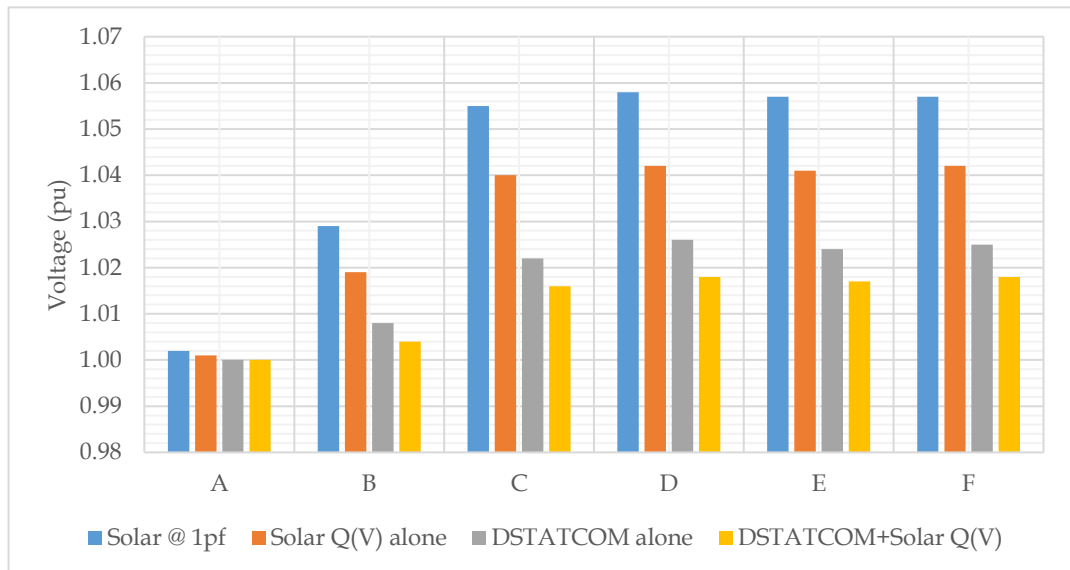


Figure 6.3 Voltage profile of 06 locations under TLC

Table 6.1 Voltage summary of the 06 locations under TLC

| | A | B | C | D | E | F |
|--------------------------------------|--------------|--------------|--------------|--------------|--------------|--------------|
| Study 1 | 1.002 | 1.029 | 1.055 | 1.058 | 1.057 | 1.057 |
| Study 2 | 1.001 | 1.019 | 1.040 | 1.042 | 1.041 | 1.042 |
| Study 3 | 1.000 | 1.008 | 1.022 | 1.026 | 1.024 | 1.025 |
| Study 4 | 1.000 | 1.004 | 1.016 | 1.018 | 1.017 | 1.018 |
| Overall Voltage Reduction (%) | 0.20% | 2.43% | 3.70% | 3.78% | 3.78% | 3.69% |

It was noted that a maximum voltage reduction of 3.78% has been obtained with the coordinated voltage control mechanism. Complete voltage profile is illustrated in figure 6.4.

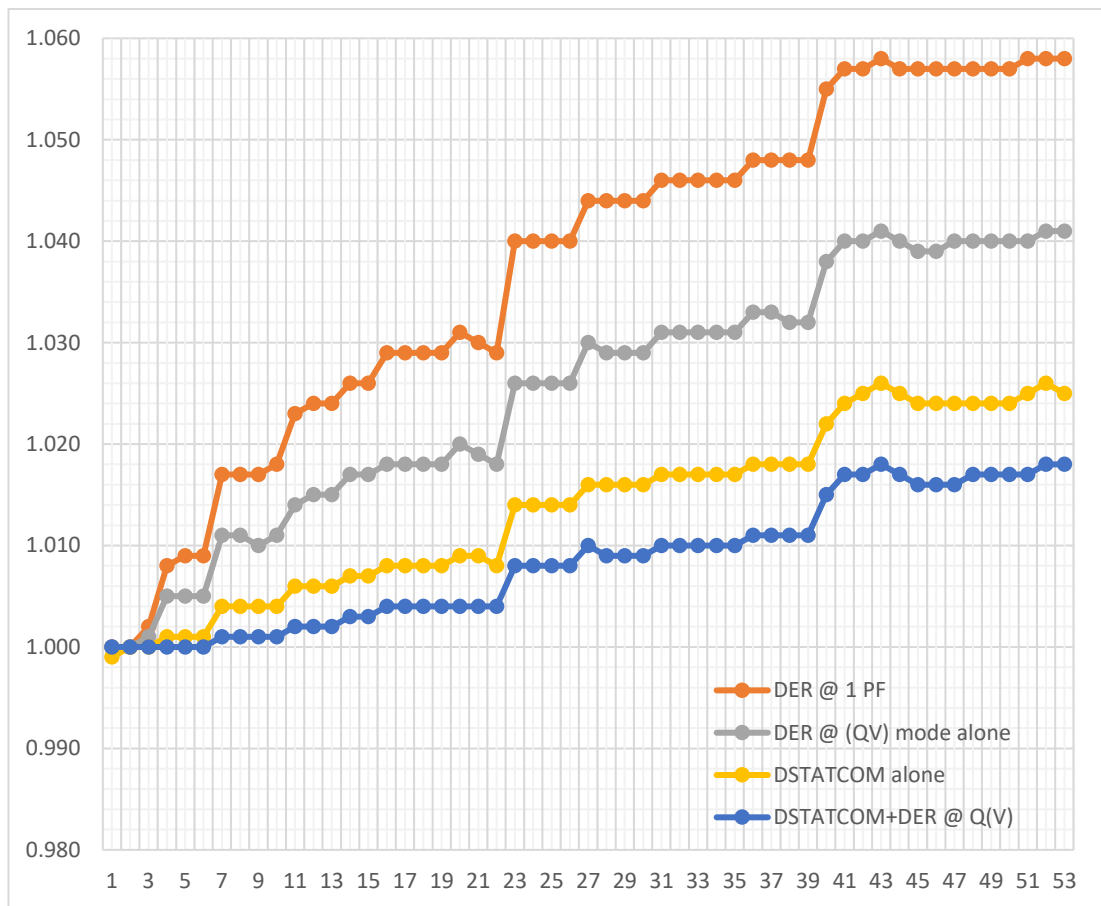


Figure 6.4 Complete voltage profile variation of Mauara feeder

6.2.2 Minimum mid-day load condition

As explained in earlier chapter 2.3.1.2, minimum mid-day load condition (MLC) was simulated in DIgSILENT PowerFactory software. The comparison of voltages under the scenario 2 (having connected 6 nos. of solar PV systems) with two different simulation packages are illustrated in figure 6.5.

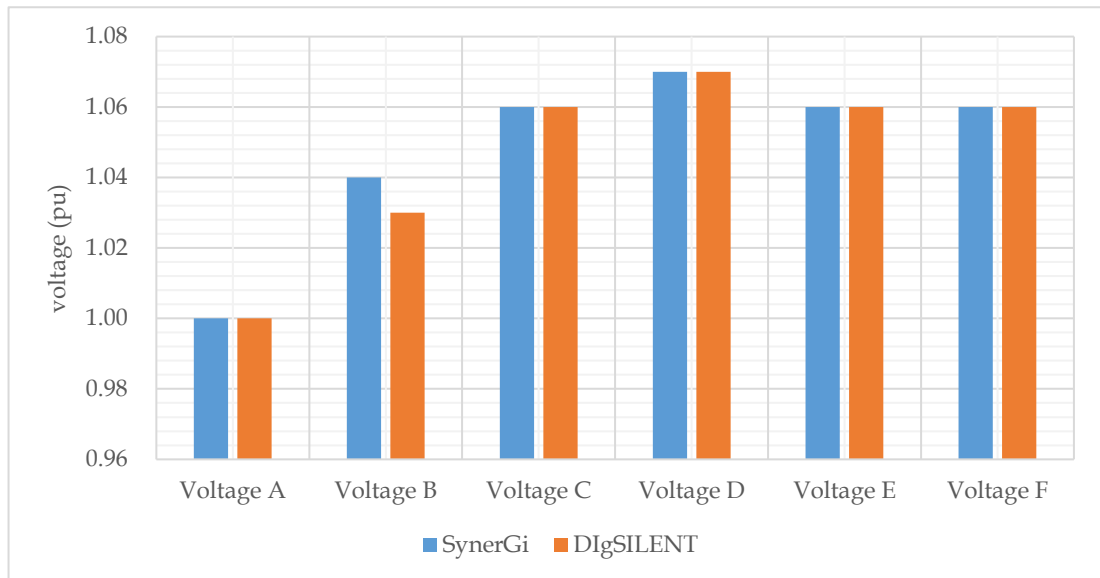


Figure 6.5 Comparison of Mauara feeder voltages under different simulation platforms

The voltages of Mauara feeder under SynerGi & DIgSILENT PowerFactory simulation software under MLC are approximately equal as per the figure 6.5. Therefore, it is understood that the DIgSILENT Powerfactory model under MLC is verified and ready to adopt the voltage control mechanism thereto.

Four (04) simulations were performed for Mauara Feeder under MLC as stated below.

Study 1 : Solar PV systems are operating under unity power factor.

Study 2 : Solar PVs operated under volt-var control mode alone. No any other voltage support devices.

Characteristics- Droop: 6% , Dead band voltage: 0.98 pu - 1.02 pu

Study 3 : Solar PVs operated under unity power factor alone. DSTATCOM is the only voltage support device which monitors 6 bus bars as mentioned in figure 6.2. *Characteristics - Droop : 6%*

Study 4 : Coordinated voltage control mechanism between solar PV and DSTATCOM. Refer appendix 13 (A13).

The voltages of six (06) locations are illustrated in figure 6.6 and the voltage summary of the each locations and overall voltage improvement of study 4 compared to the study 1 are tabulated in table 6.2.

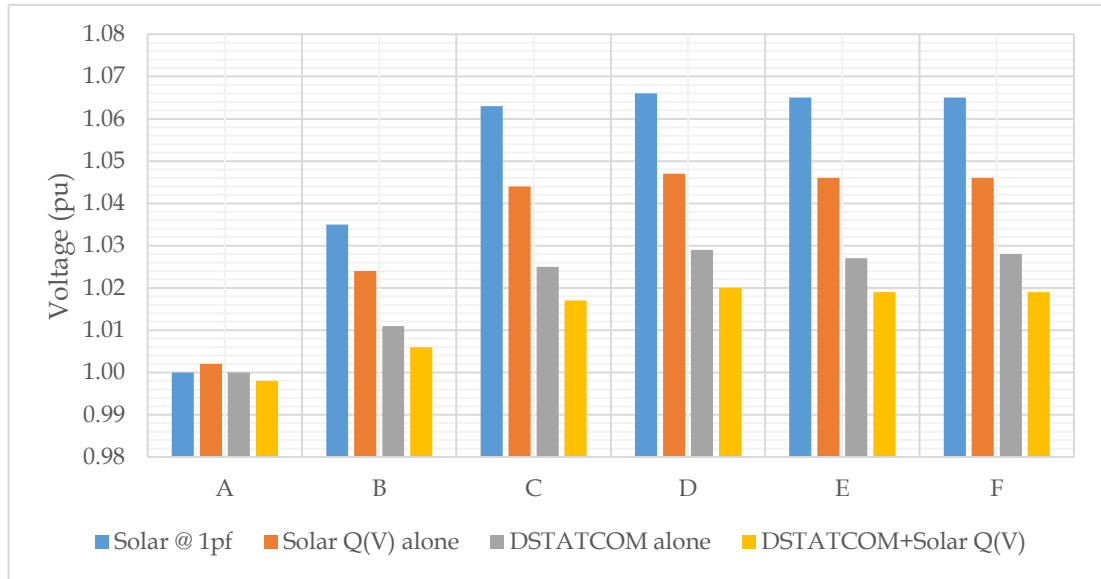


Figure 6.6 Voltage profile of 06 locations under MLC

Table 6.2 Voltage summary of the 06 locations under MLC

| | A | B | C | D | E | F |
|--------------------------------------|--------------|--------------|--------------|--------------|--------------|--------------|
| Study 1 | 1.000 | 1.035 | 1.063 | 1.066 | 1.065 | 1.065 |
| Study 2 | 1.002 | 1.024 | 1.044 | 1.047 | 1.046 | 1.046 |
| Study 3 | 1.000 | 1.011 | 1.025 | 1.029 | 1.027 | 1.028 |
| Study 4 | 0.998 | 1.006 | 1.017 | 1.020 | 1.019 | 1.019 |
| Overall Voltage Reduction (%) | 0.20% | 2.80% | 4.33% | 4.32% | 4.32% | 4.32% |

It was noted that a maximum voltage reduction of 4.33% has been obtained with the coordinated voltage control mechanism.

According to the results in table 6.2, it is evident that the DER operating at volt-var mode is marginally sufficient to maintain the voltages within the stipulated limits.

6.3 Influence of DSTATCOM Location on Voltage Profile

In order to study the influence of DSTATCOM location, DSTATCOM was connected to bus no. 39 and 52 simultaneously. The Bus nos. 39 and 52 both includes in the same LCZ which is marked in appendix 13 (A14). It is seen that the there is no voltage change except the bus nos. 50, 51 and 52 within the LCZ.

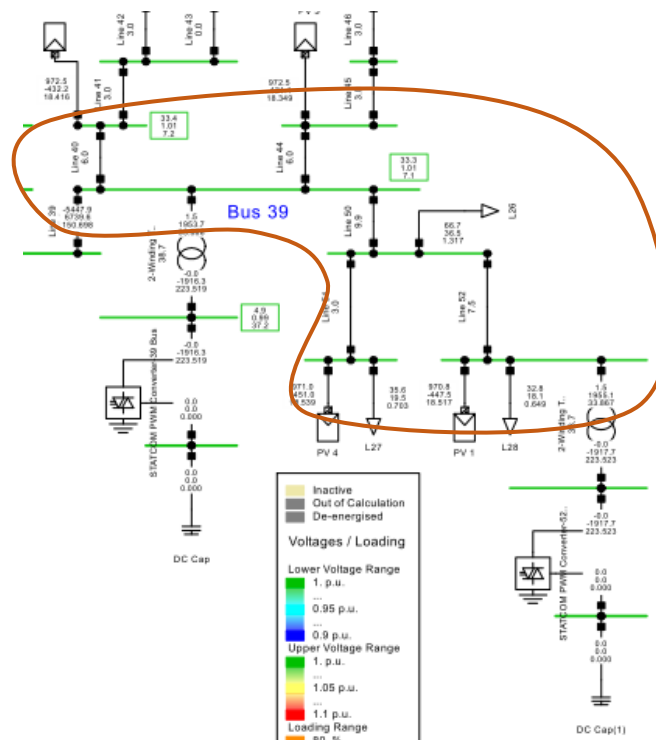


Figure 6.7 Identification of LCZs of DSTATCOMs

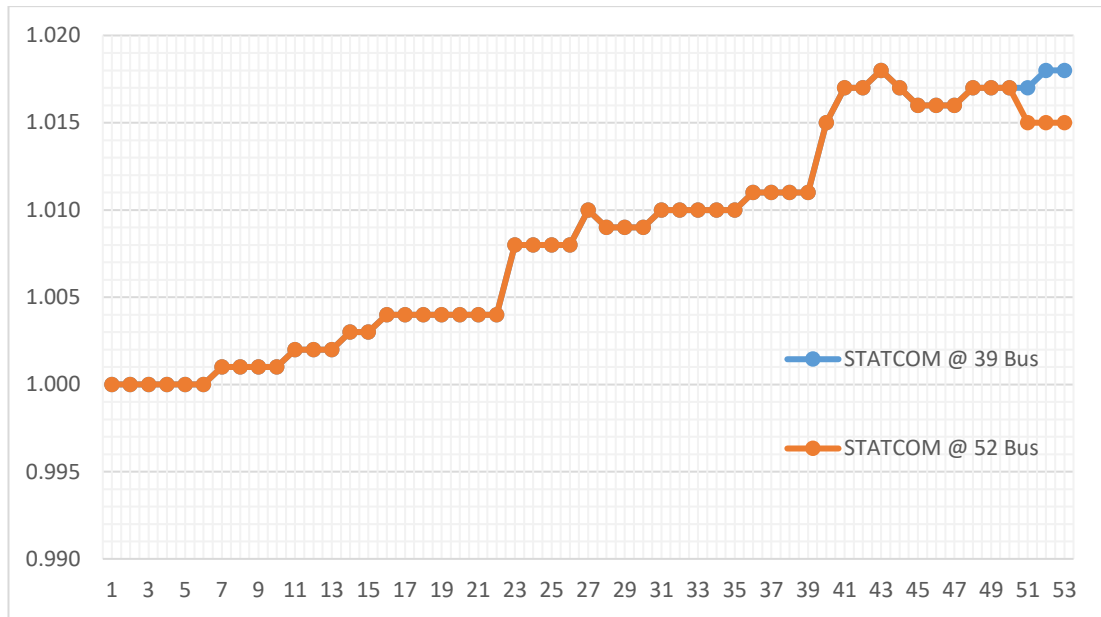


Figure 6.8 Mauara feeder voltage against DSTATCOM location

6.4 Influence of Dead Band Voltage of Solar PV on Voltage Profile

When the DER is operating under voltage-reactive power mode, dead band voltage to be defined in which reactive power compensation becomes idle. The principle, is discussed in chapter 5.2.

In earlier chapter 6.2, voltage reference was set to 1.0 pu and dead band voltage set to 0.98 pu to 1.02 pu in order to maintain the proper coordination between DER and DSTATCOM.

The dead band voltage has a direct connection with reactive power injection/ absorption as its reactive power delivering droop facilitates the relationship between voltage and the reactive power. Reactive power injection/ absorption was calculated for different dead band voltages in order to study the influence of it.

The amount of reactive power absorption against different dead band voltages were studied and mentioned in table 6.3. The same data were plotted in figure 6.9.

Table 6.3 Reactive power absorption vs dead band voltage

| Dead Band Voltage (pu) | Reactive power absorption (kVar) | | | | | |
|------------------------|----------------------------------|-------|-------|-------|-------|-------|
| | PV1 | PV2 | PV3 | PV4 | PV5 | PV6 |
| 0.00 | 489.4 | 489.4 | 489.4 | 489.4 | 489.4 | 489.4 |
| 0.02 | 489.4 | 489.4 | 489.4 | 489.4 | 489.4 | 489.4 |
| 0.04 | 450.9 | 432.6 | 423.5 | 454.3 | 454.9 | 434.7 |
| 0.06 | 335.2 | 315.6 | 305.9 | 338.9 | 339.4 | 317.9 |
| 0.08 | 218.7 | 197.6 | 187.3 | 222.6 | 223 | 200.1 |
| 0.10 | 101.2 | 78.7 | 67.8 | 105.3 | 105.7 | 81.4 |

It is clear that the increase of dead band voltage resulted in decrease of reactive power absorption, since the idling period of DER increases.

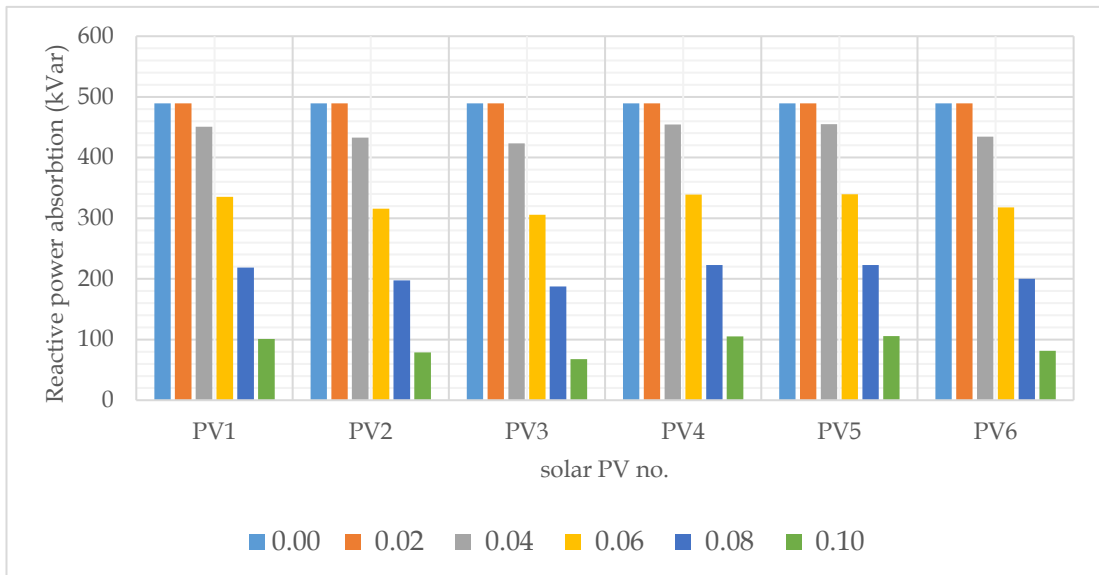


Figure 6.9 Reactive power absorption vs dead band voltage of DER

6.5 Conclusion

The developed voltage control mechanism was adopted to Mauara feeder of Embilipitiya GSS under TLC and MLC. The both control mechanisms, i.e. local control mechanism and coordinated voltage control mechanism, were simulated and results were tabled. The results show that the over voltage occurrences due to the large scale solar PV systems can be successfully omitted by proposed coordinated voltage control method.

During the MLC, local control mechanism of DER marginally sufficient to maintain the voltage at stipulated limits, i.e. 0.95pu - 1.05. However, there might be chances of over voltage occurrences due to sudden load drops in the network as the system voltage is very nearly to 1.05 pu. Therefore, it is recommended to have the coordinated voltage control mechanism which assures to lie voltages at each and every bus of the feeder within stipulated limits.

In addition, influence of the DSTATCOM location was analyzed in Mauara feeder and results show that the changing the DSTATCOM location within the LCZ would not disturb the voltage profile along the feeder. However, the voltage at the DSTATCOM connection will be changed as the reactive power absorbing point changes within the LCZ.

Furthermore, the influence of the dead band voltage was analyzed and to understood that the higher the dead band voltage lower the reactive power compensation capability of DER.

CHAPTER 7

CONCLUSIONS AND RECOMMENDATIONS

7.1 General Conclusions

With the global tendency of extracting renewable energy, solar energy has become very popular in both Sri Lanka and globally. As a result of that, it was identified that voltages violations may occur especially in lightly loaded feeders due the “Battle for Solar Energy” program.

This thesis investigated the performance of coordinated decentralized control mechanism in order to control the over voltages and maintain the voltage levels within its stipulated limits. It was analyzed the coordination between two local voltage controllers; Volt-var control of DG and DSTATCOM, can be used to increase the voltage controllability.

In this research, a novel concept of coordinated decentral control mechanism was instigated with the concept of LCZ where the network is divided in to several LCZs for the ease of controllability. Apart from the conventional DSTATCOM models, a fresh DSTATCOM model is developed to monitor each and every bus voltage within the LCZ and acts as the primary voltage control device. The volt-var control of DG was set to act as the secondary voltage support device.

Initially, the coordinated voltage control mechanism was developed in IEEE 33 bus test system. The successful implementation of the novel voltage control method then adopted to Mauara feeder of the Embilipitiya GSS which was identified as one of the feeders getting effected (or experiencing over-voltages) due to the “battle for solar energy” program.

The Mauara feeder simulations were performed under two load conditions. i.e. TLC and MLC. The summary of the feeder voltages pertaining to the said simulations are as follows.

Table 7.1 Summary of the Mauara Feeder simulations

| | TLC | MLC |
|-----------------------------------------------|------------|------------|
| Max. Voltage Point | D | D |
| Voltage prior to the coordinated control (pu) | 1.06 | 1.07 |
| Voltage with local Q(V) mode of DG (pu) | 1.04 | 1.05 |
| Voltage after the coordinated control (pu) | 1.02 | 1.02 |
| Voltage improvement (%) | 3.8 | 4.3 |

It was clearly understood by table 7.1 that the local Q(V) control of DG marginally sufficient enough to maintain the voltage within operational safe limits, i.e. 0.95pu - 1.05pu. However, the chance of violating the voltage limits is high due to following reasons, since the voltages are slightly acceptable.

1. Increase of generation with the solar PV systems in LV network during the mid-day. Accordingly, the loads sensed by the MV network during the mid-day decreases and the situation gets worse than the minimum mid-day load condition.
2. Sudden loss of load in the MV network. Accordingly, generation increases and situation gets worse than the minimum mid-day load condition.

Further, it was guaranteed that the voltage along the feeder lies below 1.02 pu with the application of coordinated decentral voltage control mechanism. The voltage profile of the distribution network was further analyzed with respect to the DSTATCOM location and the dead band voltage of the DG.

7.2 Research Findings

The research findings are as follows.

1. An evaluation of coordinated decentralized control structure that can provide both dynamic and steady state voltage support under the active distribution network environment.

2. Both voltage control devices; Volt-var control of DG and DSTATCOM, are fast-acting, thus, capable of providing reactive power into the network instantly when needed.
3. LCZ is defined to exemplify the voltage controllable area of DSTATCOM where each bus in the LCZ is actively monitored by DSTATCOM.
4. The interaction between voltage control devices are addressed when those devices in the same LCZ.

7.3 Suggestions for Future Work

Suggestions for future research are as follows.

1. In this thesis, over-voltage is only concerned as the PQ issue in the distribution network. However, investigation on harmonic issues pertaining to the DG have to be addressed.
2. It was assumed that DG provides 1MW of active power in to the distribution network, hence, DSTATCOM model in this research is used to study the static voltage improvement of the distribution network. Dynamic voltage study to be carried out based on the dynamic characteristics of the DG.
3. Economic feasibility study based on the cost benefit analysis to be performed considering the dynamic voltage study of the distribution network.
4. There are different control modes of DG as described in chapter 5.1. Identifying the best possible control mode in order to maximize the renewable energy extraction to be analyzed in different constraints of the network.

REFERENCES

1. Renewables 2018, Global Status Report (www.ren21.net) (online)
2. "100% ELECTRICITY GENERATION THROUGH RENEWABLE ENERGY BY 2050", Assessment of Sri Lanka's Power Sector, Co-publication of the Asian Development Bank and the United Nations Development Programme.
3. A. Bayod-Rújula, "Future development of the electricity systems with distributed generation," *Energy*, vol. 34, pp. 377-383, 2009.
4. Chapa udayakiran, Sk.hussain vali, "Design of Battery Energy Storage System (BESS) Support Dynamic Voltage Restorer (DVR) to reduce the rating of Voltage Source Converter (VSC) applied to IEEE 11,33 &69 bus systems," 2017 IEEE 7th International Advance Computing Conference, Hyderabad, India, 2017
5. <https://solarvest.my/large-scale-solar/> (online)
6. <http://www.energy.gov.lk/Solar/> (online)
7. "IEEE Standard for Interconnection and Interoperability of Distributed Energy Resources with Associated Electric Power Systems Interfaces," *IEEE std 1547-2018*, 2018.
8. "IEEE Recommended Practice for Monitoring Electric Power Quality," *IEEE Std 1159-2009*, 2009.
9. B. Blazic, I. Papic, "Voltage profile support in distribution networks 14; influence of the network R/X ratio", *2008 13th International Power Electronics and Motion Control Conference*, pp. 2510-2515, 2008.
10. F. Zhang *et al.*, "The reactive power voltage control strategy of PV systems in low-voltage string lines," *2017 IEEE Manchester PowerTech*, Manchester, 2017, pp. 1-6.

11. J. de Oliveira Quevedo *et al.*, "Analysis and Design of an Electronic On-Load Tap Changer Distribution Transformer for Automatic Voltage Regulation," in *IEEE Transactions on Industrial Electronics*, vol. 64, no. 1, pp. 883-894, Jan. 2017.
12. A. Kumar and R. S. Bhatia, "Optimal capacitor placement in radial distribution system," *2014 IEEE 6th India International Conference on Power Electronics (IICPE)*, Kurukshetra, 2014, pp. 1-6.
13. C. L. Masters, "Voltage rise: the big issue when connecting embedded generation to long 11 kV overhead lines," in *Power Engineering Journal*, vol. 16, no. 1, pp. 5-12, Feb. 2002.
14. De Kock, Jan; Strauss, Cobus. *Practical Power Distribution for Industry*. Elsevier. 2004. pp. 74–75.
15. J. Arrillaga, N. R. Watson, *Power System Harmonics*. Wiley. p. 126.
16. M. H. Haque, "Compensation of distribution system voltage sag by DVR and D-STATCOM," *2001 IEEE Porto Power Tech Proceedings (Cat. No.01EX502)*, Porto, Portugal, 2001, pp. 5 pp. vol.1-.
17. D. Nair, M. Raveendran, A. Nambiar, N. P. Mohan and S. Sampath, "Mitigation of power quality issues using DSTATCOM," *2012 International Conference on Emerging Trends in Electrical Engineering and Energy Management (ICETEEEM)*, Chennai, 2012, pp. 65-69.
18. J. von Appen, M. Braun, T. Stetz, K. Diwold and D. Geibel, "Time in the Sun: The Challenge of High PV Penetration in the German Electric Grid," in *IEEE Power and Energy Magazine*, vol. 11, no. 2, pp. 55-64, March-April 2013.
19. P. Pachanapan, O. Anaya-Lara, A. Dysko and K. L. Lo, "Adaptive Zone Identification for Voltage Level Control in Distribution Networks With DG," in *IEEE Transactions on Smart Grid*, vol. 3, no. 4, pp. 1594-1602, Dec. 2012.

20. N. Efkarpidis, T. Wijnhoven, C. Gonzalez, T. De Rybel and J. Driesen, "Coordinated voltage control scheme for Flemish LV distribution grids utilizing OLTC transformers and D-STATCOM's," *12th IET International Conference on Developments in Power System Protection (DPSP 2014)*, Copenhagen, 2014, pp. 1-6.
21. <https://nptel.ac.in/courses/108107114/31> (online)
22. Bhim Singh, Ambrish Chandra, Kamal Al-Haddad. *Power Quality: Problems and Mitigation Techniques*, Chichester, West Sussex, United Kingdom : Wiley, 2015, Chapter 4.4.2
23. Huilian Liao, Sami Abdelrahman, Zhixuan Liu, Jovica V. Milanović, Thomas Wood, Kai Strunz, "Methodology for optimising QoS mitigation infrastructure based on differentiated customer requirements"
24. Robert Kowalak, "Modelling of Power Electronic Compensators for the Analysis of Power System Operation", *Acta Energetica 4/17 (2013)*, pp 48–55,
25. Arif Wazir, Naeem Arbab, "Analysis and Optimization of IEEE 33 Bus Radial Distributed System Using Optimization Algorithm", *Journal of Emerging Trends in Applied Engineering* (ISSN 2518-4059), Vol. 1, No. 2, 2016
26. M. Kumar, A. Swarnkar, N. Gupta et al., "Design and operation of DSTATCOM for power quality improvement in distribution systems", *The 6th International Conference on Renewable Power Generation (RPG)*, 19–20 October 2017.
27. X. Hou *et al.*, "A General Decentralized Control Scheme for Medium-/High-Voltage Cascaded STATCOM," in *IEEE Transactions on Power Systems*, vol. 33, no. 6, pp. 7296-7300, Nov. 2018.
28. G. Farivar, C. D. Townsend, B. Hredzak, J. Pou, V. G. Agelidis, "Passive reactor compensated cascaded H-Bridge multilevel LC-StatCom", *IEEE Trans. Power Electron.*, vol. 32, no. 11, pp. 8338-8348, Nov. 2017.

29. S. Kartakis, A. Fu, M. Mazo and J. A. McCann, "Communication Schemes for Centralized and Decentralized Event-Triggered Control Systems," in *IEEE Transactions on Control Systems Technology*, vol. 26, no. 6, pp. 2035-2048, Nov. 2018.
30. Y. Xia, W. Wei, Y. Peng, P. Yang and M. Yu, "Decentralized Coordination Control for Parallel Bidirectional Power Converters in a Grid-Connected DC Microgrid," in *IEEE Transactions on Smart Grid*, vol. 9, no. 6, pp. 6850-6861, Nov. 2018.
31. O. Stursberg and C. Hillmann, "Decentralized Optimal Control of Distributed Interdependent Automata With Priority Structure," in *IEEE Transactions on Automation Science and Engineering*, vol. 14, no. 2, pp. 785-796, April 2017.

APPENDICES

A1. Power Quality in Distribution Network

Summary of the categories and characteristics of power system as per the IEEE Standard 1159-2009 are tabulated below.

Table A1.1. Power quality disturbances in distribution networks

| Categories | Typical spectral content | Typical duration | Typical voltage magnitude |
|--------------------------------|--------------------------|------------------|---------------------------|
| 1.0 Transients | | | |
| 1.1 Impulsive | | | |
| 1.1.1 Nanosecond | 5 ns rise | < 50 ns | |
| 1.1.2 Microsecond | 1 μ s rise | 50 ns–1 ms | |
| 1.1.3 Millisecond | 0.1 ms rise | > 1 ms | |
| 1.2 Oscillatory | | | |
| 1.2.1 Low frequency | < 5 kHz | 0.3–50 ms | 0–4 pu |
| 1.2.2 Medium frequency | 5–500 kHz | 20 μ s | 0–8 pu |
| 1.2.3 High frequency | 0.5–5 MHz | 5 μ s | 0–4 pu |
| 2.0 Short duration variations | | | |
| 2.1 Instantaneous | | | |
| 2.1.1 Sag | | 0.5–30 cycles | 0.1–0.9 pu |
| 2.1.2 Swell | | 0.5–30 cycles | 1.1–1.8 pu |
| 2.2 Momentary | | | |
| 2.2.1 Interruption | | 0.5 cycles–3 s | < 0.1 pu |
| 2.2.2 Sag | | 30 cycles–3 s | 0.1–0.9 pu |
| 2.2.3 Swell | | 30 cycles–3 s | 1.1–1.4 pu |
| 2.3 Temporary | | | |
| 2.3.1 Interruption | | 3 s–1 min | < 0.1 pu |
| 2.3.2 Sag | | 3 s–1 min | 0.1–0.9 pu |
| 2.3.3 Swell | | 3 s–1 min | 1.1–1.2 pu |
| 3.0 Long duration variations | | | |
| 3.1 Interruption, sustained | | > 1 min | 0.0 pu |
| 3.2 Undervoltages | | > 1 min | 0.8–0.9 pu |
| 3.3 Overvoltages | | > 1 min | 1.1–1.2 pu |
| 4.0 Voltage imbalance | | steady state | 0.5–2% |
| 5.0 Waveform distortion | | | |
| 5.1 DC offset | | steady state | 0–0.1% |
| 5.2 Harmonics | 0–100th H | steady state | 0–20% |
| 5.3 Interharmonics | 0–6 kHz | steady state | 0–2% |
| 5.4 Notching | | steady state | |
| 5.5 Noise | broad-band | steady state | 0–1% |
| 6.0 Voltage fluctuations | < 25 Hz | intermittent | 0.1–7% |
| 7.0 Power frequency variations | | < 10 s | |

A2. Overview of major FACTS devices

The two categories of power flow control devices are the conventional (mechanically switched) and power electronics-based devices in which summary and comparison are mentioned in figure A2.1 and A2.2 respectively.

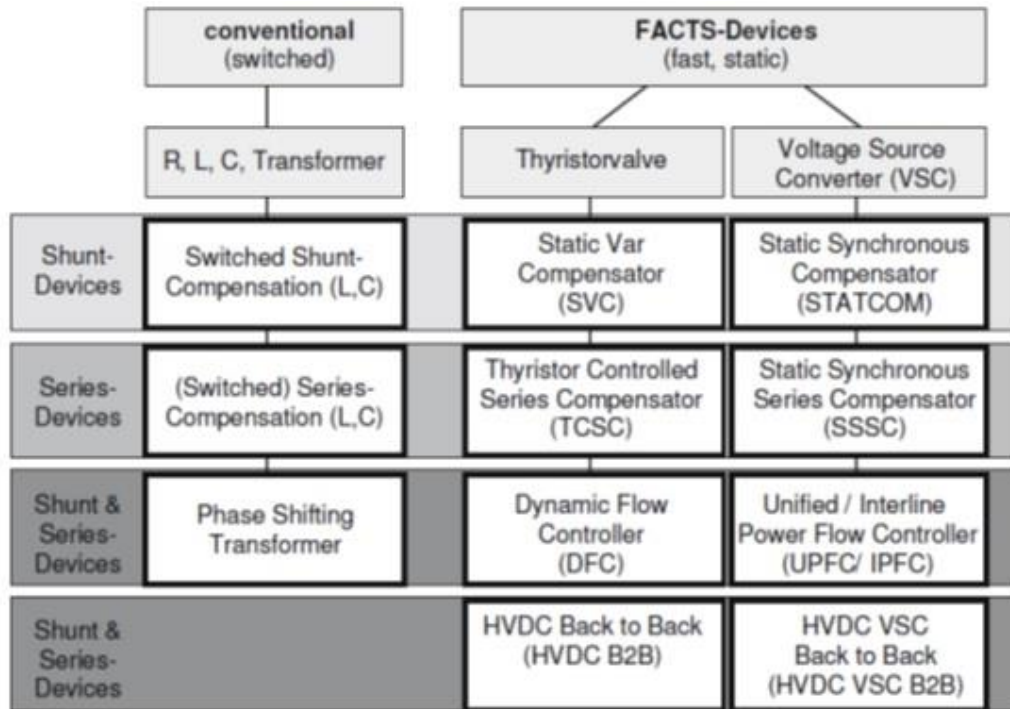


Figure A2.1. Overview of major FACTS devices

| | Speed of response | Repeated operation possible | Steps | "Inductive" control | Inertia (active power) | Cost CAPEX / OPEX |
|--------------------------------|-------------------|---------------------------------------|------------|---------------------|------------------------------------|----------------------------------------|
| Switched capacitors (reactors) | Slow | Discharge time and wear of switchgear | Fixed | No | No | Low |
| Thyristor switched capacitors | Fast | Yes | Fixed | No | No | Medium |
| SVC | Fast | Continuous | Continuous | Yes | No | Cheaper than STATCOM for large systems |
| Synchronous condenser | Fast | Continuous | Continuous | Yes | Yes | High OPEX, bad MTTR, permanent losses |
| STATCOM | Fast | Continuous | Continuous | Yes | Possible with added energy storage | High CAPEX if no hybrid solution |

Figure A2.2. FACTS comparison

A3. Summary of Power System Analysis Modelling Capability

| Type of Modelling | Purpose | Study Types | Examples of Software Packages |
|--------------------------------------------------|-----------------------------------------------------------------------------------------------------------|---------------------------------------------------------------------------------------------------------------|-----------------------------------------------------------------------------------|
| Steady state power system analysis | Assessment of voltage and thermal conditions, fault levels | Load flow, voltage step, fault level contribution of DG | DlgSILENT, DINIS, ERACS, ETAP, IPSA, Power World, PSS/E, SKM Power Tools, OpenDSS |
| Dynamic power system analysis | Assessment of the transient and dynamic behaviour of equipment e.g. generators, DFIGs, and/or the network | Transient stability, critical clearing time, dynamic voltage step/control, fault ride through | DlgSILENT, DINIS, ERACS, ETAP, IPSA, Power World, PSS/E, SKM Power Tools |
| Harmonic analysis | Assessment of harmonics, distortion levels and identification of resonances | Impedance scan, harmonic load flow (including impact of VSC) | DlgSILENT, ERACS, ETAP, IPSA, PSS SincaI, SKM Power Tools |
| Electro-Magnetic Transient (EMT) Analysis | Assessment of eletro-magnetic transients and phenomena | Insulation coordination (lightning, switching), HVDC/ FACTS equipment design, sub-synchronous resonance (SSR) | ATP-EMTP, EMTP-RV, PSCAD/ EMTDC |
| Real Time Simulation (RTS) | Closed loop and scenario testing in real time | Real time simulations, protection testing, control system testing | RTDS, Opal-RT |
| Hybrid Simulation | Assessment of multiple models/ programs in the same dynamic simulation environment | Dynamic analysis of the interaction between two systems | ETRAN (PSS/E and PSCAD) |
| Multi-Domain Analysis | Assessment of multiple systems and their interactions | Study of interactions between electrical, power electronic, mechanical and fluid dynamic systems | MATLAB (including Simulink and SPS/Simulink), DYMOLA |

DlgSILENT Power Factory Version 15 offers a number of improvements on its predecessor, including voltage profile optimization for bi-directional power flows (where voltage profile was cited as a concern by DNOs) and a techno-economic evaluation capability for grid expansion strategies.

A4. Phase Locked Loop

This Phase Locked Loop (PLL) is a device that generates an output signal whose phase is related to the phase of an input reference signal. PLL contains an internal oscillator that is synchronized by being phase locked with some grid power signal. For this case, it is locked to voltage in the system. In new model, this PLL is connected to LV bus bar.

The basic structure of a PLL is shown in figure A4.1. Phase detector produces a signal proportional to the phase difference between V (input reference signal) and V' (output signal). Loop Filter is a low pass filter to cut off higher frequency signals. Finally, voltage controlled oscillator adjust its frequency such that phase of input signal and output signal are matched.

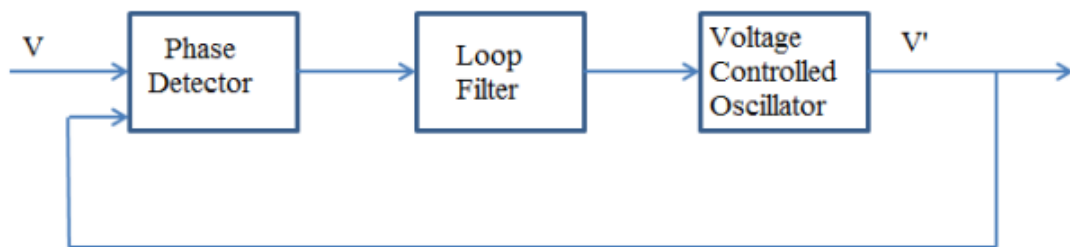


Figure A4.1 Basic Structure of a PLL

A5. Voltage-Reactive Power (Volt-Var)

An example voltage-reactive power characteristic is shown in Figure H.4. The voltage-reactive power characteristic shall be configured in accordance with the default parameter values specified in Table 8 if not specified by the Area EPS operator. If specified by the Area EPS operator, the voltage-reactive power characteristic shall be configured using values in the optional adjustable range. The voltage-reactive power characteristics shall be adjustable locally and/or remotely as specified by the Area EPS operator.

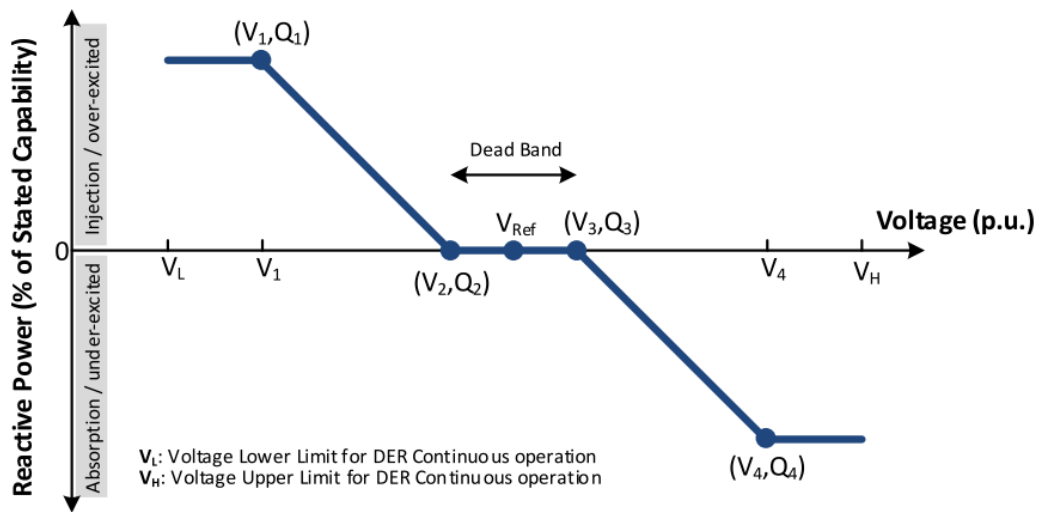


Figure H.4—Example voltage-reactive power characteristic

**Table 8—Voltage-reactive power settings for normal operating performance
Category A and Category B DER**

| Voltage-reactive power parameters | Default settings | | Ranges of allowable settings | |
|-----------------------------------|----------------------------------------------------|----------------------------------------------------|-----------------------------------------------------------------|---------------------------------------------------------------------|
| | Category A | Category B | Minimum | Maximum |
| V_{Ref} | V_N | V_N | $0.95 V_N$ | $1.05 V_N$ |
| V_2 | V_N | $V_{Ref} - 0.02 V_N$ | Category A: V_{Ref} Category B: $V_{Ref} - 0.03 V_N$ | V_{Ref}^c |
| Q_2 | 0 | 0 | 100% of nameplate reactive power capability, absorption | 100% of nameplate reactive power capability, injection |
| V_3 | V_N | $V_{Ref} + 0.02 V_N$ | V_{Ref}^c | Category A: V_{Ref} Category B: $V_{Ref} + 0.03 V_N$ |
| Q_3 | 0 | 0 | 100% of nameplate reactive power capability, absorption | 100% of nameplate reactive power capability, injection |
| V_1 | $0.9 V_N$ | $V_{Ref} - 0.08 V_N$ | $V_{Ref} - 0.18 V_N$ | $V_2 - 0.02 V_N^c$ |
| Q_1^a | 25% of nameplate apparent power rating, injection | 44% of nameplate apparent power rating, injection | 0 | 100% of nameplate reactive power capability, injection ^b |
| V_4 | $1.1 V_N$ | $V_{Ref} + 0.08 V_N$ | $V_3 + 0.02 V_N^c$ | $V_{Ref} + 0.18 V_N$ |
| Q_4 | 25% of nameplate apparent power rating, absorption | 44% of nameplate apparent power rating, absorption | 100% of nameplate reactive power capability, absorption | 0 |
| Open loop response time | 10 s | 5 s | 1 s | 90 s |

^aThe DER reactive power capability may be reduced at lower voltage.

^bIf needed DER may reduce active power output to meet this requirement.

^cImproper selection of these values may cause system instability.

A6. Active Power-Reactive Power (Watt-Var)

Example active power-reactive power characteristic is shown in Figure H.5. The target characteristic shall be configured in accordance with the default parameter values shown in Table 9. The characteristics shall be allowed to be configured as specified by the Area EPS operator using the values specified in the optional adjustable range.

The left-hand side of Figure H.5 and corresponding requirements specified in Table 9 shall only apply to DER capable of absorbing active power.

The active power-reactive power characteristics are allowed to be adjusted locally and/or remotely as specified by the Area EPS operator.

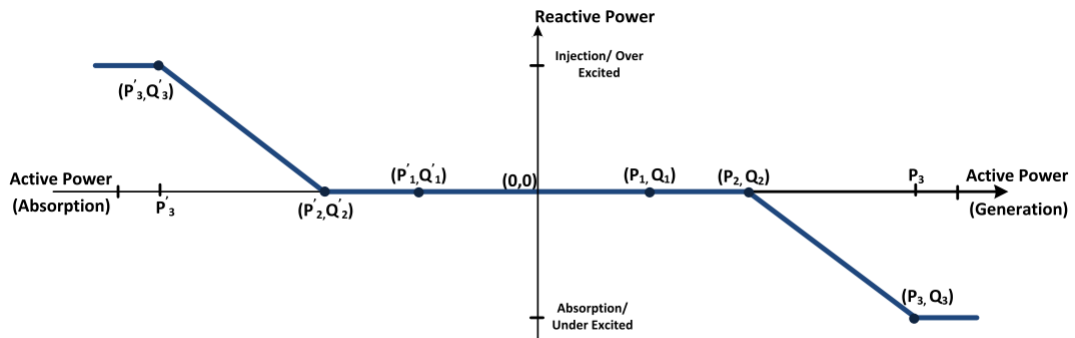


Figure H.5—Example active power-reactive power characteristic

Table 9—Active power-reactive power settings for normal operating performance
Category A and Category B DER

| Active power-reactive power parameters | Default settings | | Ranges of allowable settings | |
|----------------------------------------|-------------------------------------------------------------------|----------------------------------------------------|--------------------------------------------------------|-------------------------------------------------------|
| | Category A | Category B | Minimum | Maximum |
| P_3 | P_{rated} | | $P_2 + 0.1 P_{\text{rated}}$ | P_{rated} |
| P_2 | $0.5 P_{\text{rated}}$ | | $0.4 P_{\text{rated}}$ | $0.8 P_{\text{rated}}$ |
| P_1 | The greater of $0.2 P_{\text{rated}}$ and P_{min} | | P_{min} | $P_2 - 0.1 P_{\text{rated}}$ |
| P'_1 | The lesser of $0.2 \times P_{\text{rated}}$ and P'_{min} | | $P'_2 - 0.1 P'_{\text{rated}}$ | P'_{min} |
| P'_2 | $0.5 P'_{\text{rated}}$ | | $0.8 P'_{\text{rated}}$ | $0.4 P'_{\text{rated}}$ |
| P'_3 | P'_{rated} | | P'_{rated} | $P'_2 + 0.1 P'_{\text{rated}}$ |
| Q_3 | 25% of nameplate apparent power rating, absorption | 44% of nameplate apparent power rating, absorption | 100% of nameplate reactive power absorption capability | 100% of nameplate reactive power injection capability |
| Q_2 | 0 | | | |
| Q_1 | 0 | | | |
| Q'_1 | 0 | | | |
| Q'_2 | 0 | | | |
| Q'_3 | 44% of nameplate apparent power rating, injection | | | |

NOTE— P_{rated} is the nameplate active power rating of the DER.
 P'_{rated} is the maximum active power that the DER can absorb.
 P_{min} is the minimum active power output of the DER.
 P'_{min} is the minimum, in amplitude, active power that the DER can absorb.
 P' parameters are negative in value.

A7. Voltage-Active Power (Volt-Watt)

Two examples of these characteristics are shown in Figure H.6. The characteristic shall be configured in accordance with the default parameter values specified in Table 10 for the given DER normal operating performance category. The characteristic may be configured as specified by the Area EPS operator using the values in the adjustable range.

If enabled, the voltage-active power mode shall remain active while any of the voltage-reactive power modes described in 5.3 are enabled. For DER that do not absorb active power, P_2 , which is the minimum set point for active power generation due to overvoltage, is subject to the equipment capability. If P_2 is outside the continuous operation region of the DER, the active power generation is allowed to be reduced to the minimum DER capability instead of P_2 or DER shutting down.

DER that can inject and absorb active power, P'_2 , which is the maximum set point for active power absorption change due to system overvoltage, is subject to the equipment capability. If P'_2 is outside the continuous operation region of the DER, the active power absorption is allowed to be reduced to the maximum absorption capability instead of P'_2 or DER shutting down.

The voltage-active power characteristics curves are allowed to be adjusted locally and/or remotely as specified by the Area EPS operator.

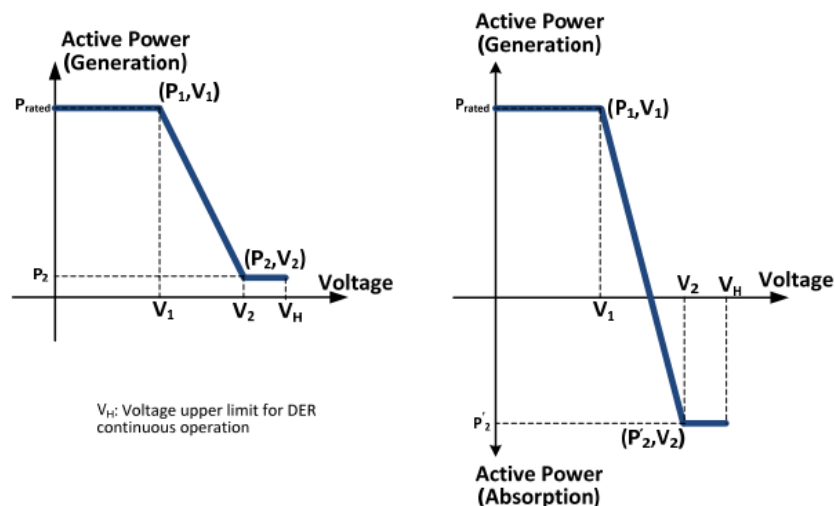


Figure H.6—Example voltage-active power characteristic

Table 10—Voltage-active power settings for Category A and Category B DER

| Voltage-active power parameters | Default settings | Ranges of allowable settings | |
|----------------------------------------------------------------------|----------------------------------------------|------------------------------|--------------|
| | | Minimum | Maximum |
| V_1 | $1.06 V_N$ | $1.05 V_N$ | $1.09 V_N$ |
| P_1 | P_{rated} | N/A | N/A |
| V_2 | $1.1 V_N$ | $V_1 + 0.01 V_N$ | $1.10 V_N$ |
| P_2 (applicable to DER that can only generate active power) | The lesser of $0.2 P_{rated}$ or P_{min}^a | P_{min} | P_{rated} |
| P'_2 (applicable to DER that can generate and absorb active power) | 0 ^b | 0 | P'_{rated} |
| Open Loop Response Time | 10 s ^c | 0.5 s | 60 s |

^a P_{min} is the minimum active power output in p.u. of the DER rating (i.e., 1.0 p.u.).

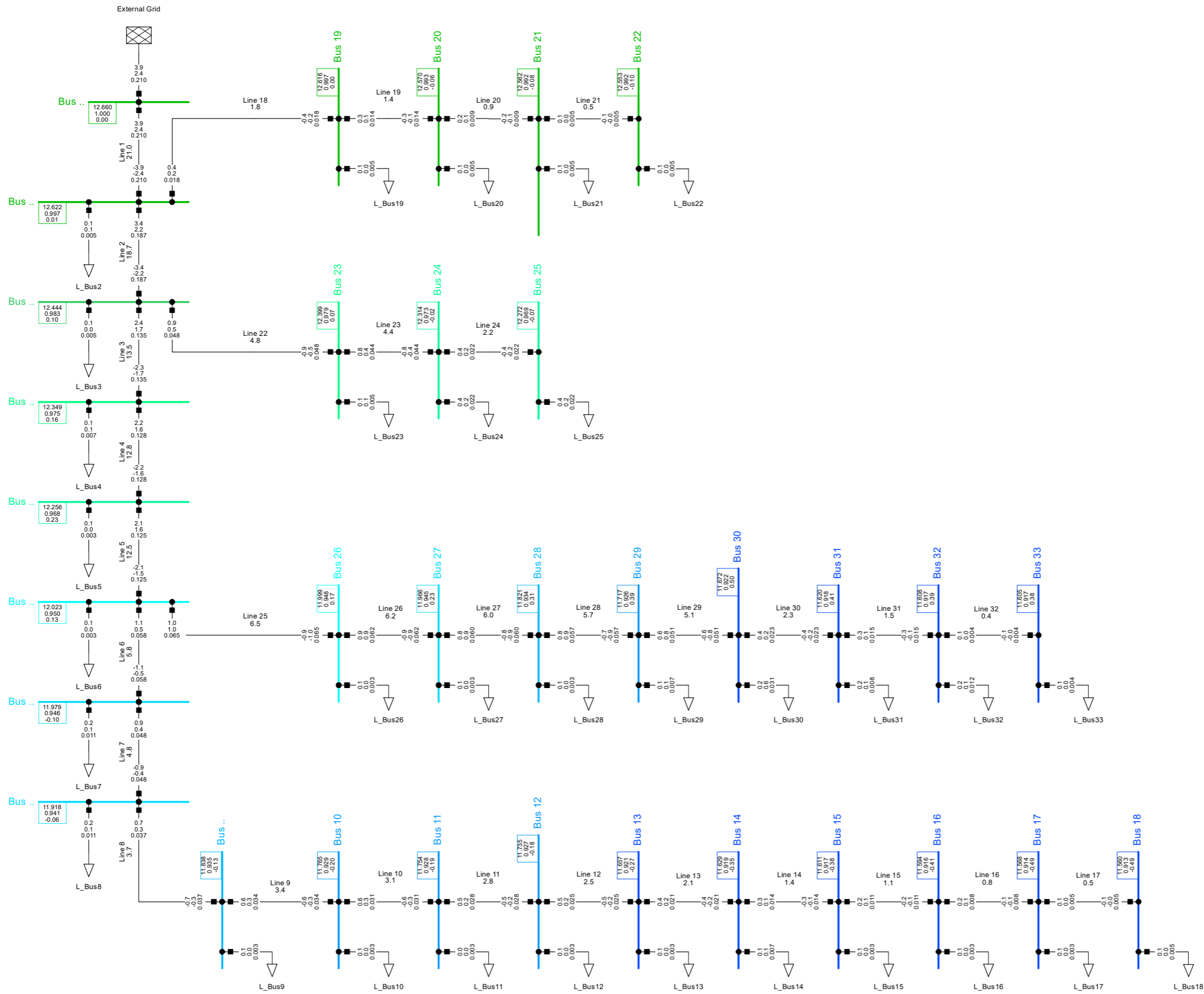
^b P'_{rated} is the maximum amount of active power that can be absorbed by the DER. ESS operating in the negative real power half plane, through charging, shall follow this curve as long as available energy storage capacity permits this operation.

^cAny settings for the open loop response time of less than 3 s shall be approved by the Area EPS operator with due consideration of system dynamic oscillatory behavior.

A8. Records Generated for IEEE 33 Bus Network in DIgSILENT PowerFactory

A8.1 Single Line Diagram

A8.2 Bus Voltages Diagram



Legend

- Inactive (Yellow box)
- Out of Calculation (Grey box)
- De-energised (Dark Grey box)

Voltages / Loading

Lower Voltage Range

- 1. p.u. (Green)
- 0.95 p.u. (Cyan)
- 0.9 p.u. (Blue)

Upper Voltage Range

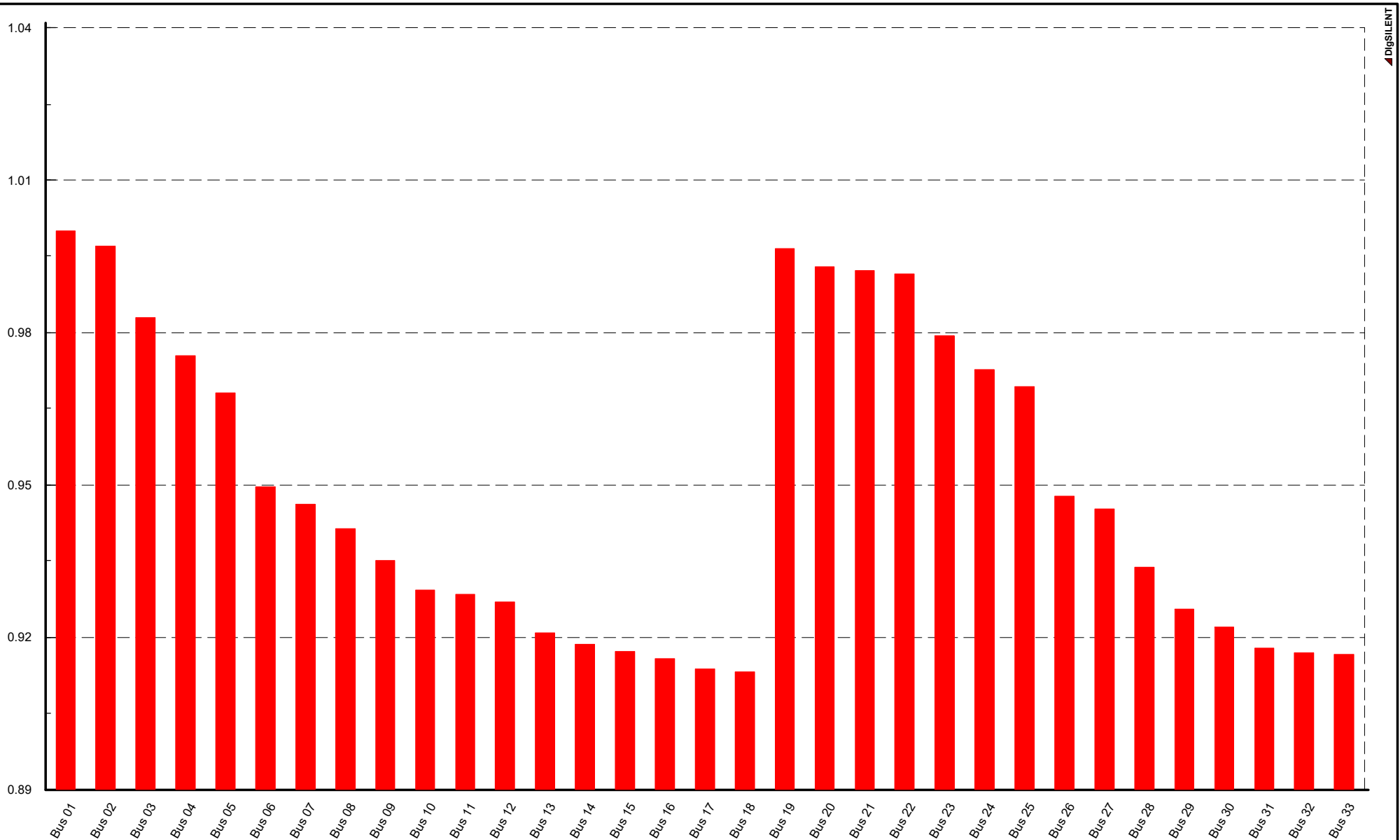
- 1. p.u. (Green)
- 1.05 p.u. (Yellow)
- 1.1 p.u. (Red)

Loading Range

- 80. % (Yellow)
- 100. % (Red)

| | |
|--------------------------------------|---------------------------|
| Load Flow Balanced | |
| Nodes | Branches |
| UI Line-Line Voltage, Magnitude [kV] | P Active Power [MW] |
| u Voltage, Magnitude [p.u.] | Q Reactive Power [Mvar] |
| phi Voltage, Angle [deg] | I Current, Magnitude [kA] |

| | |
|-----------------------|---------------------------|
| PowerFactory 2018 SP5 | Project: |
| | Graphic: 33-Bus with Solo |
| | Date: 5/12/2019 |
| | Annex: |

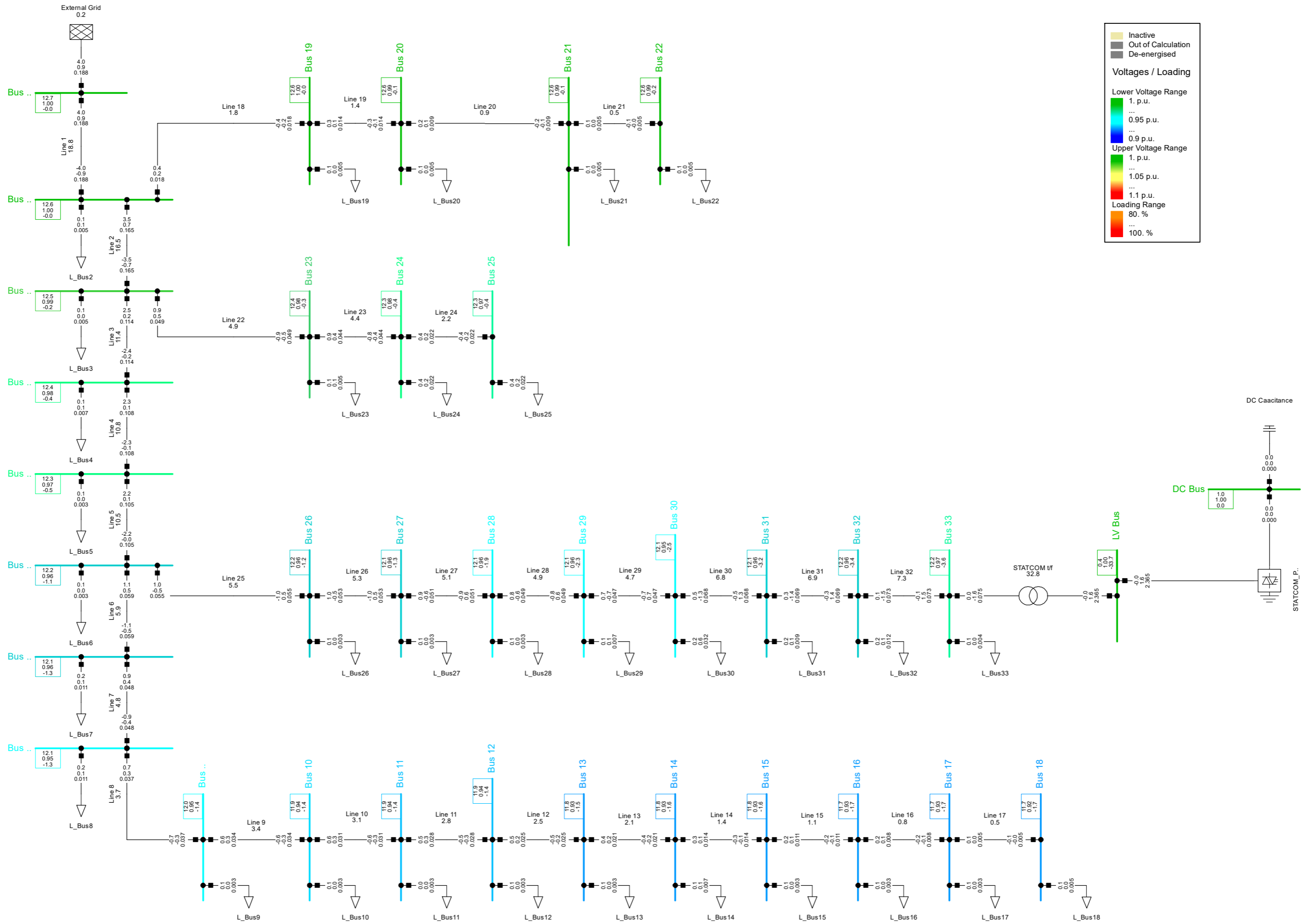


■ Voltage, Magnitude in p.u.

**A9. Records Generated for IEEE 33 Bus Network with DSTATCOM in
DIgSILENT PowerFactory**

A9.1 Single Line Diagram

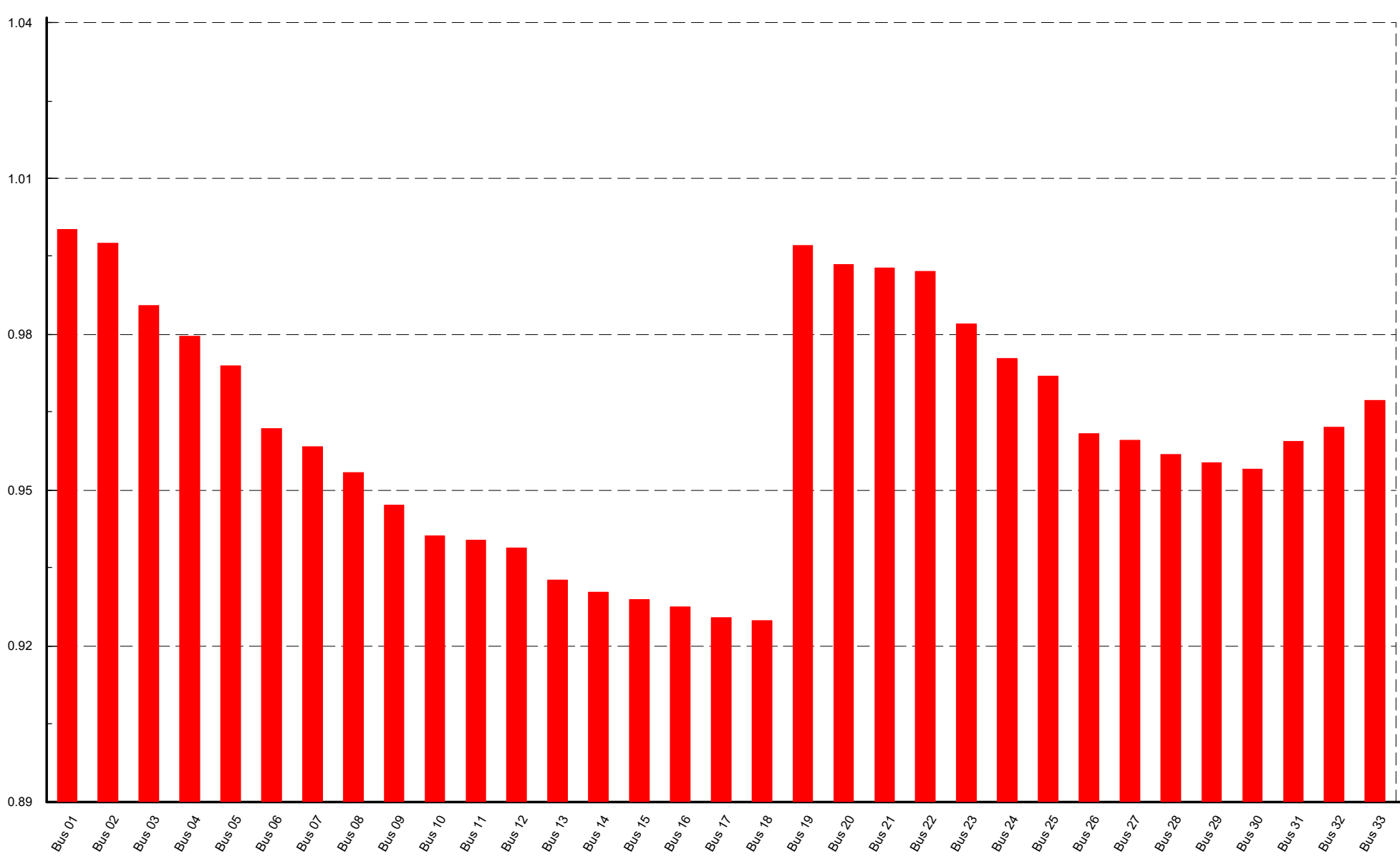
A9.2 Bus Voltages Diagram



Simulation RMS,balanced 10:000 s

| Nodes | Branches |
|--------------------------------------|---------------------------|
| UI Line-Line Voltage, Magnitude [kV] | P Active Power [MW] |
| u Voltage, Magnitude [p.u.] | Q Reactive Power [Mvar] |
| phiu Voltage, Angle [deg] | I Current, Magnitude [kA] |

| | |
|-----------------------|------------------|
| PowerFactory 2018 SP5 | Project: |
| | Graphic: Network |
| | Date: 5/12/2019 |
| | Annex: |

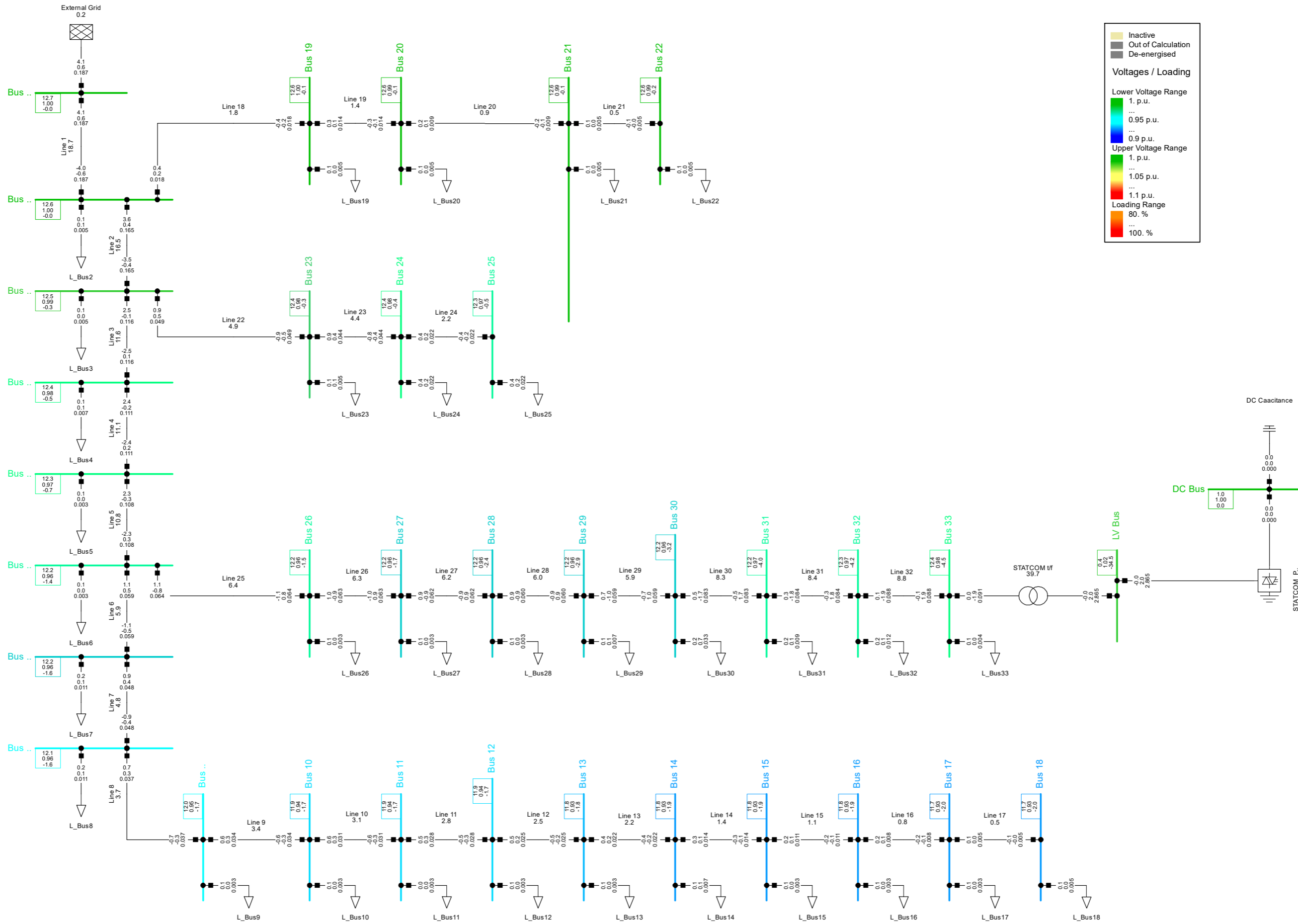


■ Voltage, Magnitude in p.u.

**A10. Records Generated for IEEE 33 Bus Network with modified DSTATCOM
in DIgSILENT PowerFactory**

A10.1 Single Line Diagram

A10.2 Bus Voltages Diagram



Legend

- Inactive (Yellow)
- Out of Calculation (Grey)
- De-energised (Dark Grey)

Voltages / Loading

Lower Voltage Range

- 1. p.u. (Green)
- 0.95 p.u. (Cyan)
- 0.9 p.u. (Blue)

Upper Voltage Range

- 1. p.u. (Yellow)
- 1.05 p.u. (Orange)
- 1.1 p.u. (Red)

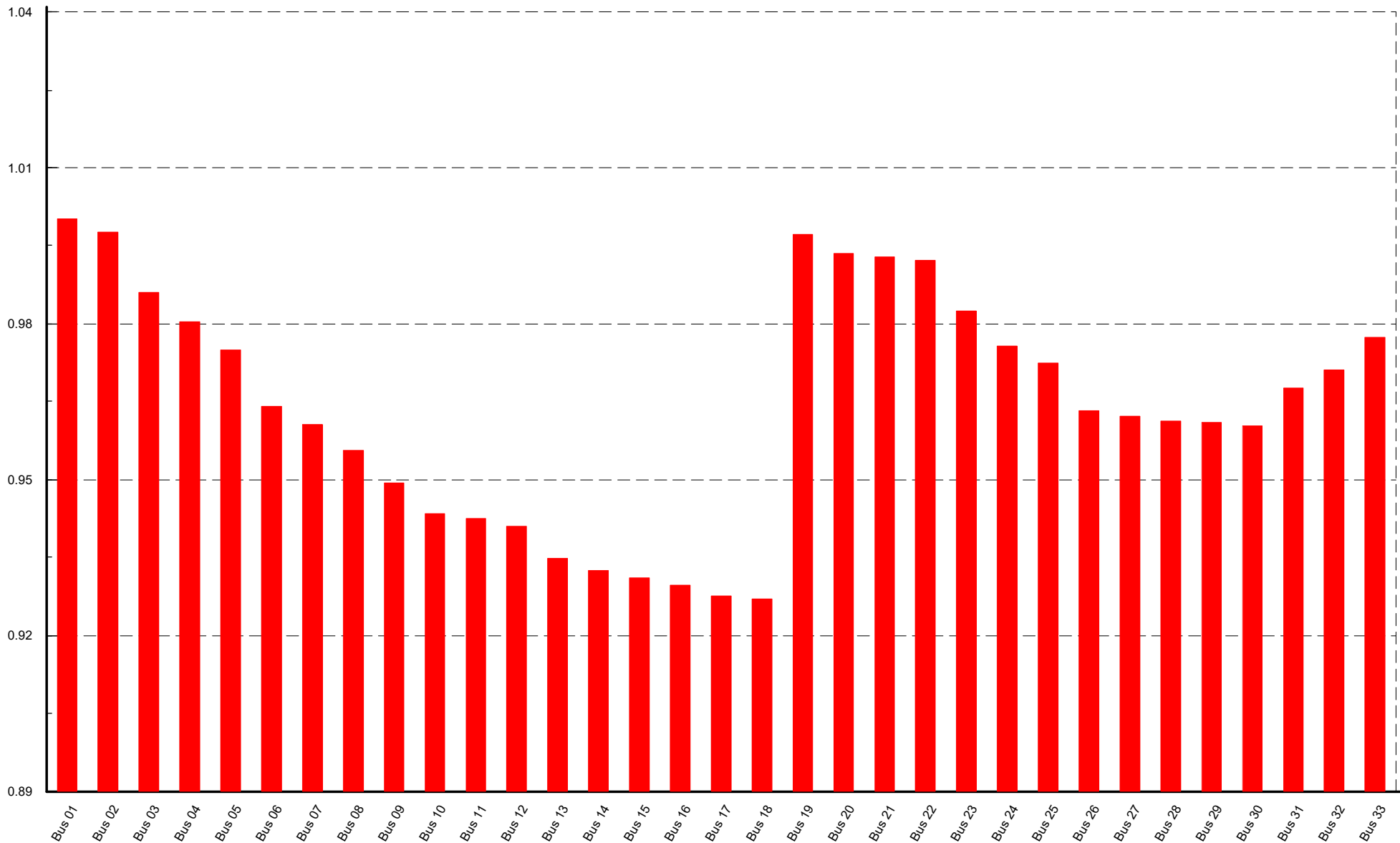
Loading Range

- 80. % (Yellow)
- 100. % (Red)

Simulation RMS,balanced 10:000 s

| Nodes | Branches |
|--------------------------------------|---------------------------|
| UI Line-Line Voltage, Magnitude [kV] | P Active Power [MW] |
| u Voltage, Magnitude [p.u.] | Q Reactive Power [Mvar] |
| phiu Voltage, Angle [deg] | I Current, Magnitude [kA] |

| | |
|-----------------------|------------------|
| PowerFactory 2018 SP5 | Project: |
| | Graphic: Network |
| | Date: 5/12/2019 |
| | Annex: |

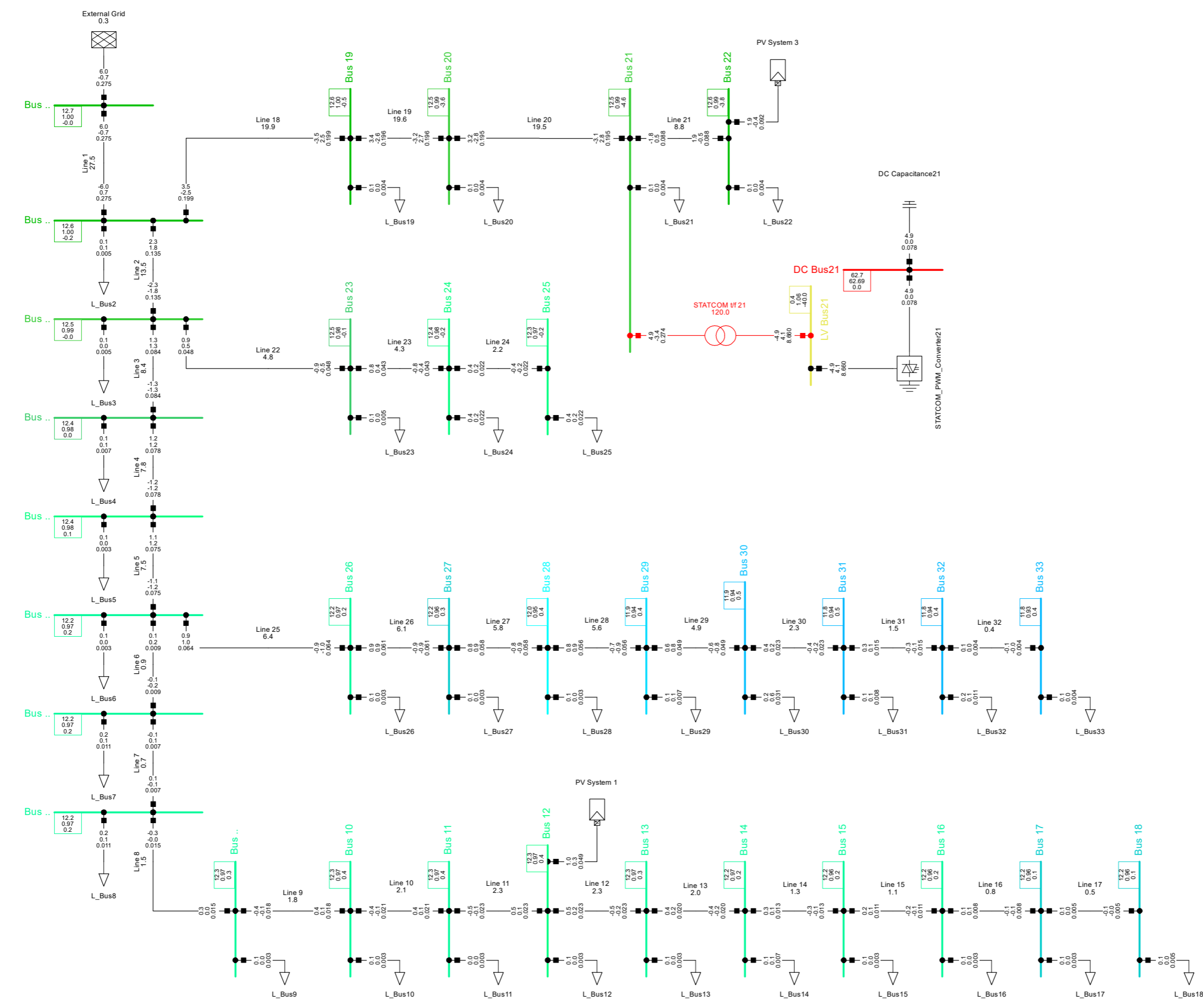


■ Voltage, Magnitude in p.u.

**A11. Records Generated for Coordinated Voltage Control between DSTATCOM
& Solar PV of IEEE 33 Bus Network in DIgSILENT PowerFactory**

A11.1 Single Line Diagram

A11.2 Bus Voltages Diagram



Legend

- Inactive (Yellow)
- Out of Calculation (Grey)
- De-energised (Dark Grey)

Voltages / Loading

Lower Voltage Range

- 1. p.u.
- 0.95 p.u.
- 0.9 p.u.

Upper Voltage Range

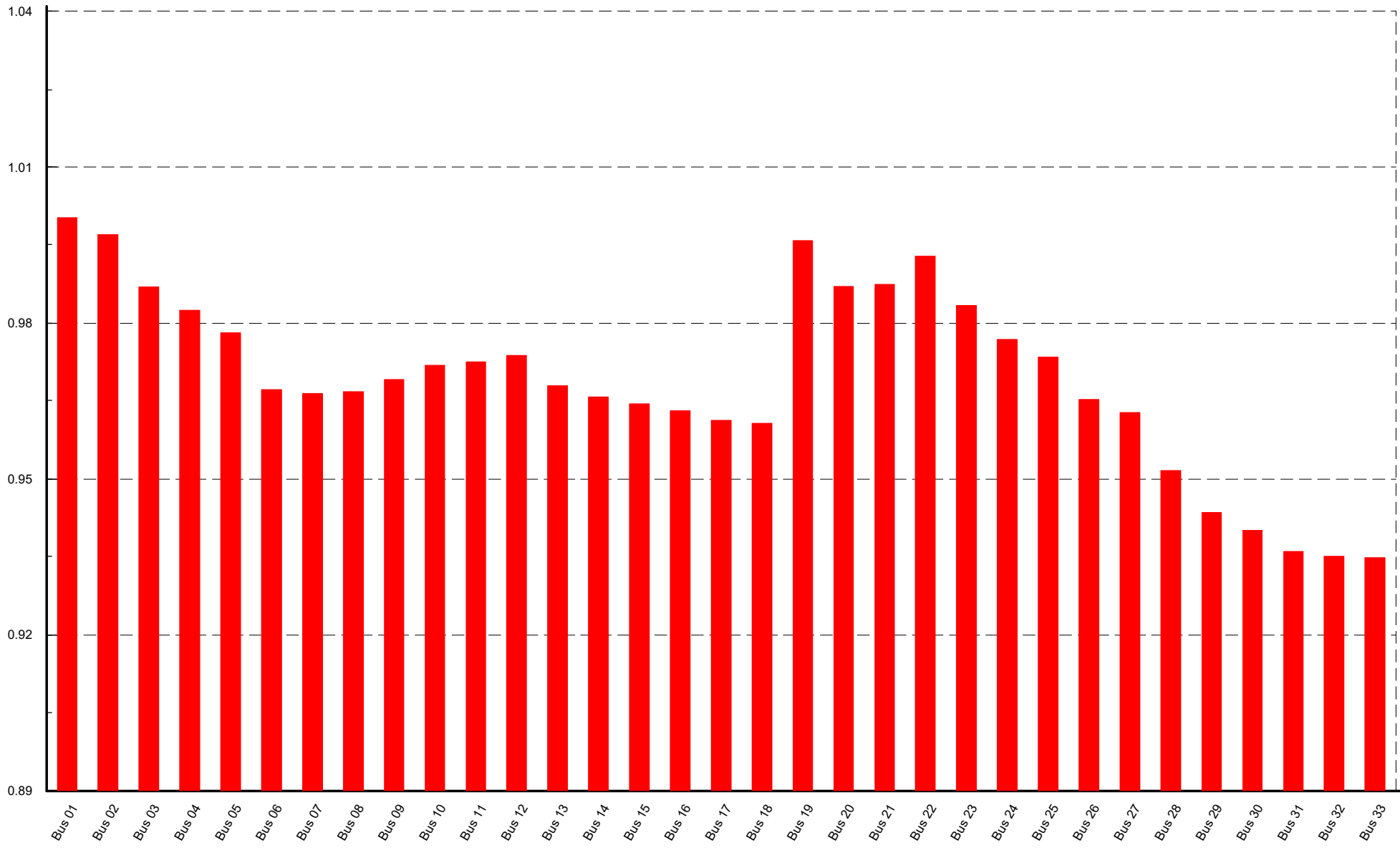
- 1. p.u.
- 1.05 p.u.
- 1.1 p.u.

Loading Range

- 80. %
- 100. %

| | |
|-------------------------------------|---------------------------|
| Simulation RMS,balanced 10:000 s | |
| Nodes | Branches |
| U Line-Line Voltage, Magnitude [kV] | P Active Power [MW] |
| u Voltage, Magnitude [p.u.] | Q Reactive Power [Mvar] |
| phi Voltage, Angle [deg] | I Current, Magnitude [kA] |

| | |
|-----------------------|------------------|
| PowerFactory 2018 SP5 | Project: |
| | Graphic: Network |
| | Date: 5/12/2019 |
| Annex: | |

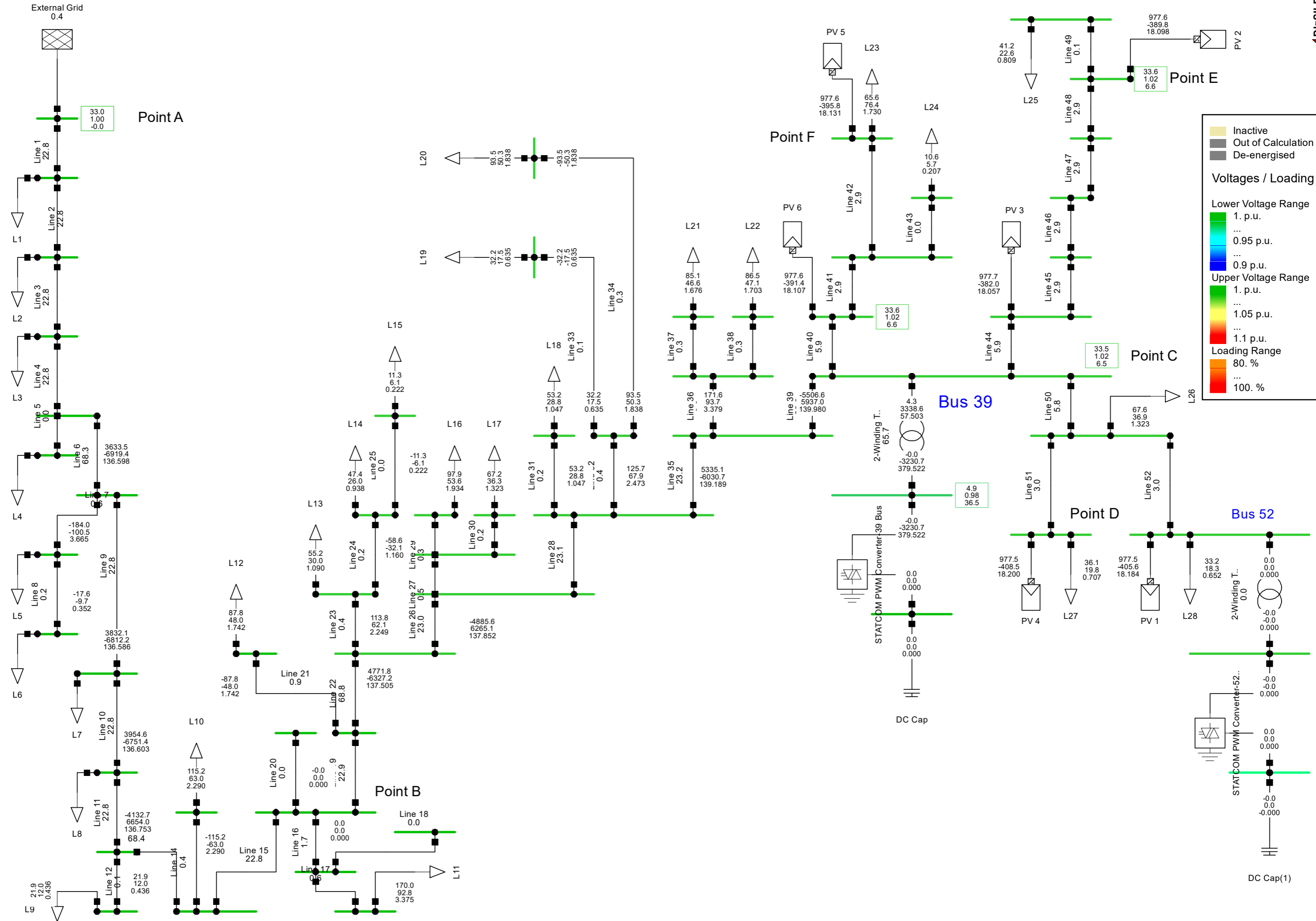


■ Voltage, Magnitude in p.u.

A12. Records Generated for Coordinated Voltage Control between DSTATCOM (@ 39 bus) & DER of Mauara Feeder in DIgSILENT PowerFactory under TLC

A12.1 Single Line Diagram

A12.2 Bus Voltages Diagram



Legend

- Inactive (Yellow)
- Out of Calculation (Grey)
- De-energised (Dark Grey)

Voltages / Loading

Lower Voltage Range

- 1. p.u. (Green)
- 0.95 p.u. (Cyan)
- 0.9 p.u. (Blue)

Upper Voltage Range

- 1. p.u. (Green)
- 1.05 p.u. (Yellow)
- 1.1 p.u. (Red)

Loading Range

- 80. % (Orange)
- 100. % (Red)

Point A

Point B

Point F

Point E

Point D

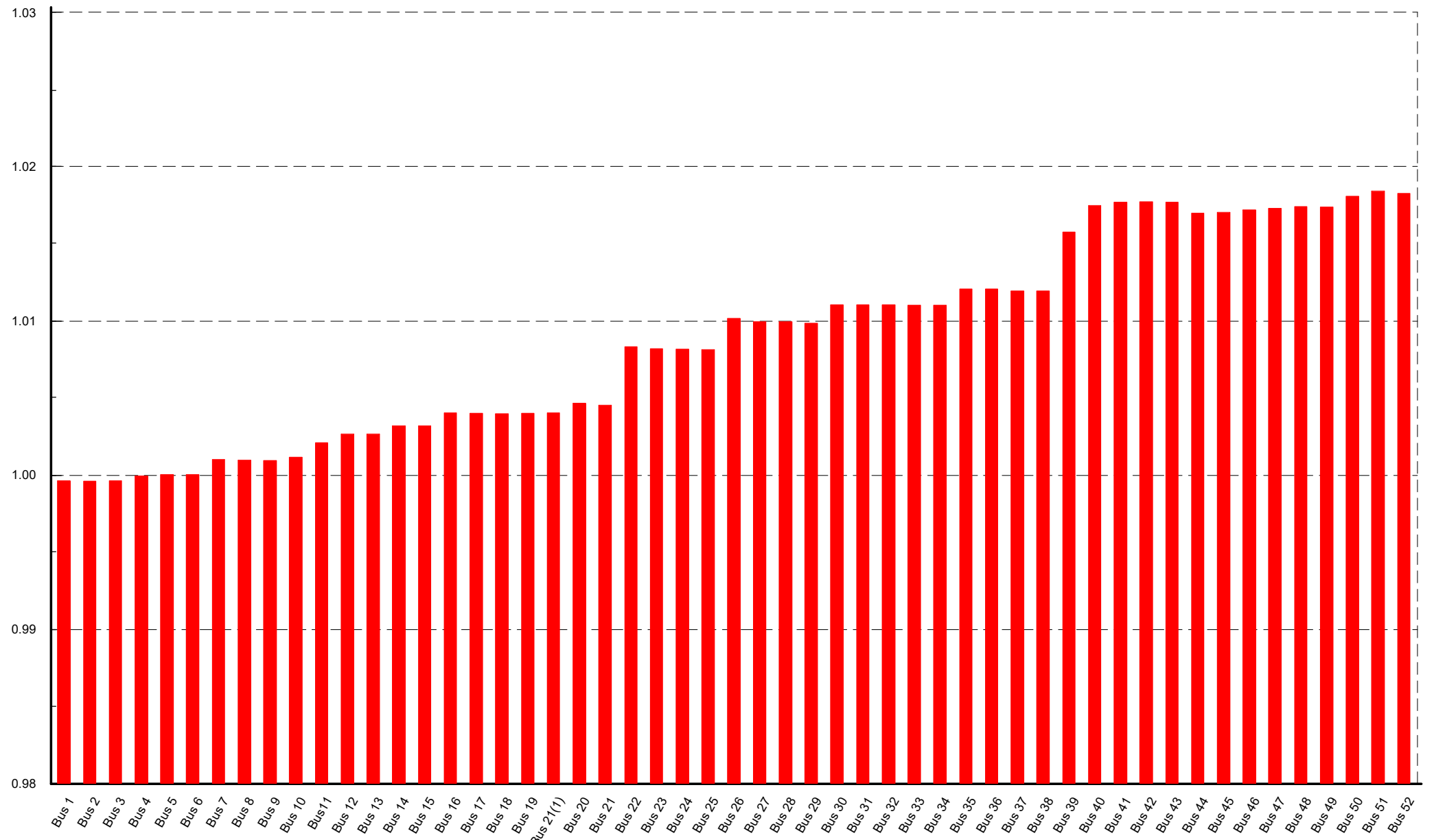
Point C

Bus 39

Bus 52

DC Cap

DC Cap(1)

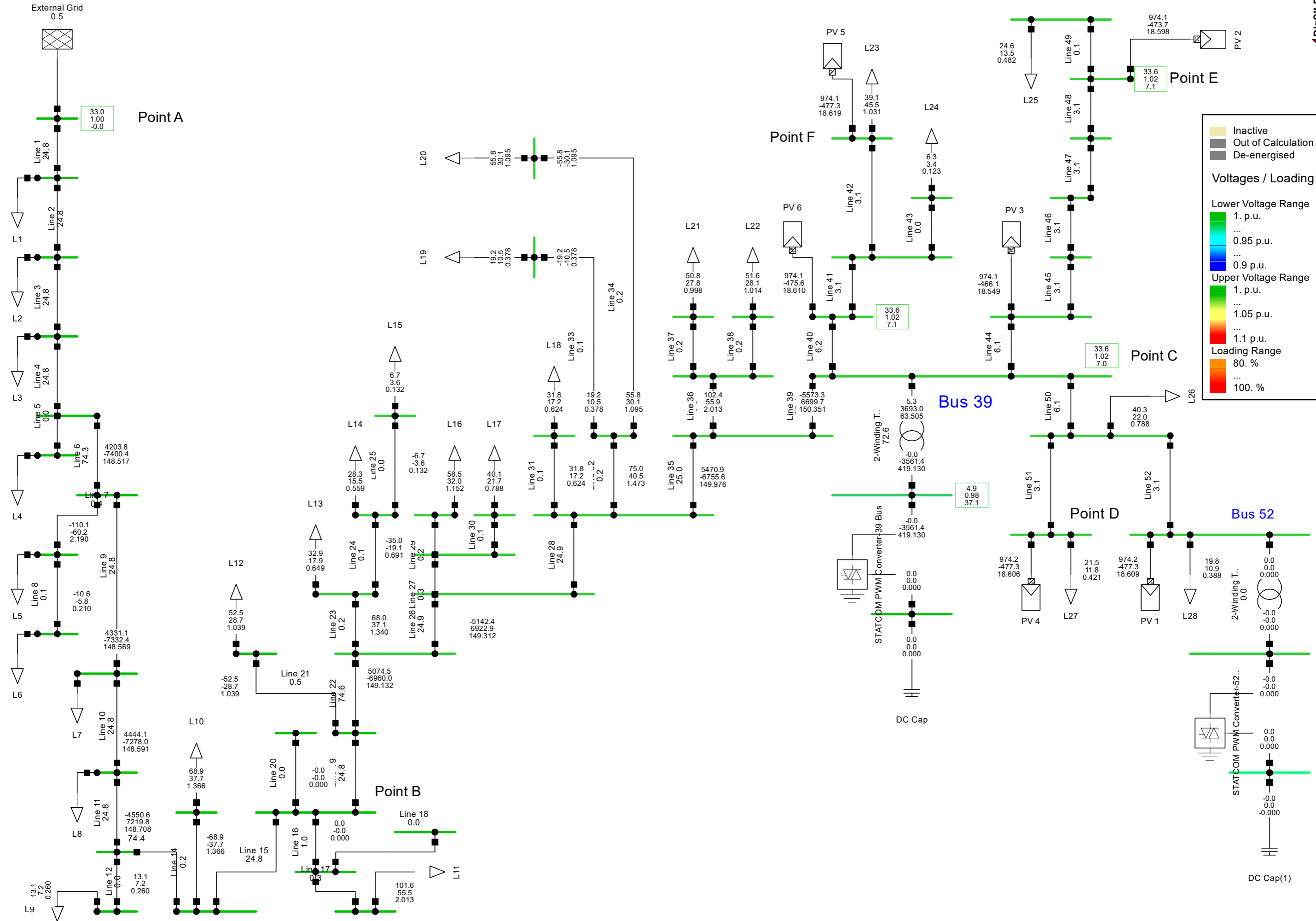


■ Voltage, Magnitude in p.u.

A13. Records Generated for Coordinated Voltage Control between DSTATCOM (@ 39 bus) & DER of Mauara Feeder in DIgSILENT PowerFactory under MLC

A13.1 Single Line Diagram

A13.2 Bus Voltages Diagram



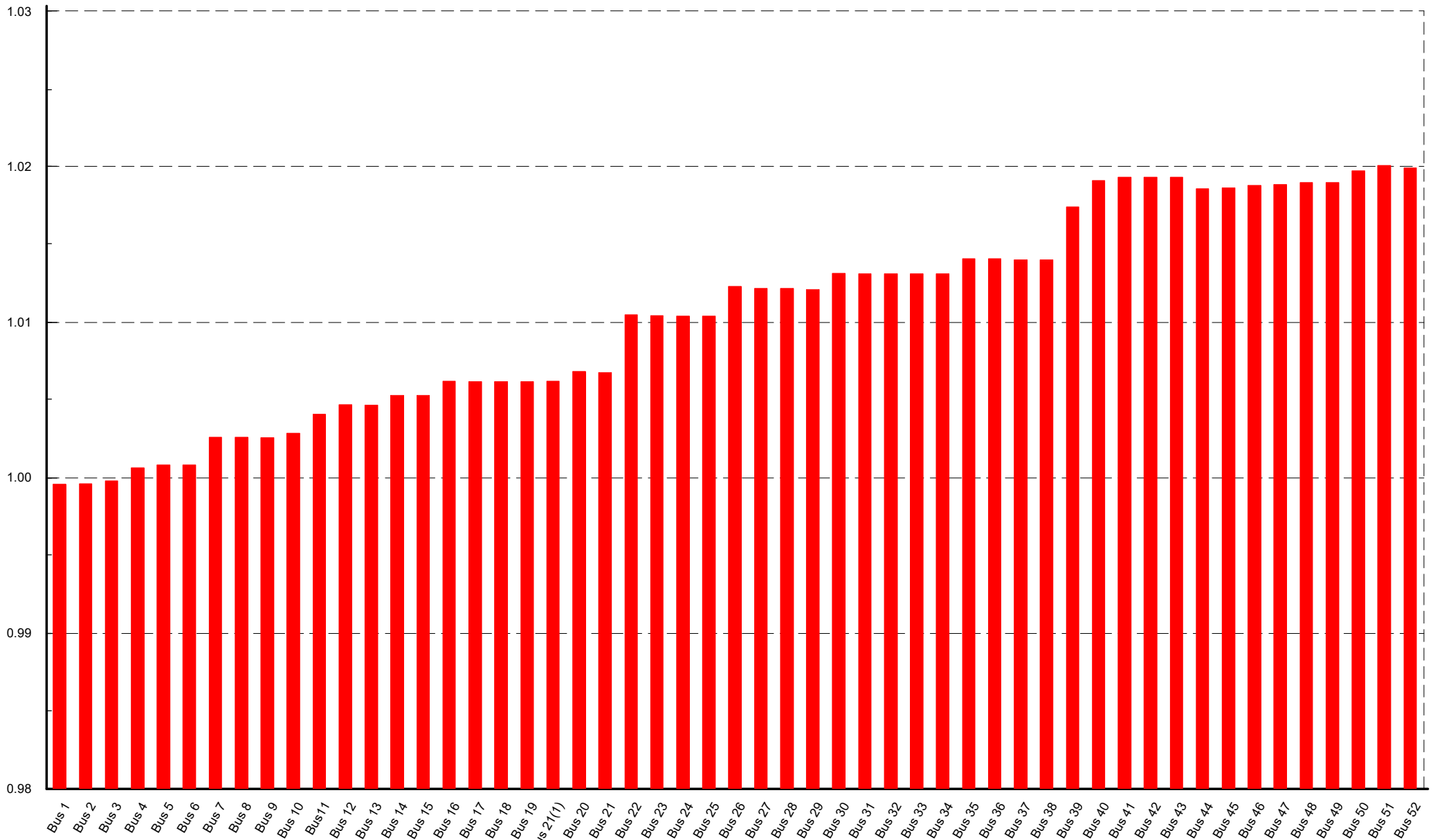
Inactive
Out of Calculation
De-energised

Voltages / Loading

Lower Voltage Range
1. p.u.
...
0.95 p.u.
...
0.9 p.u.

Upper Voltage Range
1. p.u.
...
1.05 p.u.
...
1.1 p.u.

Loading Range
80. %
...
100. %



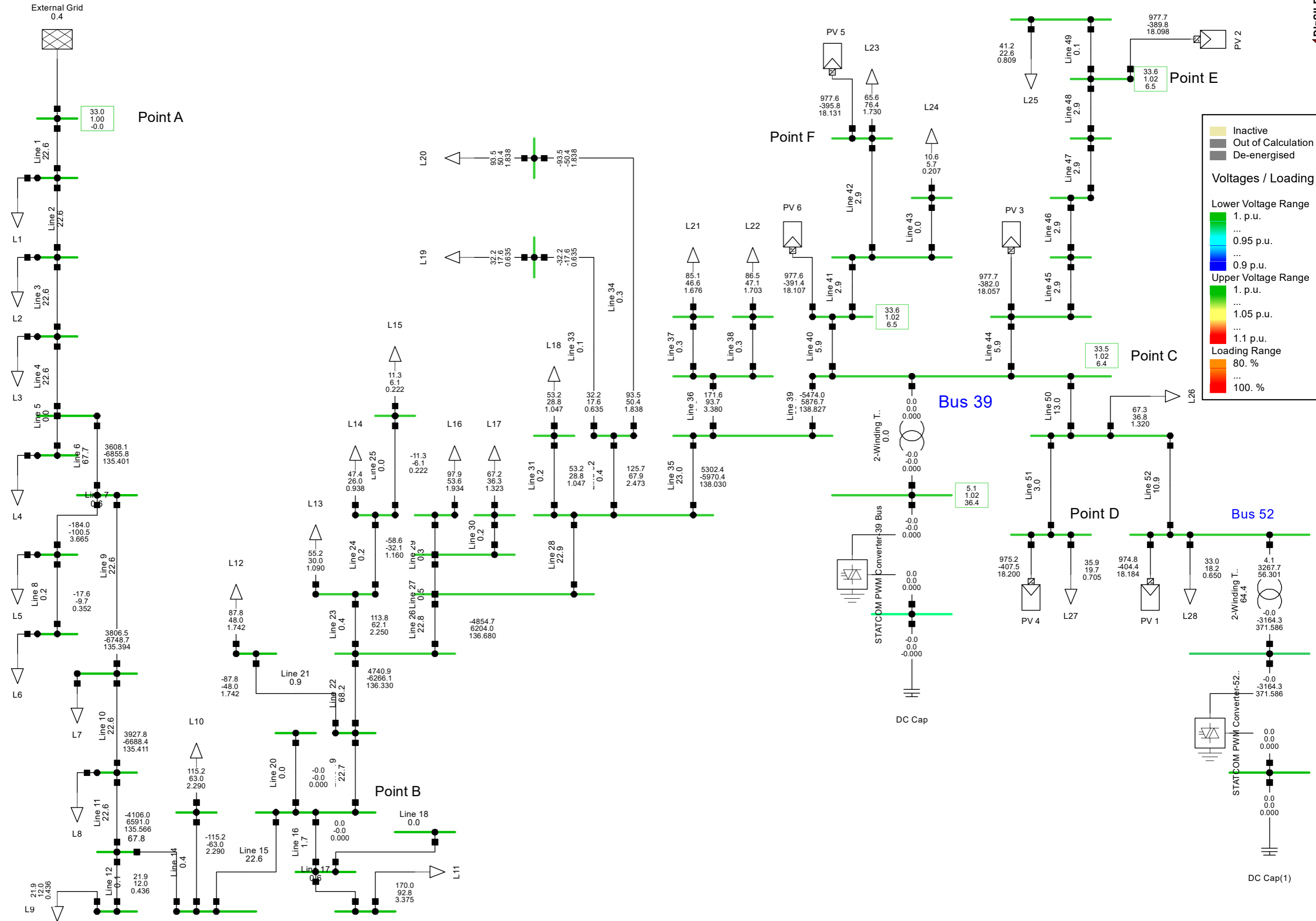
■ Voltage, Magnitude in p.u.

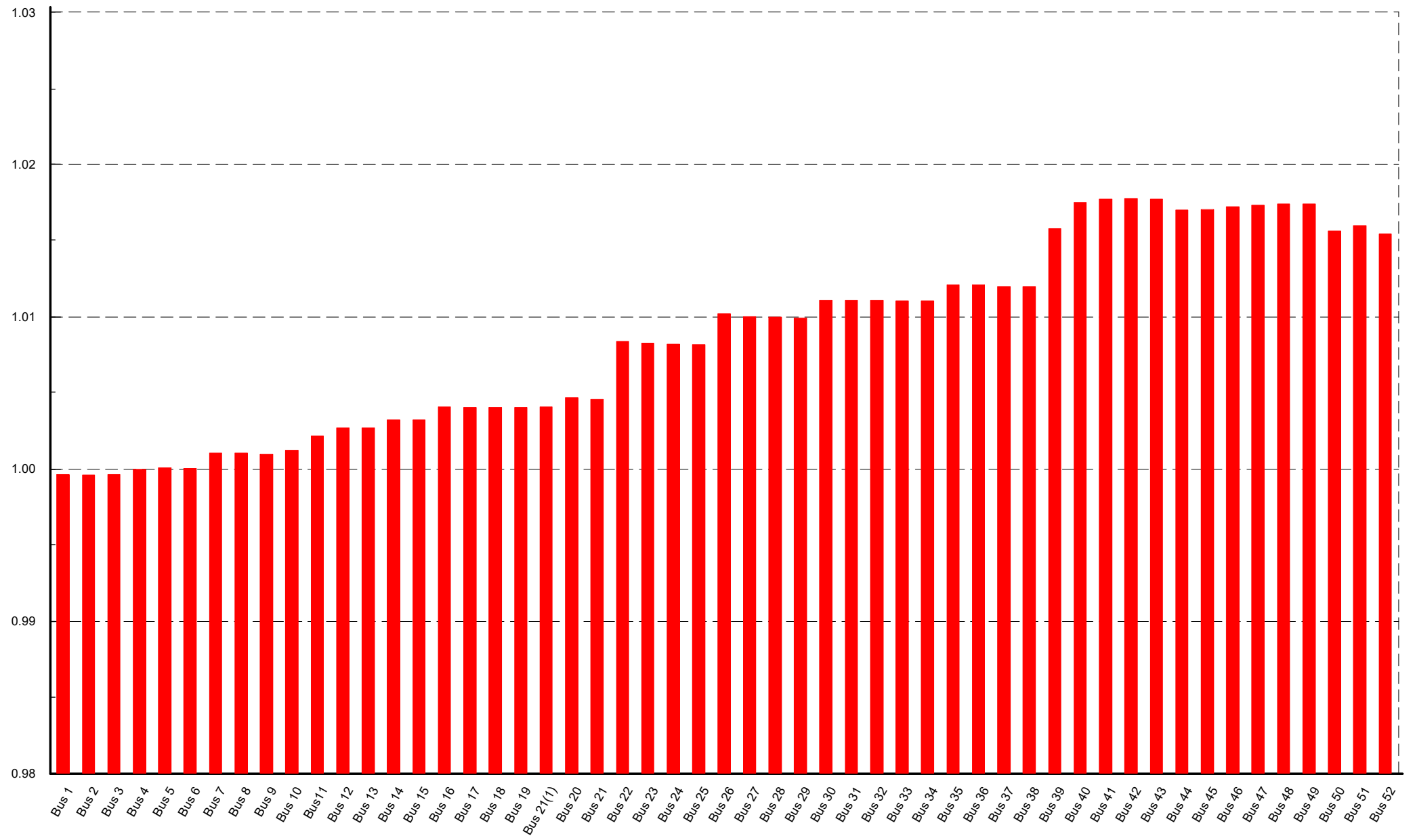
DIGSILENT

**A14. Records Generated for Coordinated Voltage Control between DSTATCOM
(@ 52 bus) & DER of Mauara Feeder in DIgSILENT PowerFactory**

A14.1 Single Line Diagram

A14.2 Bus Voltages Diagram





■ Voltage, Magnitude in p.u.